5.04 Observation and Measurement Techniques

G. M. Turner, Victoria University of Wellington, Wellington, New Zealand

J. L. Rasson, Institut Royal Meteorologique, Dourbes, Belgium

C. V. Reeves, Earthworks BV, Delft, The Netherlands

5.04.1	**Introduction**	94
5.04.1.1	Instrumentation	95
5.04.1.2	Vector Magnetometer Sensors	96
5.04.1.2.1	The induction coil	96
5.04.1.2.2	The fluxgate	97
5.04.1.2.3	The SQUID	98
5.04.1.3	Scalar Magnetometers	99
5.04.1.3.1	Proton precession magnetometers	99
5.04.1.3.2	Overhauser effect proton magnetometers	101
5.04.1.3.3	Optically pumped magnetometers	101
5.04.2	**Magnetic Observatories**	103
5.04.2.1	Special Magnetic Conditions in an Observatory	103
5.04.2.2	Geomagnetic Observations Using the Baseline Concept	104
5.04.2.2.1	Absolute measurements of field components	104
5.04.2.2.2	Measuring the angular orientation of the geomagnetic field	106
5.04.2.2.3	Variation measurements: variometers	108
5.04.2.2.4	Instrument certification and calibration	109
5.04.2.2.5	Obtaining definitive absolute data	110
5.04.2.3	The INTERMAGNET Magnetic Observatory Network	111
5.04.2.4	Fully Automatic Magnetic Observatories	112
5.04.2.5	Magnetic Repeat Station Surveys	113
5.04.2.6	Products and Services Magnetic Observatories Can Provide	113
5.04.3	**Magnetic Surveys for Geological Exploration**	113
5.04.3.1	Mapping Magnetic Anomalies	114
5.04.3.2	The Origin of Magnetic Anomalies	115
5.04.3.3	Instrumentation Applied to Magnetic Surveying	118
5.04.3.3.1	Ground surveys	118
5.04.3.3.2	Airborne survey techniques	119
5.04.3.4	Design and Execution of Surveys	119
5.04.3.4.1	Practical airborne magnetometry	119
5.04.3.4.2	Elimination of nongeological influences (aircraft, temporal changes)	120
5.04.3.5	Data Presentation, Enhancement and Interpretation Methods	122
5.04.3.6	The Link between Magnetic Properties of Rocks and Regional Geology	124
5.04.3.7	Satellites and Space Probes	126
5.04.4	**Paleomagnetic Methods**	127
5.04.4.1	Sampling	127
5.04.4.1.1	Introduction	127
5.04.4.1.2	Consolidated rocks	128
5.04.4.1.3	Unconsolidated (lake and deep sea) sediments	129
5.04.4.2	Rock Magnetometers	130
5.04.4.2.1	Introduction	130
5.04.4.2.2	Astatic systems	130
5.04.4.2.3	Spinner magnetometers	131
5.04.4.2.4	Cryogenic magnetometers	132

5.04.4.3	Progressive Demagnetization Techniques	134
5.04.4.3.1	Introduction	134
5.04.4.3.2	Thermal demagnetization	135
5.04.4.3.3	Alternating field (AF) demagnetization	136
5.04.4.4	Data Analysis and Statistics	136
5.04.4.4.1	Progressive demagnetization data	136
5.04.4.4.2	The statistical treatment of paleomagnetic data	138
5.04.4.4.3	Field tests	139
5.04.4.4.4	Poles	142
References		143

Nomenclature

***f* frequency**	(Hz)	***M* magnetization**	($A\ m^{-1}$)
***m* magnetic moment**	($A\ m^2$)	***Q* Koenigsberger ratio**	(dimensionless)
***B* magnetic induction (field)**	(T)	***R* resistance**	(Ω)
***C* capacitance**	(F)	***T*, T_C, T_B temperature, curie temp., blocking temp.**	(°C or K)
***D*, *I* or *Dec*, *Inc* declination, inclination**	(degrees)	***V* voltage (signal or emf)**	(V)
***E* energy**	(J)	***X*, *Y*, *Z* N, E, Down components of geomagnetic field (induction)**	(T)
***F* total geomagnetic field**	(T)	γ **gyromagnetic ratio**	($Hz\ T^{-1}$)
***H* magnetic field intensity**	($A\ m^{-1}$)	λ, ϕ **latitude, longitude**	(degrees)
***H* horizontal component of induction**	(T)	μ **magnetic permeability**	
***I* moment of inertia**	($kg\ m^2$)	τ **torque**	(N m)
***K* mass (specific) susceptibility**	($m^3\ kg^{-1}$)	τ **relaxation time**	(sec,yr)
***L* angular momentum (spin)**	($kg\ m^2\ s^{-1}$)	ϕ **magnetic flux**	($T\ m^2 = Wb$)
***L* inductance**	(H)	χ **volume susceptibility**	(dimensionless)
		ω **angular frequency**	($rad\ s^{-1}$)

5.04.1 Introduction

The geomagnetic field is a complex function of space and time, with contributions of both internal and external origin. Historically, knowledge of the morphology and variability of the field has been important in navigation, in understanding atmospheric and ionospheric processes, including radio transmission, as well as in geophysical studies of Earth's interior (the core, mantle, and the tectonic plates of that make up the lithosphere). The purpose of this chapter is to describe the instruments and practices used to observe and measure the full range of features of the geomagnetic field.

The significance of the predominantly dipole nature of the main field was recognized by Gilbert over 400 years ago; secular variation was documented at about the same time. The nondipole part of the field that originates from the core manifests itself at the surface as features that typically extend over thousands of kilometers. The International Geomagnetic Reference Field (IGRF, website) is a spherical harmonic model designed to accurately describe the spatial features of the field originating from the core. Much of the data incorporated into the IGRF comes from the global network of permanent geomagnetic observatories (INTERMAGNET, website).

By contrast, the remanent magnetization of crustal bodies typically results in magnetic anomalies of much smaller extent (up to tens or hundreds of kilometers). These are generally charted and studied through regional or local magnetic surveys.

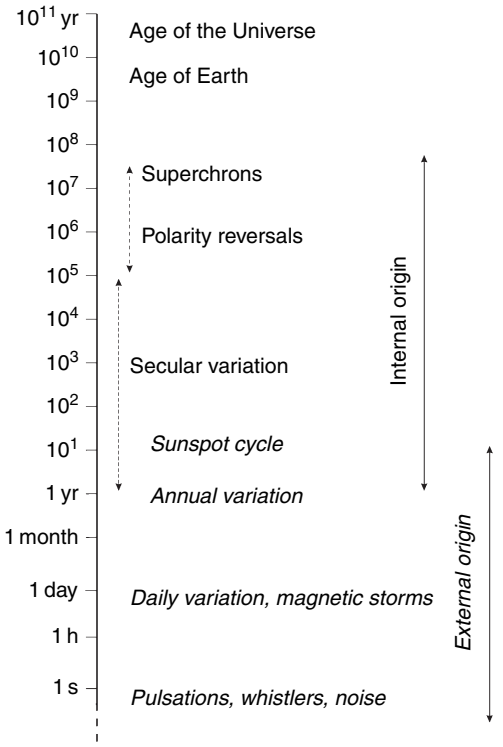

Figure 1 Time variations of the geomagnetic field in relation to the age of Earth and the Universe, indicating which are of internal and which are of external origin.

In addition, the field has been observed to undergo a very broad spectrum of time variations, extending well beyond the limit of real time and historical observations (**Figure 1**). Perhaps the most astounding of these is the phenomenon of polarity reversals found only in the paleomagnetic record. Time-varying signals reaching Earth's surface from the core are attenuated due to the conductivity and permeability of the mantle, so that periodicities less than about an year cannot be detected. The shorter period magnetic field variations that are observed originate externally – from variations in the solar wind and the interplanetary magnetic field, and their interactions with the magnetosphere.

Although the vast majority of measurements of the geomagnetic field are made on Earth's surface, magnetometers are routinely flown in space probes and satellites, offering hugely superior spatial coverage. Modern models of the main field incorporate satellite measurements, while aeromagnetic measurements make a huge contribution to modern survey work.

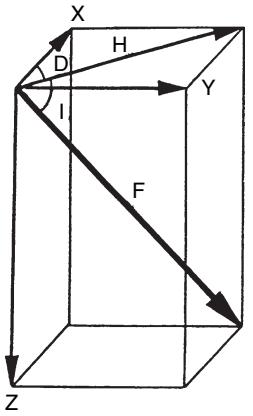

Figure 2 Decomposition of the geomagnetic vector, showing components used when describing the vector in Cartesian (x, y, z), cylindrical (D, H, Z) and spherical (D, I, Z) coordinate systems.

In order to describe the (instantaneous) geomagnetic field vector completely, three independent components must be specified. The three coordinate systems commonly used are as follows:

- Cartesian: X (North component), Y (East component), Z (vertical component, positive downwards);
- Cylindrical: D (magnetic declination angle, positive east of north), H (horizontal component), Z (as above);
- Spherical: D (as above), I (magnetic inclination angle, positive below horizontal), F (intensity of magnetic field).

The relations between these different systems are illustrated in **Figure 2**.

5.04.1.1 Instrumentation

The earliest known compass, made in China around the first century AD, was a spoon-shaped piece of lodestone, balanced on a horizontal plate so that it aligned with Earth's magnetic field, the handle pointing south. Although originally designed for the purpose of divining favorable orientations (*feng shui*), these early instruments were the forerunners of an extensive range of measuring instruments and navigational compasses based on pivoted or suspended magnets.

The magnetic compass is simply a needle balanced to rotate in a horizontal plane until it comes to rest in the plane of the magnetic meridian (with north, rather than south, now being the

principal sense). It was the first scientific instrument to employ a needle moving over a graduated scale, and though most moving needle instruments have by now been superseded by digital meters, the compass remains the simplest and easiest means of finding directions in remote locations, since it has no electronics and needs no power supply.

Very early compass-makers appear to have been unaware of the vertical component of the geomagnetic field. However, by the mid-sixteenth century, Hartmann and Norman had both noted and measured the angle of inclination, using a magnetized needle pivoted to rotate in the vertical north–south plane: a dip needle.

The dip needle was also used to make the first measurements of the intensity of the magnetic field. Small oscillations of the needle about its equilibrium position have a period given by $T = 2\pi\sqrt{I/(mB)}$, where I and m are the moment of inertia and the magnetic moment of the needle, and B is the magnetic field. The first recorded intensity measurements were made by de Rossel on the d'Entrecasteaux expedition of 1791–94 (Lilley and Day, 1993). Both the d'Entrecasteaux measurements, and those of Alexander von Humboldt, made between 1798 and 1803, clearly show the increase of intensity with latitude which is expected of a predominantly geocentric axial dipole (GAD) field.

Many of the first-generation magnetic field-measuring instruments were based on pivoted or suspended magnet systems. These include the quartz horizontal magnetometer (QHM) and the balance magnétique zero (BMZ) instruments used extensively in observatories, the astatic and parastatic rock magnetometers used in many of the pioneering paleomagnetic studies, variometer-type instruments used in early magnetic surveys and exploration work, and the Gough—Reitzel magnetometer commonly used until recently in magnetometer array studies.

From the 1950s onwards these elegant but delicate instruments have gradually been replaced by more robust electrical and electronic instruments such as the induction coil, and the fluxgate, which capitalizes on the high-permeability materials that were developed at the time. Electrical feedback systems have played a major role in stabilizing the response of these instruments. Still later, computer interfacing and data logging have led to partial or complete automation of many operations.

The most recent generation of magnetometers has grown out of research on magnetic properties at the atomic level, and the development of superconducting materials and devices, which are, in principle, capable of counting individual quanta of magnetic flux, and thus reaching the theoretical limit of resolution. These include the proton precession magnetometers (PPMs) and Overhauser effect magnetometers, used extensively in observatories, and the Superconducting quantum interference device (SQUID) which has revolutionized paleomagnetic measurements.

In this section we describe the principles of operation of the main types of sensors used in geomagnetism and paleomagnetism. Their incorporation into practical magnetometers is covered in the following sections on geomagnetic observatories, magnetic surveys, and paleomagnetism.

The induction coil, fluxgate, and SQUID are vector sensors: their orientation in space determines which component of the ambient field is measured. The proton precession, Overhauser and optically pumped magnetometers (OPM), on the other hand, are insensitive to the direction of the ambient magnetic field, and measure only its magnitude. This property stems from the fundamental physical principles put to work in their operation: Larmor precession, electron spin resonance, and Zeeman splitting.

5.04.1.2 Vector Magnetometer Sensors

5.04.1.2.1 The induction coil

The induction coil, or search-coil magnetometer is one of the simplest modern magnetometers: in principle, when the magnetic flux, ϕ, threading through a conducting circuit varies, an emf or voltage signal is induced in the circuit in accordance with Faraday's Law of electromagnetic induction. The induced voltage, V_i, is proportional to the rate of change of the magnetic flux.

In practice the flux linkage is enhanced by winding many turns of conducting wire on a core of high-permeability ferromagnetic material. For a solenoid of N turns, each of cross-sectional area A, and a core of relative permeability μ, $\phi = \mu NAB$, where B is the component of the magnetic field parallel to the axis of the solenoid.

For magnetic field variations of frequency ω, along the axis, $B = B_0 e^{-i\omega t}$, and the theoretical induced voltage is

$$V_i = -\frac{d\phi}{dt} = NA\mu(i\omega)B_0 e^{-i\omega t}$$

This signal must be amplified, and the actual measured voltage depends also on the resistance, inductance, and capacitance of the coil as well as the size of any damping resistor and the gain of the amplifier.

Due to their simplicity, induction coils are widely used for many applications, for instance in geophysical prospecting and metrology. In magnetic observatories they are used to monitor rapid variations of the geomagnetic field, such as pulsations. With suitable circuitry, induction coils can be designed to measure variations with frequencies between 10^{-4} and 10^{+7} Hz and fields from fractions of femto-tesla to tens of teslas (Korepanov *et al.*, 2001).

5.04.1.2.2 The fluxgate

The operation of a fluxgate sensor depends on the nonlinear relation between induced magnetization and magnetizing field in high-permeability easily saturated materials such as ferrites, permalloy, metallic glasses, and mu-metal.

Various different designs exist: most have two cores, either as two separate linear cores, or as two halves of a ring fluxgate.

The general principle of operation is described below for the case of the Vacquier two-core design shown in **Figure 3**. Identical primary coils are wound around the two high-permeability cores. The drive current (of frequency 50–1000 Hz) is of sufficient amplitude to saturate the cores during most of each cycle. The primary windings are connected in series opposition, so when the drive current is applied, the axial magnetic fields are out of phase (**Figure 4(a)**). If there is a steady ambient magnetic field, B_{amb}, parallel to the core axis, as shown in **Figure 3**, then when it augments the field in one coil, it reduces the total field in the other and vice versa (**Figure 4(b)**). The effect of the ambient field is thus that, during any given half-cycle, the core in which the field is augmented will be saturated for more of the half-cycle, while the core with the reduced field will be saturated for less of the half-cycle. The situation

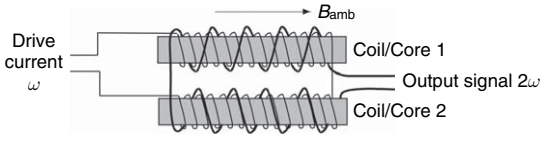

Figure 3 A two-core fluxgate magnetometer (Vacquier design).

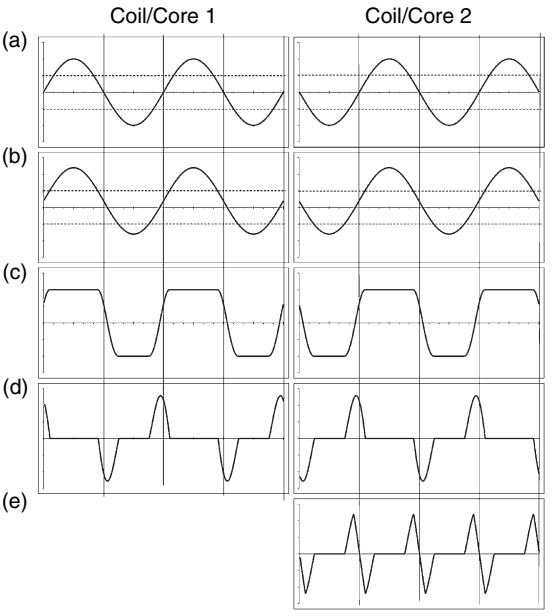

Figure 4 Signal processing in a two-core fluxgate sensor. (a) Sinusoidal drive current, frequency ω. In the absence of the iron cores, the drive signal results in antiphase magnetic fields in coils 1 and 2; (b) Addition of the ambient field B_{amb}, as shown in **Figure 3**, results in an asymmetry; (c) So, core 1 is saturated for more of the first half-cycle than core 2, while core 2 is saturated for more of the second half-cycle than core 1; (d) the magnetic flux changes in secondary coils 1 and 2 are therefore not synchronous, resulting in induced emf pulses as shown; (e) the output signal is the sum of the emfs in secondary coils 1 and 2, which has a dominant frequency of 2ω.

reverses in the next half-cycle of the driving signal (**Figure 4(c)**). This asymmetry between the magnetization of the two cores leads directly to an asymmetry between the rates of change of flux in the secondary coils (**Figure 4(d)**). The secondary coils are oppositely wound and series connected as shown (**Figure 3**), so the asymmetry results in a nonzero output twice per cycle, that is, at twice the frequency of the driving signal (**Figure 4(e)**). For small fields the amplitude of this second harmonic is proportional to the component of the ambient field parallel to the fluxgate axis. A phase-sensitive detector, with its reference signal set to twice the frequency of the driving signal is generally used to produce a DC output that is proportional to the ambient field.

In practical applications a feedback arrangement is almost always employed to cancel the field being measured, and hence linearize the response. Fluxgate sensors are highly directional, measuring only the

field component parallel to the fluxgate axis. An arrangement of three orthogonal fluxgates may therefore be used to obtain the intensity and direction of the total field vector. If three independent units are used in close proximity; for example, in a spacecraft, problems can arise due to interference of the separate feedback systems. This has been overcome in the Compact Spherical Coil system, as used in the Oersted and CHAMP satellites, where all three sensors see the whole feedback field (Nielsen *et al.*, 1995).

The first fluxgate-type device was built and described by Aschenbrenner and Goubau (1936). Airborne fluxgates were used extensively during the Second World War for submarine detection. Subsequent developments mean that modern fluxgates have many applications: they are used for navigation on land and sea, as vector magnetometers in almost all space flights, in observatories, and in many medium-resolution rock magnetometers.

5.04.1.2.3 The SQUID

The development of the SQUID or superconducting quantum interference device, as a magnetic field sensor heralded a new era in sensitivity, particularly in paleomagnetic rock magnetometers.

The superconductivity of mercury was discovered by Kammerlingh Onnes in 1911, when he found that, below about 4 K, its electrical resistivity effectively vanished. Other metal superconductors, more suitable for the construction of practical devices, include niobium ($T_C = 9.2$ K) and lead ($T_C = 7.2$ K). More recently superconducting ceramic materials, for example, oxides of lanthanum or yttrium, with barium, strontium or calcium and copper, have been discovered with transition temperatures of 90 K and higher. However, practical sensors utilizing these 'high-temperature' superconductors have not yet been developed.

Superconductivity may be explained by the Bardeen, Cooper, Schrieffer (BCS) theory (Bardeen *et al.*, 1957). At sufficiently low temperatures a weak interaction causes electrons to form pairs. Such 'Cooper pairs' have boson-like properties; in particular, in the absence of an exclusion principle, they occupy a single quantum state, and may be described by a single coherent wave function. The pairing of electrons is critical to the theory. In the normal state, electrical resistivity results from collisions, or scattering of conduction electrons by the ions of the crystal lattice. In the superconducting state, one electron of the Cooper pair effectively distorts the lattice, allowing the other free passage.

Another property of the superconducting state is the exclusion of magnetic flux from the bulk of the superconducting material (Meissner effect). If an external magnetic field exists through a ring of superconductor then, as it is cooled through the critical temperature, superconducting currents will be generated to cancel it. However, if the current exceeds a certain value, I_c, the superconductivity is lost, and the material reverts to its normal resistivity. The moment this happens the current drops and flux enters the ring. With the lowering of the current, superconductivity is restored. However, to maintain the coherency of the electron-pair wave function, the current can drop only by quantized amounts, and correspondingly only quantized amounts of flux may enter the ring. This flux quantum, ϕ_o, is equal to $h/2e = 2.09 \times 10^{-15}$ Wb. In principle, the number of flux jumps may be counted to give a measure of the strength of the external magnetic field. This effect is utilized in the SQUID.

Josephson (1962) predicted that a supercurrent should be able to pass through a thin layer of dielectric material sandwiched between two superconductors, if the wave functions of the electrons extend into the junction and join up coherently. A similar effect is achieved by creating a very narrow bridge or weak link between two pieces of superconductor.

The term SQUID has been applied to two types of devices that have evolved from the basic Josephson junction. The simpler concept is that of the DC SQUID. It consists of two Josephson junctions or weak links arranged symmetrically in a ring of superconductor. Magnetic flux through the ring will result in equal and opposite phase shifts of the wave functions across the two junctions. Interference therefore occurs between the currents in the two branches of the device, in a manner analogous to the interference of light waves in a double-slit experiment. The current is maximum if the flux is equal to an integral number of flux quanta, but is reduced to zero for an odd number of half-quanta.

The first superconducting rock magnetometers used radio frequency (RF)-driven SQUIDS (Goree and Fuller, 1976). These are not strictly interference devices, but rather single weak links contained in a ring or cylinder of superconducting material. The operation of a device similar to the Dayhem bridge used in the first superconducting rock

magnetometers built by Superconducting Technologies Inc. (SCT) is illustrated in Figure 5.

The sensor is driven by an RF signal of frequency 20–30 MHz, through a coil wound around the outside. The amplitude of the RF signal is sufficient to exceed the critical current of the weak link. When this occurs the loop momentarily becomes resistive and a flux quantum is admitted before superconductivity is regained, as described above. This produces a pulse in the sensor coil. Figure 5(a) illustrates the situation when the critical current corresponds to 0.75 flux quantum; with no bias field, the output consists of two positive pulses and two negative pulses per cycle. The addition of an external magnetic field biases the RF signal, and changes the positions in the cycle at which the critical current is exceeded. Figure 5(b) shows that the positions of the pulses have been shifted, and from these shifts the DC field can be obtained. A common arrangement to avoid problems of nonlinearity and drift is to apply negative feedback, so the sensor is always at its most sensitive state, and to monitor the feedback signal needed to achieve this.

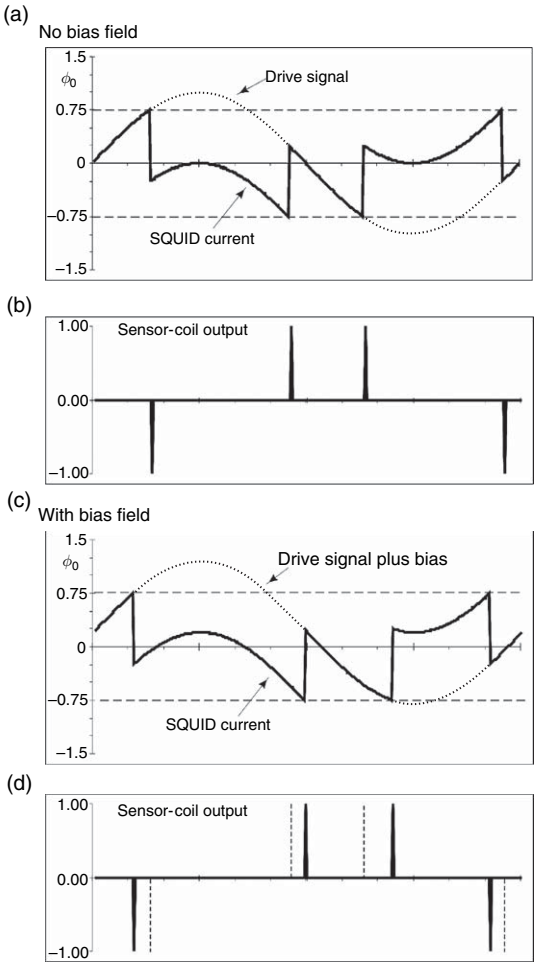

Figure 5 Signal processing by a weak link SQUID sensor, with and without a direct biasing field. (a) Sinusoidal drive signal that causes the super-current to exceed the critical value at 0.75 ϕ_0, at which point the flux through the SQUID jumps by ϕ_0. The bold curve shows the resulting SQUID current. (b) At each flux jump a pulse is induced in the sensor coil. (c) and (d) are the corresponding curves for the case of a direct bias field and show that the pulses in the sensor coil are offset by the direct field.

5.04.1.3 Scalar Magnetometers

5.04.1.3.1 Proton precession magnetometers

Thanks to groundbreaking work on nuclear magnetic induction by Bloch (1946) and its application to the measurement of weak magnetic fields by Packard and Varian (1954), the PPM became available from the late 1940s. It allows the absolute measurement of the scalar magnetic field at the push of a button. In the PPM the magnetic field is found by measuring the frequency of the Larmor precession of the proton magnetic moment about the ambient field, the protons being provided by a sample of water or other proton-rich fluid.

The spin angular momentum and magnetic moment vectors of the proton, $\mathbf{L}$ and $\mathbf{m_p}$ are parallel. Their ratio is a scalar constant known as the proton gyromagnetic ratio, γ_p.

$$\gamma_p = \frac{m_p}{L} = 2.67522205(23) \times 10^8\,\mathrm{Hz\,T^{-1}}\ \text{(CODATA 2002, NIST website)}$$

In an external magnetic field, $\mathbf{B}$, the magnetic moment experiences a torque and this results in a change in the angular momentum vector:

$$\boldsymbol{\tau} = \mathbf{m}_p \times \mathbf{B} = \frac{\mathrm{d}\mathbf{L}}{\mathrm{d}t}$$

$\mathbf{L}$ is parallel to $\mathbf{m}$, while the torque is perpendicular to $\mathbf{m}$, so $\mathbf{d}L$ is perpendicular to $\mathbf{L}$, and the effect is to make $\mathbf{L}$ and $\mathbf{m}$ precess about the direction of $\mathbf{B}$ (Figure 6). This is Larmor precession, and its frequency is given by

$$\omega_{\mathrm{Larmor}} = 2\pi f = \gamma_p B$$

Hence a measurement of the Larmor frequency and division by the proton gyromagnetic ratio leads directly to the intensity of the ambient magnetic field. In practice the 'shielded' proton gyromagnetic ratio, γ', is used instead of γ. This takes account of the diamagnetism of water (or other proton-rich

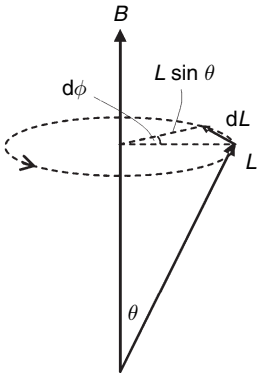

Figure 6 Larmor precession of the proton angular momentum vector, **L**, about the ambient magnetic field vector, **B**, in response to the torque, **m** x **B**, on the magnetic moment vector of the proton, **m**, which is parallel to **L**. See text for more details.

fluid) and the shape of the sample (usually taken to be spherical). For a spherical sample of water at 25°C

$$\gamma' = 2.67515333(23) \times 10^8\,\mathrm{Hz\,T^{-1}}\ \text{(CODATA 2002, NIST website)}$$

A PPM sensor is therefore ideally a spherical container filled with water, or other proton-rich fluid. A surrounding coil supplied with a direct current produces a direct field several orders of magnitude larger than the Earth's field, and aligns the magnetic moments of the protons. This is to partially remove the random orientation due to the thermal agitation of the protons. After the few seconds, necessary to obtain sufficient alignment, this DC field is removed and the proton magnetic moments precess about the ambient (geomagnetic) field vector. An emf induced by the precessing protons is then observed for a few seconds by a pick-up coil, until thermal agitation drowns the signal again (Primdahl, 2002). The observed signal is an exponentially decaying sinusoid at the Larmor frequency f. The emf signal in the geomagnetic field ranges from 850 to 3400 Hz and its amplitude is typically of a few microvolts. The signal-to-noise ratio is dependent upon the strength of the field; therefore, a PPM works better in strong fields. Often the same coil is used for the polarizing and pick-up operations. For maximum signal, the polarizing DC field should be applied at right angles to the field to be measured, in order to maximize the rotating component and the emf pick-up by the coil. Cylindrical coils will therefore have dead zones for certain orientations of the sensor, where the emf signals disappear in the noise. Toroidal coils have been used to eliminate this spatial dependency on the signal-to-noise ratio.

Efforts to improve the PPM have also addressed the way in which the frequency measurement is performed. In early PPMs, the frequency, f, of the output signal was multiplied by an integer M using a phase-locked loop. The resulting signal at frequency Mf was then counted by a digital counter for a time duration D. D was set by a custom-cut quartz crystal, serving as a frequency reference, and whose frequency F was adjusted to provide the correct scaling according to the value of γ'_p. For instance, the Geometrics G816 PPM used $M = 64$ and $F = 2.857252$ MHz. The interval D spanned 2^{20} cycles of F, about 0.37 s. The final count C was then equal to the magnetic field, B, in units of nT:

$$C = \frac{64 \times 2^{20}}{2857252} f = 23.4872 f = \frac{2\pi}{\gamma'_p} f \cdot 10^9\ \mathrm{nT}$$

Nowadays, PPM frequency-measuring schemes are assisted by microcomputers and digital signal processors. This computing power allows use of every part of the proton precession signal, to adopt noise-canceling techniques and to extract qualitative information on the measurement (Sapunov *et al.*, 2001; Jankowski and Sucksdorff, 1996; Primdahl, 2002). Elaborate statistical analysis on the digitized time series of the decaying precession signal and Fourier techniques are used in proprietary algorithms by PPM manufacturers in order to increase the true resolution of their PPMs.

Factors affecting the accuracy of the PPM originate in the following

1. Erroneous frequency measurement. This is the most easily avoided error as frequency standards are readily available for control either as precision oscillators or by broadcasting (time signals or global positioning system (GPS)). The reference oscillator in the PPM's electronics should regularly be checked against a frequency standard.
2. Magnetically unclean sensors, which distort the field to be measured. This contamination will result in 'heading errors' where the magnetometer readings will depend upon the sensor orientation.
3. Failure to adhere to the conditions defining γ'_p: nonspherical sample (Primdahl *et al.*, 2005), use of another proton-rich fluid than water (Hrvoic, 2001), etc.
4. Mechanical rotation. Clockwise or anticlockwise sensor rotation around the magnetic field direction will add or subtract to the precession frequency. This effect is readily noticed in PPMs on board rotating platforms such as rockets or satellites (Alexandrov and Primdahl, 1993).

A drawback of the PPM is the low sampling rate, and the dead times corresponding to the polarization phases, when no data can be obtained. The low signal-to-noise ratio of the standard proton precession signal makes it difficult to perform geomagnetic field measurements with repeatability better than 0.1 nT. The latter limitations result in an instrument with an overall accuracy of 0.2 nT in a field of about 50 000 nT.

PPMs are used extensively in ground, marine, and airborne magnetic surveys; they are routinely carried on space probes and satellites, and are almost ubiquitous in geomagnetic observatories. Provided its frequency reference is checked and adjusted regularly, the PPM is an excellent realization of the International Magnetic Standard (IMS) (see Section 5.04.2).

5.04.1.3.2 Overhauser effect proton magnetometers

In 1953, Overhauser predicted an effect now known as dynamic nuclear polarization (Overhauser, 1953a, 1953b), which enhances the initial alignment of the proton magnetic moments considerably. His idea was to impose an appropriate RF signal on the atom and thereby excite the electronic spins to higher, non-thermal equilibrium states, a process now known as electron spin resonance or ESR. Because of a quantum mechanical coupling between the electron and the nuclear spins, as the excited electron spins try to equilibrate to their lower states they would reorient the nuclear spins. The nuclear-spin polarization achieved in this way would be increased by a factor of about 1000, the ratio of the electronic to the nuclear magnetic moments. The idea was met with much skepticism: it was even deemed by some to contravene the second law of thermodynamics until late 1953 when it was verified experimentally by Carver (Carver and Slichter, 1953, 1956).

Dynamic nuclear polarization of the proton magnetic moments is employed in the Overhauser PPM, where it increases the signal-to-noise ratio and lowers the power requirements, since little or no direct current is required for continuous polarization. An Overhauser PPM sensor should consist of a container filled with a proton-rich fluid having at the same time free electrons available for RF ESR. This is obtained by dissolving a substance containing free radicals such as Tempone, Proxyl, or Trityl into the fluid (Primdahl, 2002). A cavity resonator, supplied by an RF generator via a coaxial cable, surrounds the fluid container. A coil also surrounds the container, which plays a similar pick-up and polarization role as in the standard PPM. Three different polarization schemes are known and in use at present, each requiring specific free radical substances and RF excitation characteristics (Sapunov *et al.*, 2001).

The increased complexity in the chemistry of the fluid and the electronics of the sensor results in a much improved signal-to-noise ratio for the Overhauser instrument compared to the standard PPM. Noise levels and a repeatability approaching 1 pT are achieved, but the absolute accuracy is no better than the 0.2 nT of the standard PPMs, mainly because no testing and certification procedures exist to improve this figure (see below).

By avoiding the power-hungry direct field polarization of standard PPMs, the Overhauser magnetometer can achieve relatively low-power operation, which is an advantage for an instrument intended to operate continuously in an unattended mode. A single reading uses about 1 W s (1 J) and the standby power supply can be as low as 50 mW.

A drawback of the Overhauser PPM stems from the unknown long-term reliability of the device, compared with the tried and tested standard PPM. The single electron of the free radical makes it somewhat unstable chemically. The useful lifespan of the dissolved free radical is often specified as being between 5 and10 years, and signal degradation in the best devices has been observed for continuous operation much longer than this.

5.04.1.3.3 Optically pumped magnetometers

Like proton magnetometers, OPMs are scalar instruments but, unlike the standard PPM, they deliver a continuous stream of data, in the form of a frequency that depends on the magnitude of the magnetic field. OPMs are based on the Zeeman splitting of the electron energy levels of some alkali metal and helium atoms in a magnetic field. The optical pumping scheme allows measurement of this energy splitting – and therefore the magnetic field – with very high resolution (Alexandrov and Bonch-Bruevich, 1992).

The state of an alkali metal (or metastable ^{4}He) atom is determined primarily by its outermost (valence) electrons. In the presence of a magnetic field, atomic energy levels are split by an amount that is proportional to the magnitude of the field: this is the Zeeman effect. Optical 'pumping' (Kastler, 1950) refers to the populating of one of these Zeeman sublevels at the expense of another.

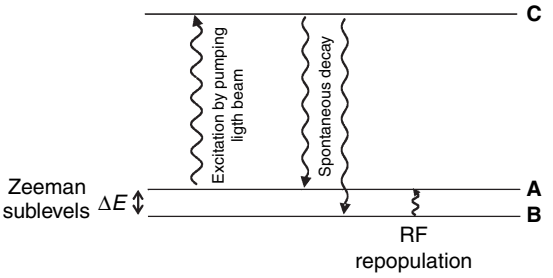

Figure 7 Schematic representation of the energy states of an atom in an optically pumped magnetometer. A and B are Zeeman sublevels, split by an amount ΔE in the presence of a magnetic field. C is a substantially higher energy state. See text for details of the optical pumping and RF repopulation processes.

The basic principle of optically pumped magnetometers is illustrated in **Figures 7** and **8**. A monochromatic light beam of suitable polarization is shone into a cell containing gaseous atoms of the alkali metal or helium. The wavelength and polarization are such that atoms from only one of the Zeeman sublevels, A, are excited to some higher state, C. After a very short time in state C, these excited atoms relax spontaneously to A or B with equal probability. Eventually, this process (excitation from only A, but relaxation to either A or B) leads to a situation with all the atoms in state B, and none in A. The light beam will no longer be absorbed – the cell becomes transparent to it.

Transmission of the light beam through the cell (to a photo-diode) serves as a switch to a coil around the cell that transmits an RF signal. The frequency of this RF signal is adjusted (via suitable feedback) until it corresponds to the Zeeman splitting between A and B. When this occurs A is repopulated and the light beam is once again able to excite atoms to state C, that is, light is again absorbed and the cell loses its transparency. This cycle therefore provides the basis of the feedback mechanism, while the RF frequency, f, provides the means to calculate B, the magnitude of the ambient magnetic field.

The Zeeman splitting, $\Delta E = \mathbf{\Delta}\,\mu \cdot \mathbf{B} = \mathrm{hf}$, where $\Delta\mu$ is the difference between the components of the atomic magnetic moment parallel to the magnetic field between the two sublevels. This is calculated from the quantum mechanics of the particular atom, using the Breit Rabi polynomial formula. The linear term is roughly equal to $28/(2I-1)$ Hz nT^{-1}, where I is the nuclear spin number, and determines the basic sensitivity of the magnetometer (**Table 1**). In some cases (e.g., potassium, helium) the Zeeman spectrum is 'resolved', and the polynomial coefficients can be calculated directly from fundamental physical constants: then the OPM has absolute accuracy (Alexandrov and Bonch-Bruevich, 1992; Gilles *et al.*, 2001).

The change in optical transmission upon application of the resonating RF signal depends in detail on the direction of the incident light beam relative to the

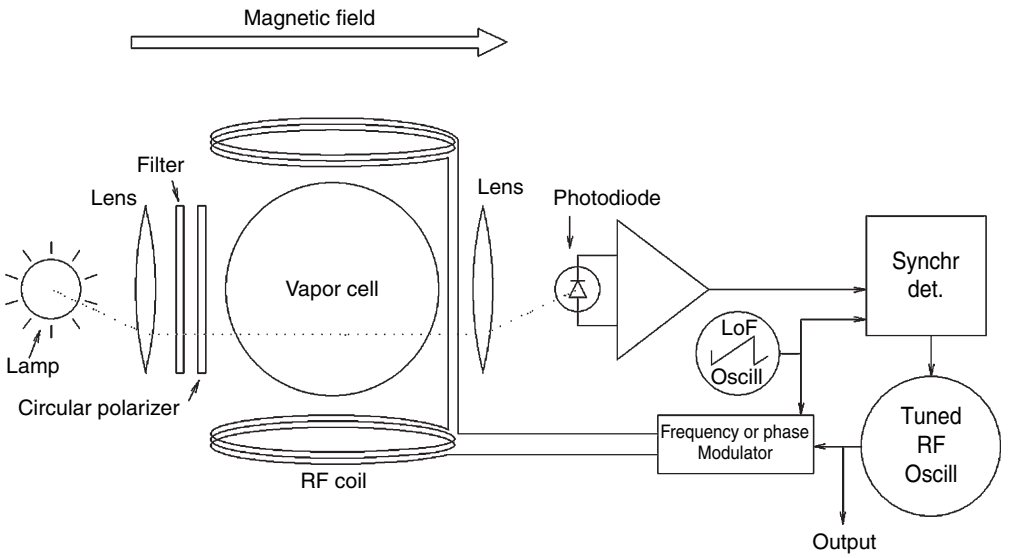

Figure 8 The operation principle of an M_z-mode optically pumped magnetometer. The RF frequency is usually in the hundreds of kilohertz while the low frequency, LoF, scans the spectral line at 10∼100 Hz by modulating the frequency of the RF signal.

Table 1 OPM sensitivities and vaporization temperatures (depending on cell size)

Substance	Basic sensitivity (Hz nT^{-1})	Vaporization temperature (°C)
^{23}Na	7.00	100–130
^{39}K	7.00	40–60
^{41}K	7.00	40–60
^{87}Rb	7.00	25–35
^{85}Rb	4.66	25–35
^{135}Cs	3.50	20–30
^{4}He	28.0	–

ambient magnetic field. This has led to two categories of OPMs: M_z-mode OPM's, where the quasi-stationary change of the transmitted light intensity is monitored, and M_x-mode OPMs in which the modulation of an auxiliary light beam at the RF frequency is detected.

OPM's have a high sensitivity – some approaching noise levels of 0.1 pT Hz$^{-1/2}$. This makes them attractive for magnetic prospecting and aeromagnetic surveying, as well as for space-based observations. Their high cost, due largely to the short lifetime of the gas discharge lamp, has limited their use in observatories.

Rb and Cs are preferred by magnetometer designers, as their low vaporization temperatures are easy to achieve, and result in longer lifetimes; some have been measuring continuously for more than 10 years. ^{135}Cs, ^{85}Rb, and ^{87}Rb can all be used, but only ^{87}Rb has a well-resolved spectrum in the geomagnetic field range, making it suitable for an absolute observatory magnetometer. The first digital magnetic observatory was based on a rubidium OPM (Alldredge and Saldukas, 1964). Caesium OPMs are used extensively in aeromagnetic survey work. ^{39}K and ^{41}K also have resolved spectra in the geomagnetic field range and produce instruments of high sensitivity. However, the chemical reactivity of potassium, together with its higher vaporization temperature reduce the life of the vapour cell considerably. Furthermore, to achieve a high sensitivity requires a cell 150 mm or more in diameter, making a potassium OPM rather bulky. The fundamental physics of ^{4}He is rather simpler; however, there are technical problems to be overcome in its application (Gravrand *et al.*, 2001; Blinov *et al.*, 1984). Helium OPMs have been flown on several satellites and space missions.

5.04.2 Magnetic Observatories

A global network of geomagnetic observatories was proposed and initiated by Gauss and Weber in 1834 – the original set of observations providing the data for Gauss' first spherical harmonic analysis of the geomagnetic field. Nowadays geomagnetic observatories are charged with the task of maintaining continuous permanent records of all three components of the field. Measurements are made at intervals of between 1 h and 1 s and are referred to universal time. A resolution of 1 – 0.01 nT is required. Vector measurements using, for example, fluxgate instruments are often complemented by scalar measurements of intensity to improve absolute accuracy. Geomagnetic observatory data is collected, collated, and disseminated by the World Data Centers (WDC). Nowadays near-real-time data is available through the INTERMAGNET website (see Section 5.04.2.3). Recently, the Virtual Global Magnetic Observatory Network has made geomagnetic data sets available online via search engines and object-building internet applications (Papitashvili *et al.*, 2006).

5.04.2.1 Special Magnetic Conditions in an Observatory

A magnetic observatory should be constructed so that only the natural magnetic field is present. Therefore, all buildings intended to house magnetic instruments are made from nonmagnetic material (**Figure 9**). Additionally, the location is selected so that it is not situated on a local magnetic anomaly, be it from geological or artificial origin. Consequently, the magnetic field is very homogeneous: the magnetic field lines are parallel. Magnetic field differences within the observatory are very small and spatial gradients are low (<1 nT m^{-1}). For the observation procedures to be valid, temporal magnetic field variations must be identical (within the observational error) inside the entire observation space.

As extremely high degrees of precision and accuracy are required in both angular and component measurements (~1 arcsec and 0.1 nT), recording instruments must be installed on specially constructed, highly stable 'pillars'. Horizontal directions are referenced to True North; therefore, a target should be available whose azimuth is known to the same accuracy and precision. Over time, these finely tuned conditions may degrade through secular changes in the environment or unauthorized introduction of

Figure 9 The geomagnetic observatory of Dourbes, showing the construction of the pavilions housing the observing instruments. To the left is the underground vault for the variometers: a high thermal inertia coupled with thick insulation ensures a low daily temperature variation in the vault. In the center is the absolute measurement pavilion, housing the reference pillar for the observatory. To the right, a technical pavilion for mains appliances and offices.

magnetic material to the observatory premises. Therefore, observatory conditions should be checked regularly and corrected if and as necessary.

5.04.2.2 Geomagnetic Observations Using the Baseline Concept

A complete description of the geomagnetic field requires the independent measurement of three angular or field components (see Section 5.04.1). The geomagnetic field varies with time, so observatory instrumentation must be of the recording type. At present, state-of-the-art component and orientation magnetometers, while potentially very sensitive and fast (up to the pT resolution at 100 Hz sampling rate), are not yet capable of measuring and recording all the field components continuously, with the required absolute accuracy. Therefore, a two-step observatory measurement procedure is generally employed:

1. A variometer is used to measure the variation of the field components about baseline values, in a continuous and unattended way, at the required sampling rate, say 1/minute.
2. Absolute measurements are performed manually (say 1/week) by an observer with adequate instrumentation (DIflux, proton magnetometer) to establish the values of the baselines mentioned in (1). Here the expression 'absolute measurement' means that the process of observation of the geomagnetic field must be fully traceable to metrological SI standards, and that the orientation of the geomagnetic vector is measured with respect to the local vertical and to geographic North.

If one can show that (1) the baselines remain stable between absolute measurements, and (2) the gradient between the variometer and the absolute measurement site is constant, then post-processing can be carried out to merge the two data sets and produce a final record having the accuracy of the absolute instrument, at the sampling rate of the variometer. It is expected that in the future fully automatic observatories will be available (see Section 5.04.2.4 on observatory automation) where the absolute measurement will also be made unattended.

5.04.2.2.1 Absolute measurements of field components

5.04.2.2.1.(i) The International Magnetic Standard (IMS) Before the advent of truly absolute instruments such as the PPM (Section 5.04.1.3), based on fundamental principles of physics, absolute measurement of the geomagnetic field intensity was complicated and prone to many sources of error. The concept of an IMS was therefore introduced by Wienert (1970). The IMS is an ideal, hypothetical instrument with no systematic error, against which observatories' quasi-absolute instruments, such as quartz horizontal magnetometers (QHMs) and balances magnétique zero (BMZs) (see below) could be checked.

5.04.2.2.1.(ii) Absolute measurement of the horizontal component, H, by the Gauss method Although rarely used nowadays, Gauss' method, devised in 1832, is of historical interest and importance. It enables measurement of both H and the magnetic moment, m, of a magnet, using only the magnet and a compass, and making measurements of

only length, mass, time, and angle. In the past, this procedure was the cornerstone of the absolute determination of magnetic field.

1. The magnet is first suspended from its centre of mass and allowed to swing in the horizontal plane about its equilibrium position in the magnetic meridian. The period of oscillation, T, is measured. T is given by

$$T^2 = 4\pi^2 \frac{I}{mH}$$

where I is the moment of inertia of the magnet (about an axis through its center and perpendicular to its length), and can be calculated from measurements of its length and mass. The value of the product mH can therefore be found in terms of T and I.

2. The magnet is next laid in an East–West orientation and the compass placed a distance r from its center on the extrapolation of its axis. The compass needle experiences the resultant of the horizontal component of Earth's magnetic field, H, in a northerly direction, and the axial field of the dipole, H_r^* (* indicates the field on the axis of a dipole, moment m, a (large) distance r from its center is $H_r = 2\mu_0 m/(4\pi r^3)$), in an easterly direction.

The angle, α, of the compass needle from north is therefore given by

$$\tan\alpha = \frac{H_r}{H}$$

from which m/H can be found. Once both the product and the quotient of m and H are known, each can be found separately and the absolute measurement task is complete. For the highest accuracy it is necessary to consider further parameters (Laursen and Olsen, 1971) such as torsion of the suspension fiber, time changes in H, more accurate field patterns, and interactions of the axial magnet and compass needle, etc.

5.04.2.2.1.(iii) Quasi-Absolute measurement of H and Z using the QHM and BMZ The QHM was invented by Lacour in 1934, it was modified and developed by Lamont, and a Soviet version was developed at IZMIRAN. Although not strictly fulfilling the requirements of an IMS, the QHM provided valuable measurements in many observatories, particularly before the advent of the proton magnetometer. Its robustness, compactness, and practical design ensured its use until the 1980s, and the QHM is still used in some parts of the world.

An axial magnet, of moment m, suspended by a quartz fiber, is able to swing in the horizontal plane. The upper suspension point of the fiber is rotated until the mechanical torsion of the fiber equals exactly 360°, using the magnetic moment of the horizontal field on the magnet for detaining it. A total rotation of $360 + \theta$, where θ is the angle through which the magnet itself has turned is read from a graduated horizontal disk. If the torsion constant, τ, of the fiber is known, the horizontal component of the field, H, can be found by equating the torques on the magnet due to the fiber and due to H (Laursen and Olsen, 1971):

$$H = \frac{360\,\tau}{m \sin\theta}$$

Measurements made with a QHM are only quasi-absolute because they depend on recalibration of the torsion constant at 1–2 year intervals. The elastic properties of the quartz fiber and the magnetic moment of the magnet are temperature dependent, necessitating a temperature correction to each measurement made with the QHM.

The key part of the BMZ is a magnet balanced on knife edges so it is free to pivot about a horizontal axis. The vertical component of the ambient field is cancelled by a large magnet above the housing and fine adjustment of the position of a smaller magnet below the housing. The null position of the pivoted magnet is achieved by monitoring, through a telescope, the reflection of a light beam from a mirror mounted on the magnet.

Like the QHM, the BMZ requires careful calibration, and measurements made with it must be corrected for temperature, particularly of the upper magnet. It is therefore also a 'quasi-absolute' instrument.

5.04.2.2.1.(iv) Absolute measurements with the proton vector magnetometer (PVM) Although the proton precision magnetometer (PPM) is a scalar instrument, meaning it measures only the magnitude of the magnetic field vector, irrespective of direction (Section 5.04.1.3), its accuracy and simplicity of use have motivated researchers to devise ways in which it can be used for field component measurements as well. The PPM is placed inside a system of coils, by means of which known, auxiliary horizontal or vertical components can be added to the ambient geomagnetic field (**Figure 10**). Knowing the

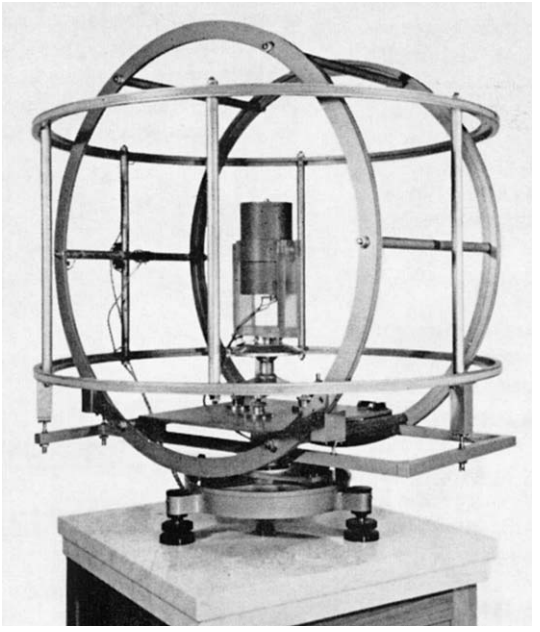

Figure 10 A proton vector magnetometer, able to make absolute measurements of the horizontal and vertical component of the geomagnetic field. Note the special adjustments to individually level and orient the two sets of Helmholtz coils.

direction of the auxiliary field means that, in principle, information on the direction of the ambient field can be obtained from a comparison of PPM measurements made with and without the auxiliary field. A current generator able to set the coil current to about 1 part in 10^6 is required for results aiming at the 0.1 nT level of accuracy.

Considering the triangle defined by the ambient geomagnetic field vector, **F**, and an applied horizontal auxiliary field, $\mathbf{F}_a$(**Figure 11**), the magnitude of the resultant vector, $\mathbf{F}_r$ which will be measured by the proton magnetometer is given by

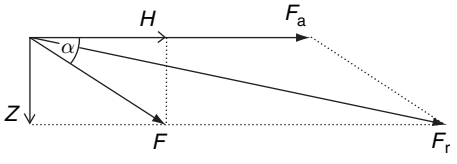

Figure 11 Diagram illustrating the principles of the PVM absolute component measurement. F is the ambient magnetic field vector, with horizontal and vertical components H and Z, respectively; F_a is the additional field (in this case horizontal) supplied by the auxiliary coil system. F_r is the total resultant field. See text for discussion.

$$F_r^2 = F^2 + F_a^2 + 2FF_a\cos\alpha = F^2 + F_a^2 + 2F_aH$$

where $H = F\cos\alpha$ is the horizontal component of **F**, that is, the component in the direction of the auxiliary field. Direct use of this equation to find H requires knowledge of F and F_a. F is obtained simply from a PPM measurement with no auxiliary field. F_a however, requires accurate calibration of the coil system which is difficult to achieve to the same accuracy. Several methods of obtaining the horizontal H and vertical Z component of the geomagnetic field that avoid the need for this have been described. These generally involve switching the direction of an accurately constant auxiliary field, increasing F_a in multiples (de Vuyst and Hus, 1966), or varying F_a to minimize F_r (Hurwitz and Nelson, 1960).

The crucial aspect of the proton vector magnetometer (PVM) set-up is the need for accurate spatial orientation of the current carrying coils – which can be quite bulky. The magnetic axes should be oriented exactly along the local vertical or horizontally towards the magnetic cardinal directions (**Figure 10**). Orienting the mechanical symmetry axis of the coils often is not enough, and special manipulations must be performed to compensate for the non-coincidence of the magnetic and mechanical axes. Ultimately, a leveling precision of 3 arcsec must be achieved for H accuracy measurements of 0.7 nT in a typical mid-latitude geomagnetic field.

Another drawback of the PVM method is that it needs quiet field conditions – the measurements involve several steps, during which the field should remain steady. It is therefore difficult to implement in high-latitude observatories, subject to frequent and large geomagnetic variations.

The PVM was being superseded by the DIflux (see below) at the end of the twentieth century, but it may well be revived again in the future; with smaller and faster proton sensors and compact coil systems available, it can be installed on the telescope of a nonmagnetic theodolite, alleviating the orientation and leveling problem (Sapunov *et al.*, 2006).

5.04.2.2.2 Measuring the angular orientation of the geomagnetic field

5.04.2.2.2.(i) Declinometer The magnetic declination is the angle between the geodetic and magnetic meridian planes. The magnetic meridian plane can be defined as the vertical plane containing the magnetic axis of a magnet suspended so as to move freely in the horizontal plane.

These definitions lead to a straightforward principle for the absolute measurement of the magnetic declination – measuring the azimuth of the magnetic axis of a freely horizontally suspended magnet.

This conceptually simple procedure is not easy to realize, especially if accuracies of the order of the arc second are to be attained. Technical solutions (Laursen and Olsen, 1971) have to be found in order to suspend the magnet freely in a horizontal plane, to observe the orientation of its axis, and to measure angles between the meridians with the required accuracy, and to eliminate rheological effects, such as hysteresis and anelasticity, in the suspension fiber.

As a result the declinometer, or magnetic theodolite, was developed. It consists of a torsion head suspending the magnet in the required position. This head is mounted together with a telescope on a vertical-axis rotation table, indexed by a graduated circle. The telescope performs the dual task of observing a distant target with known azimuth, and to collimate on the magnet-end mirror. This mirror is mounted on the magnet with its optical plane normal to the magnet's magnetic axis. Angles can typically be obtained to an accuracy of 0.1 arcmin or even 1 arcsec.

The declinometer has been superseded nowadays by the DIflux, which offers operational simplification and an increased accuracy (see below).

5.04.2.2.2.(ii) Inclinometer Historically the first inclinometer – the 'dip circle' – was built as a needle magnet free to move around a horizontal E–W axis. A vertical graduated circle, centered on this axis, allowed measurement of the angular position of the magnet in the magnetic meridian, and this gave the magnetic inclination. Despite clever procedures to eliminate the effect of gravity and to minimize collimation errors, the dip circle never achieved the high accuracy required in a magnetic observatory.

Another inclinometer, known as the 'earth inductor' with better metrological characteristics was introduced at the beginning of the twentieth century. This device was the first in geomagnetic observatories to use an 'electronic' sensor as a null indicator. This apparatus uses the emf induced by the geomagnetic field in a coil rapidly spinning about one of its diameters, as an indicator of its orientation relative to the field vector. When the coil's spin axis is collinear with the field, no emf is generated. Small deviations from colinearity can be amplified with high gain to give a restoring signal limited only by system noise. The early amplifiers were galvanometers deflecting light spots, and the rectification of the small alternating emf's by mechanical rotating contacts was not always satisfactory. Parasitic DC offsets were eliminated by observation with the coil oriented in symmetrical positions. Play in the bearings of the spin axis was probably the main limiting factor of accuracy. A modern version of the earth inductor, the Turbomag (Schnegg and Fischer, 1991), uses hydrodynamic bearings and contactless transfer of the emf to the observer.

In principle, the earth inductor could have been used for declination measurement also but, apart from the Turbomag, this did not occur probably because the addition of a telescope would have made it too bulky. Nevertheless, the earth inductor paved the way for the development of the DIflux which will be examined below.

5.04.2.2.2.(iii) DIflux (DIM) For angular measurements, state-of-the-art instrumentation is now provided by a device called the 'DIflux' or declination/inclination magnetometer (DIM), which is assembled from a nonmagnetic theodolite and a fluxgate sensor mounted on a telescope. The magnetic axis of the fluxgate should be parallel to the optical axis of the telescope (**Figure 12**). The DIflux was first described by Tenani (1941). By the 1970s it had reached an advanced level of development (Meyer and Voppel, 1954; Serson and Hannaford, 1956; Trigg, 1970). Further developments by Daniel Gilbert, Jacques Bitterly, and Jean-Michel Cantin at IPG Paris have resulted in levels of precision,

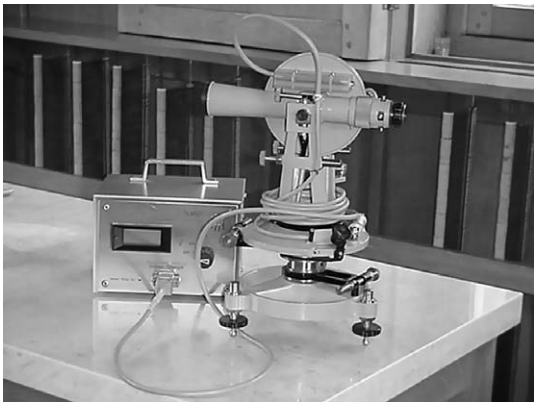

Figure 12 A DIflux with its electronic console. This instrument is able to measure the geomagnetic inclination and declination. A single-axis fluxgate sensor is located on top of the theodolite's telescope so that the magnetic axis is parallel to the telescope optical axis.

accuracy, resolution, and ease of use that make it currently the preferred instrument for angular measurements both in the observatory and in the field (Bitterly *et al.*, 1984).

The measurement principle takes advantages of the directional properties of the fluxgate; only the projection of the geomagnetic vector on the fluxgate axis is measured. Using the theodolite, an observer can orient the fluxgate in any direction while monitoring its electronic output and keeping track of its orientation in space via the theodolite's graduated horizontal and vertical circles. Usually, the preferred orientations of the fluxgate correspond to its magnetic axis being perpendicular to the geomagnetic field vector; then, the electronic output is close to zero and a high signal amplifier gain can be applied. The declination measurement involves setting-up the telescope axis into the horizontal plane, with the fluxgate axis normal to the magnetic meridian, so as to obtain a null from the fluxgate electronics. For inclination, the horizontal axis of the theodolite is set normal to the geomagnetic meridian and a fluxgate null is again sought. The essence of the measurement is therefore to determine the orientation of a plane perpendicular to the geomagnetic field vector. The plane's orientation is defined by two orthogonal lines in it, one horizontal and one in the geomagnetic meridian.

In practice a series of four measurements for declination and two for inclination (Lauridsen, 1985) is usually made, to minimize errors. The accuracy of a measurement with a DIflux depends on the accuracy and the magnetic cleanliness of the theodolite. The accuracy of a theodolite can be assessed by appropriate measurement techniques (Deumlich, 1980) and the magnetic cleanliness can also be measured and sometimes corrected to be below a given limit. We can therefore classify the 'clean' DIflux as an absolute instrument. In that sense it belongs to the family of the IMSs as defined in Section 5.04.2.2.

Instrumental errors originate in imperfect parallelism of optical and magnetic axes of telescope and fluxgate sensor, and in residual magnetization of the fluxgate core. Since the geomagnetic field may vary during a series of measurements, an external D and I variometer must keep track of this change if we want to have a truly absolute spot measurement of D or I. The proven best way to do that is by measuring the baseline of the variometer with the four D and two I measurements of the DIflux.

The DIflux performs well in equatorial and midlatitude zones. The DIflux can also be operated in polar regions where the geomagnetic field vector is close to vertical. However, because the horizontal components are small (<2000 nT), horizontal angular measurements are not convenient there. Direct measurements of the small X and Y components using the fluxgate, properly oriented along geodetic North–South and East–West and with a scale factor directly determined with a proton magnetometer, are preferred (Gilbert *et al.*, 1988).

A problem facing the DIflux nowadays is in the supply of nonmagnetic theodolites. Therefore, the future is uncertain for the DIflux, and the development and marketing of a fully automatic DIflux would bring a solution (Section 5.04.2.4).

5.04.2.2.3 Variation measurements: variometers

In the present context, a variometer is a magnetometer designed to monitor the time changes of a magnetic field component relative to a fixed baseline. The variometers installed in magnetic observatories measure a variety of vectorial components depending upon the reference system used (see above). The most popular orientations are D, H, Z and X, Y, Z. The latter ensures that the variometer orientation will not have to be modified over time due to secular variation of the geomagnetic field.

The essential quality of a variometer is its ability to maintain a stable baseline between two absolute measurements. This means that it should have a very low drift over time and a very small dependence on temperature, pressure, humidity, etc. A variometer should respond to variations in the selected component only: contamination from other components must be eliminated. This often reduces to ensuring the correct orientation of the sensors. In the case of multiaxis sensors, the quality may be measured by the orthogonality of the set-up being close to perfection. The quality of the installation of the variometer must also to be considered: tilts or rotation of the pillar on which the variometer is installed will appear in the variometer's recording as a component variation.

5.04.2.2.3.(i) Classical magnet-based instruments

Recording variometers originally used suspended magnets and photographic recording. They provided, and still do provide, much of the geomagnetic data going to the magnetic observatories databanks. Being suspended they are not

affected by pillar tilt and being mechanical they do not suffer from electrical noise; however, their sensitivity and dynamic range are limited, and they are now costly to maintain.

5.04.2.2.3.(ii) Digital variometers Many observatories now have electronic variometers with a digital data acquisition system that may be uploaded directly to data centers. Introduced from the late 1960s, electronic variometers were expected to obviate the disadvantages of photographic variometers, namely the lack of dynamic range and sensitivity. It was also felt that they would be more economical, being easier to install and offering the possibility of unattended operation. However, the introduction of these new instruments has come with some drawbacks, as the electronic components are less robust against electromagnetic/electrical disturbances than the mechanical configuration of suspended magnets. Many digital variometer installations have been lost as a result of a lightning strike on the observatory. Also, as the sensors are no longer suspended, the new instruments are more sensitive to tilt. The acquisition system samples an analog signal at discrete intervals, so low-pass filtering at at least twice the Nyquist frequency is necessary to avoid aliasing. This proves to be a problem with sensors such as proton magnetometers.

The sensors of digital variometers presently in use in magnetic observatories are mainly fluxgates (Rasmussen, 1990) or scalar magnetometers surrounded by backing-off coils (Alldredge and Saldukas, 1964; GEM website). Suspended (hanging or taut-fiber) magnets are still used in some designs, notably Bobrov, with attitude-restoring feedback coils (Jankowski *et al.*, 1984). As the necessary filtering cannot be applied to PPMs and as they are too slow to measure the high-frequency portion of the geomagnetic spectrum, OPMs should be used for variometric multiaxis recording (Gravrand *et al.*, 2001; Alexandrov *et al.*, 2004).

Perhaps the biggest problem with currently used variometers is their vulnerability to temperature variations. An instrument with a temperature coefficient of $0.1 - 1.0\,\mathrm{nT\,K^{-1}}$, in an environment that undergoes temperature variations of up to 10 K may result in errors of 10 nT, or 30% of the typical daily variation in a component of the field. Clearly it is desirable to use variometers with low temperature coefficients to minimize temperature changes and to correct for temperature variation wherever possible.

5.04.2.2.4 Instrument certification and calibration

The community of geomagnetic observatories has always been concerned to set standards in order to maintain the quality of geomagnetic data produced and collated.

Not only should metrological standards be examined, but also other parameters that affect instrument performance, for example, temperature coefficients of variometers should also be monitored.

5.04.2.2.4.(i) Variometer certification The factors that affect a variometer's certification can in principle be deduced from an inspection of their baselines, which are obtained from measurements with absolute instruments. This is true for instrumental parameters like long-term stability, orthogonality, and scale factor accuracy. However, except for scalar measurements, the diurnal effects of temperature cannot be detected unless half a dozen or so absolute measurements are taken per day. This is not yet routinely possible. Therefore, the certification of a variometer is best obtained by intercomparison with a master variometer. This has been often realized at the 'Workshops on Geomagnetic Observatory Instruments, Data Acquisition and Processing' organized by International Association of Geomagnetism and Aeronomy (IAGA) every other year since 1987. Even better is the continuous running of two variometers set-up in slightly different conditions at the same observatory.

Some variometers have sufficient dynamic range for measuring the full field in all three axes. It is then possible to perform an experiment where the measuring variometer is oriented in various directions with respect to the field while a scalar magnetometer is recording close by. One may then equate the calculated modulus obtained from the variometer measurements to a reading taken from the scalar magnetometer. This will lead to a redundant set of equations from which a rotation matrix describing the errors of the variometer (orthogonality and scale factors) can be extracted. Subsequent correction of the variometer with the matrix operator will then provide a variometer reading with quasi-PPM accuracy (Merayo *et al.*, 2000; Gravrand *et al.*, 2001) for whatever orientation in space.

5.04.2.2.4.(ii) Calibration of scalar magnetometers Most scalar magnetometers do not in principle need to be calibrated, since their operation is traceable to fundamental physical constants. This is particularly

true for the PPM, where, in addition to an accurate, precise value of the proton gyromagnetic ratio, only calibration of the frequency reference is required. The situation is more complicated for the absolute OPMs where several physical constants are required. Some, like the Landé factors for K, have not been determined to a high degree of precision, and these dominate the error budget of the OPM. Instrumental effects like light shifts and phase errors in electronic signals also need to be taken into account. The result of this is that scalar OPMs are quoted with varying and sometimes conflicting accuracies. A consensus exists, however, that the agreement between PPMs and OPMs is at the 0.1 nT level in a 50 000 nT field. This corresponds to 2 ppm. Two techniques exist for inter-comparing scalar magnetometers. The magnetometer exchange procedure (Rasson, 2005) is carried out in the ambient field and will therefore only give a difference for that value. The other technique uses artificial fields in a field stabilizer (Shifrin *et al.*, 2000) and will provide inter-comparison over an extended range of fields.

5.04.2.2.4.(iii) Certification of DIflux (DIM) Since the DIflux performs angle measurements, we cannot strictly speak of absolute measurements, as there need not exist a standard for angles. Nevertheless, a critical assessment of the accuracy can be made by investigating the angular accuracy (Deumlich, 1980) and the magnetic hygiene of the fluxgate-bearing theodolite.

Provided those two checks give results that comply with specified levels of accuracy, the DIflux can be declared certified. Note, however, that the two are not independent; an uncertainty (of, say 0.1 nT) in the fluxgate readings results in a corresponding uncertainty in declination or inclination ($\sim$1 arcsecond in declination, in a horizontal field of 20 000 nT).

Another frequently used procedure for certifying DIfluxes is through participation in the 'Workshops on Geomagnetic Observatory Instruments, Data Acquisition and Processing' already mentioned. One of the main activities in this kind of international workshop is the measurement of the baseline of a stable onsite variometer by all the participating DIfluxes. As all devices should measure the same constant baselines, any deviation of an instrument indicates a fault either in the angle reading or in the magnetic hygiene of the DIflux.

5.04.2.2.5 Obtaining definitive absolute data

As mentioned above, definitive geomagnetic field data at a magnetic observatory are obtained from two streams of data: variometric measurements and absolute measurements. Merging the two data sets is not a trivial or unique procedure and it requires all the skill of the observatory staff to result in an accurate time-series, giving the absolute value of the vector at each variometric sample. Important factors that impact on the procedure are

1. baseline stability of the variometer,
2. accuracy of the absolute measurements,
3. frequency and regularity of absolute measurements, and
4. data gaps in the variometer time-series.

Items (1) and (2) have been dealt with in earlier sections. Items (3) and (4) lead directly to the main problem facing definitive data production – the adoption of baselines.

In the simplest case of spherical coordinates for both absolute and variometric data, we have the fundamental magnetic observatory relationships between absolute (D, I, F) and variometric measurements ($\mathrm{d}D$, $\mathrm{d}I$, $\mathrm{d}F$):

$$D = D_0 + \mathrm{d}D$$

$$I = I_0 + \mathrm{d}I$$

$$F = F_0 + \mathrm{d}F$$

The subscript 0 indicates the baseline. In an ideal world with perfect instruments, the baselines would be merely constants, but instrumental drift due to temperature effects, mechanical creep, and pillar instabilities make the baselines wander in an unpredictable way. Values of the baselines D_0, I_0, and F_0, which are known every time an absolute measurement is taken (say one per week), vary slightly with time. But a value of the baselines must be available for every sample taken by the variometer. Adopting a baseline therefore entails the interpolation of the baseline from a sampling at one per week to the variometer sampling typically at one per minute. This can be conveniently done by fitting a mathematical expression like a low-order polynomial or a spline function to the baseline data sampled at one per week (**Figure 13**).

A final quality control should be made when the definitive data series has been obtained, in order to ensure that no errors resulting from faulty data processing software have occurred. A simple way of

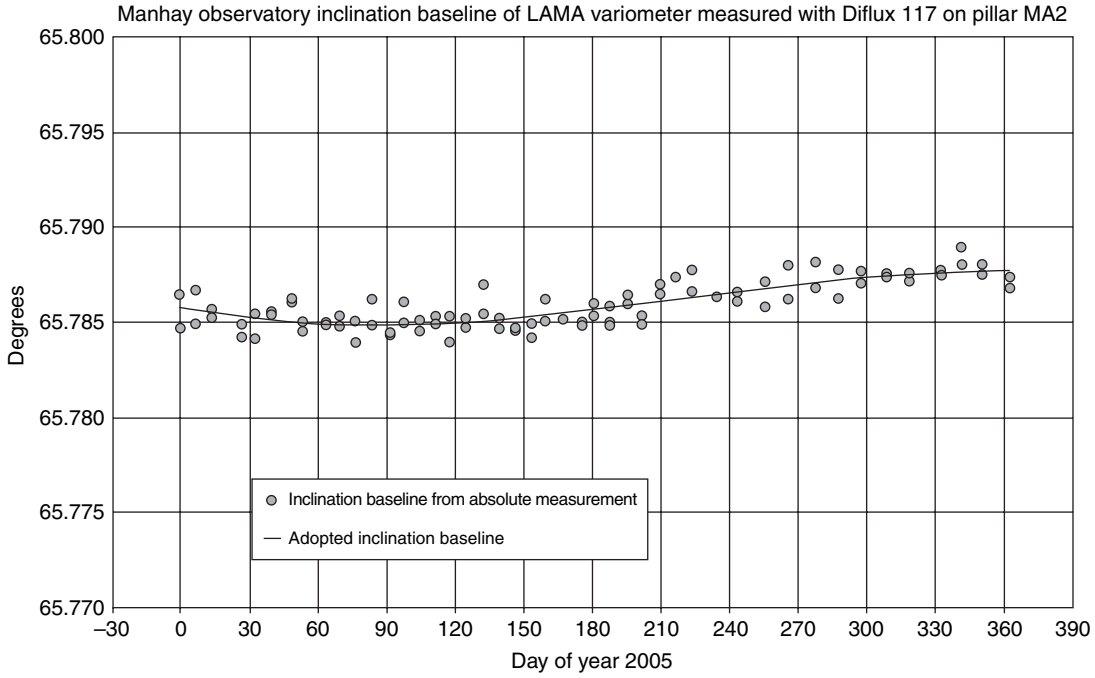

Figure 13 Illustration of the baseline (here measuring the magnetic inclination, *I*) in the MAB observatory for a whole year. Note the sensitive vertical scale of 0.005°/division, corresponding to about 5 nT/div. in *Z*. In this case, a third-order polynomial, fit by a least-squares procedure, has been adopted as a smooth baseline. The differences between measured and adopted baseline are of the order of 0.001°.

doing this is to go back to the absolute measurements performed during the data time series under consideration: the absolute spot measurements and the definitive data should agree. The adopted baselines should also agree with the absolute data baseline determinations.

5.04.2.3 The INTERMAGNET Magnetic Observatory Network

The International Real-time Magnetic Observatory Network (INTERMAGNET) was created in order to establish a worldwide cooperation of digital magnetic observatories. The networked observatories agreed to adopt modern standard specifications for measuring and data-logging equipment and to make data available in close to real time. Moreover, INTERMAGNET extends technical support for maintaining and upgrading existing magnetic observatories as well as for establishing new ones.

INTERMAGNET defines standards for the measurement and recording of the geomagnetic field, considering the state of the art. INTERMAGNET is constituted from existing groups who undertake geomagnetic observatory measurement. The acronym IMO is used to indicate an INTERMAGNET magnetic observatory (Green *et al.*, 1998).

Presently, INTERMAGNET data consists of time series of the geomagnetic vector, sampled at the round minute and carefully filtered to avoid aliasing effects. This data, collected at the IMOs represented on **Figure 14** (full squares), is continuously available from the geomagnetic information nodes (GINs, crossed circles) within 72 h. The data come in different accuracies and delays: reported (as recorded – near real-time), adjusted (corrected for artificial spikes and jumps), and definitive (reduced to baseline so that they have absolute accuracy). The latter are made available a few months after the end of each year at the earliest and finally with the production of a yearly CD-ROM.

People needing real-time data use the reported or adjusted data, available from the GINs in daily ASCII files either in INTERMAGNET imfv1.22 or IAGA 2002 format (e-mail request or ftp).

Access to recent definitive data is through the website (INTERMAGNET website). Older data are available on the CD-ROMs and at the website. Definitive data come in monthly files in a dedicated binary code. Multiplatform Java-based browsers are

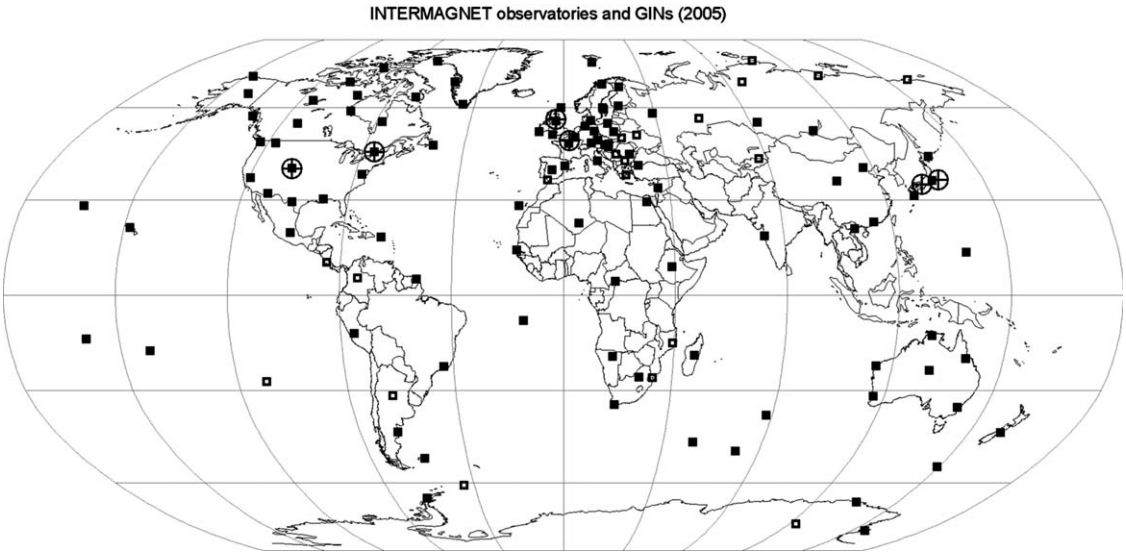

Figure 14 INTERMAGNET magnetic observatories as full squares and geomagnetic information nodes (GIN) as crossed circles representing the global coverage of the network in 2005. Open squares indicate some possible future IMOs (Robinson–Sterling pseudo-cylindrical projection).

available for easy perusal, inspection, and format conversion.

The data are available at no cost for *bona fide* scientific users. If any commercial aspects are involved, the user should contact the IMO directly for a financial arrangement.

All practical details about the data and their access are available from the website where the Technical Manual is also available for download.

5.04.2.4 Fully Automatic Magnetic Observatories

If the globe is one day to be covered by a uniform distribution of magnetic observatories separated by no more than say 2000 km, it will be necessary to install some in very remote and hard-to-access places such as on the deep sea-bottom (Chave *et al.*, 1995), on remote islands, and in inhospitable deserts. This is unlikely to be accomplished with classical observatories running the traditional way. Therefore, there is a need for fully automatic magnetic observatories.

Technology already exists for some geomagnetic measurements to be executed automatically.

1. Variometers are able to work for long time spans in an automatic mode, provided their baselines are regularly checked by absolute measurements. Only severe (>1 degree of arc) rotational motions need to be monitored, but this task can also be performed automatically.
2. Provided electrical power is available, the magnitude of the geomagnetic field can be measured easily and absolutely by a scalar PPM in an unattended way for long periods. This is because a PPM does not require orientation or mechanical or electronic adjustments in order to produce absolute data.

Two approaches have been followed for obtaining automation of observatories:

1. The first is to set up a very precise (in terms of scale factor and orthogonality), stable, and temperature-insensitive variometer in a fixed orientation, in a clean geomagnetic environment. Then, baseline checks as far apart as 1 year may be acceptable (Gravrand *et al.*, 2001).
2. The second approach is to automate the full absolute measurement protocol, which comes down to automating the DIflux measurements, since the modulus can be measured automatically by a PPM (Rasson, 1996; van Loo and Rasson, 2006).

Some magnetometer set-ups flown on satellites have already reached a level of quality in baseline stability and precise orientation with respect to the stars such that they can truly be considered as automatic magnetic observatories in orbit (Nielsen *et al.*, 1995).

5.04.2.5 Magnetic Repeat Station Surveys

From the point of view of secular variation measurement, a magnetic repeat station plays the role of a miniature magnetic observatory, with elementary infrastructure and an observation schedule reduced to one measurement session every few years. This section on repeat surveys is therefore included with magnetic observatories, although, we are strictly dealing with a survey operation.

Instrumentation used during repeat surveys is nowadays similar to that used in an observatory. As pillars are seldom possible in the field, a nonmagnetic tripod is often used for setting up the DIflux and PPM.

For declination measurement, a device for measuring the geodetic azimuth of a distant target is necessary, at least when the repeat station is first installed. Provided there is sunshine, a theodolite with a solar filter is useful for this since then the astronomically known position of the sun can provide the target's azimuth (Rasson, 2005). Often the DIflux used for the magnetic measurements can be used for the sun sightings.

If the sun is not visible, a gyrotheodolite can be used. The true North direction is then obtained by sensing the direction of Earth's rotation axis by way of a suspended gyroscope. Differential GPS is also a possibility, but needs occupation of both the repeat station and target by the measuring team. A good topographic map may also help obtain the azimuth of the target.

When a measurement of the magnetic field is performed at a repeat station, it is a spot value measurement which can be notably different from the mean value at the site. Mean values, normally taken over one full year, are usually required in a repeat survey.

The difficulty then is to obtain this mean from a single measurement session at the station. Several procedures have been designed, where the spot measurement is linked in some way to a nearby observatory, where the annual mean is known. All methods try to eliminate or mitigate the main source of error in this linkage – differential field variations, mainly diurnal, between station and observatory.

The magnetic field variations at the repeat station site are recorded for a few days with a dedicated variometer. The spot value measurements are then used to establish the baselines of the onsite variometer. Several daily means can then be computed with absolute accuracy. Subtracting the corresponding daily means at the nearby observatory will then produce the difference in field elements Station – Observatory. The annual mean can then be obtained by simple addition.

The onsite spot value measurements are used to compute the baselines of a nearby magnetic observatory variometer. These baselines are subtracted from the baselines obtained from absolute measurements made at the observatory and give the difference in field elements Station – Observatory. The annual mean can then be obtained by simple addition. This method supposes that the (diurnal) variations are similar at both the station and observatory, at the time of the spot measurements. This method hence works well for a close-by observatory or for measurements taken when the diurnal variation at both places is small: dusk, sunrise, or sunset.

Onsite spot value measurements are performed at night, when the diurnal variation is negligible. With such a measurement, it is considered that an undisturbed field is obtained and that it reflects truly the secular variation. Direct comparison with a nearby observatory, also situated in the dusk zone, is allowed.

Obviously, quiet magnetic conditions are required for accurate results. IAGA has published a detailed guide for magnetic repeat survey practice (Newitt *et al.*, 1996), where the reader can find all the necessary practical information to set-up a magnetic repeat station network.

5.04.2.6 Products and Services Magnetic Observatories Can Provide

As mentioned in the introduction, magnetic observatories have a very practical purpose, as well as contributing to our knowledge of magnetic field of internal and external origin, and our understanding of Earth's deep interior. Navigation is a notable practical application, but there are also others like space weather, metrology, and magnetic signature determination. **Table 2** is an attempt to list, as completely as possible, the products and services a magnetic observatory is able to provide.

5.04.3 Magnetic Surveys for Geological Exploration

The general aim of a magnetic survey is to improve the resolution of the IGRF through a greater sampling density and/or frequency. This might be at a

Table 2 Products and services provided by geomagnetic observatories

Products/Services	Users
Value of the magnetic declination for various epochs and/or locations	Topographic and cartographic services, oil and gas companies, harbours, air traffic services, airports, military
Value of the secular variation of the magnetic declination	Topographic and cartographic services
International Geomagnetic Reference Field generation, magnetic charts	Topography, aeronautical mapping and safety services, maritime coastal and fluvial mapping, military
Time series of geomagnetic field	Aeromagnetic and marine surveyors, high-precision directional drilling for gas and oil, Earth orbiting satellite safety, space weather, military
Geomagnetically induced currents: nowcasting and forecasting	National and international electricity mains providers and operators, other cable network operators
High precision *in situ* measurements of the magnetic declination or other components	Airports, military, topography
Set-up and certification of compass roses (aircraft compass calibration and compensation facility)	Airports
Measurement of magnetic orientation of aircraft runways	Airports
Measurement of magnetic signatures of equipment, mechanical or electronic components	Manufacturers of magnetic resonance, military
Calibration and check of magnetic compasses	Leisure equipment industry, geometers, surveyors, antenna orientation for satellite TV
EM radiation standards of safety and security, Electrosmog	Government public safety agencies
Keeping of the magnetic induction metrological standards in the Earth's field range	Metrological community

regional level to better depict high-order features of the main field. Such low-density regional surveys are often repeated (reoccupying the same sites as far as possible) at 5–10 year intervals to monitor secular variation, and are discussed in Section 5.04.2.5.

At a more local level, surveys may be designed to resolve crustal magnetic anomalies (e.g., at a scale of 1:250 000), ore deposits or buried volcanic features (e.g., 1:20 000), or may be even smaller-scale investigations of sites of archaeological or environmental interest (e.g., 1:1000). Such surveys may be conducted over land, sea, or from the air. Usually only scalar (intensity) measurements are made but at fractional nT sensitivity. Absolute accuracy is of relatively little importance so such surveys are seldom rigorously linked to observatories, but meticulous care must be taken with the correction of temporal variations in the field. PPMs are ideally suited to local survey work on the ground, being inexpensive, quick and easy to use, and readily portable. Airborne surveys, of which many millions of line-km are flown each year, now usually employ cesium vapor magnetometers. At sea, a proton magnetometer may be towed behind a survey ship.

The main problem with making three-dimensional (3-D) vector measurements at sea and from the air is the lack of a stable reference frame. Accurate navigation and determination of the vertical are essential and these factors ultimately limit the accuracy of results. A trade-off must usually be made between accuracy, which is improved by averaging over a number of measurements, and spatial resolution, which is compromised by such averaging. Most applied magnetic surveying therefore measures only the scalar magnitude of the total geomagnetic field, including the contribution of local anomalies.

5.04.3.1 Mapping Magnetic Anomalies

Local magnetic disturbances attributable to certain types of rock have long been recognized. Where these rock types are of economic importance, their magnetic effect may be used as a means of detecting them, even where the rocks are at depth or concealed below soil cover or overburden. Instrumentation to measure such local variations or 'anomalies' in the geomagnetic field in exploration mode – that is, carrying out a survey by making observations repeatedly in a pattern of observation points distributed systematically over a given search area – evolved rapidly during the second half of the twentieth

century and eventually became the basis of an airborne geophysical survey industry that now sets the pace in geological reconnaissance worldwide. By comparison, even with the aid of aerial photographs and satellite imagery, traditional geological mapping on the ground is prohibitively slow and expensive in many large areas of the world remote from modern infrastructure. Aeromagnetic surveys enable the groundwork to be done more selectively and efficiently and therefore play a significant role in mineral and petroleum exploration (Reeves, 2007).

Ground-based magnetometer surveys are still used to 'follow-up' selected anomalies mapped in airborne surveys in more detail, prior to drilling, etc., and have developed into specialized systems for particular localized applications such as engineering site investigations, detection of unexploded ordnance (UXO), and archeology. At sea, magnetometers are often towed behind marine research vessels. While this is slow and expensive on its own, cruises carried out primarily for other purposes can simultaneously conduct magnetometer traverses at little additional cost. Hence, applications of surveying with magnetometers are to be found in the air, on the ground, and at sea.

In recent decades essentially all magnetometers employed for work of this type have been electronic magnetometers that measure only the scalar magnitude of the magnetic field, regardless of its direction. This eliminates any need for precise orientational reference and so simplifies survey practice. After correction for temporal variations and subtraction of an appropriate IGRF, the anomaly recorded is then the component of the local-source anomaly in the direction of the main geomagnetic field (see Section 5.04.3.2). This is universally understood as the 'total field anomaly' in exploration magnetometry. Some increase in surveys that measure magnetic field gradients (either vertically or in a specified horizontal direction) has occurred in recent years. Advantages include improved resolution of near-surface sources. Usually gradients are measured by subtraction of the readings from two scalar sensors separated by a small distance.

Magnetometers have also been mounted in earth-orbiting satellites, most successfully in the OERSTED and CHAMP satellites of recent years. However, at satellite altitudes, the amplitudes of anomalies attributable to lithospheric sources are no more than about 30 nT and the resolution of detail no better than the altitude of the satellite, setting a rather coarse limit of 300–400 km for the scale of geological detail that is resolvable. (Chapter 5.06).

The production of magnetic anomaly maps and images in general has evolved rapidly in the last 50 years as a result of (1) improved, now exclusively electronic, magnetometer and ancillary instrumentation; (2) computer software and hardware to gather and process large volumes of data; and (3) image-processing techniques to display results in image format that lead to a largely intuitive appreciation of the geological information content.

5.04.3.2 The Origin of Magnetic Anomalies

While most rocks are only very weakly magnetic, any rock containing a quantity of a ferrimagnetic mineral such as magnetite distributed through its mineral fabric may display magnetic properties. The magnetization may be a long-lived, virtually permanent feature of the rock, having its origins in the geological history of the rock itself – for example, when it cooled through its Curie temperature (see Section 5.04.4) – and described as a remanent magnetization M_r with a direction that is, in general, unknown. On the other hand, the rock may have a certain magnetic (volume) susceptibility χ, in which case it will acquire an induced magnetization simply due to its presence in the present-day geomagnetic field. Such induced magnetization, M_i , is proportional to the product of the magnetic susceptibility and the inducing field and will be in the direction of the inducing field:

$$M_i = \chi F$$

Both types of magnetization may be present and their relative importance is quantified by the Koenigsberger ratio, Q:

$$Q = M_r / M_i$$

Considering, for simplicity, a single body of magnetized rock isolated within a large volume of nonmagnetic country rock, the magnetic rock body will possess a magnetic field that will be evident within its immediate vicinity and over a certain volume of space thereabout. This will be the case whether the magnetization of the rock is induced, remanent, or a combination of both. A scalar magnetometer measuring the total field strength within the vicinity of this body will experience the magnitude of the vector sum of the geomagnetic field and the local field due to the magnetic rock body (**Figures 15** and **16**). In the vast majority of cases, the latter is found to

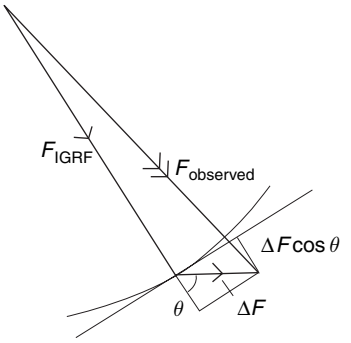

Figure 15 By convention, the 'total field anomaly' is the difference between the observed total field value, $|\mathbf{F}_{observed}|$, and the geomagnetic field value predicted by the IGRF, $|\mathbf{F}_{IGRF}|$. As long as the local anomaly is much smaller than the geomagnetic field, the total field anomaly so defined is a close approximation to the component of the magnetic field of the local source in the direction of the geomagnetic field, $\Delta F \cos\theta$.

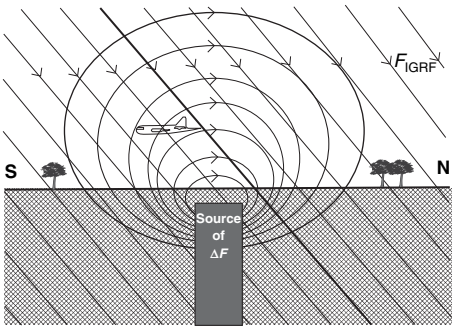

Figure 16 In the vicinity of a magnetized rock body, the passing magnetometer experiences the influence of both the ambient geomagnetic field, modeled by the IGRF, $\mathbf{F}_{IGRF}$, and a local-source field, $\Delta\mathbf{F}$.

be at least two orders of magnitude smaller than the former. The former is predictable at any given location from models of the geomagnetic field – the model provided by the IGRF (IGRF-10, website) being the one used almost universally in magnetic surveying.

What is measured by the surveying magnetometer is the vector sum of the global and local contributions and, by convention, the so-called 'total field magnetic anomaly' is what is left when the magnitude of the predicted field (IGRF) is subtracted from the observed field magnitude, once temporal variations have been eliminated. Figure 15 illustrates that, to a close approximation, the anomaly defined as above is the component of the local-source field in the direction of the geomagnetic field. As a result of the

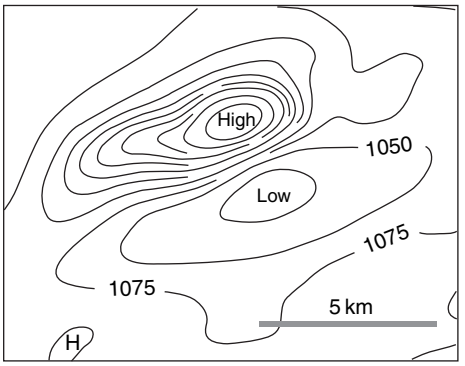

Figure 17 A typical aeromagnetic anomaly pattern in the vicinity of a single, compact and isolated geological source, showing both positive and negative parts (southern hemisphere). Contour interval 25 nT.

variations in the direction of the local magnetic field around the rock body, there will, in general, be areas where the local field tends to reinforce the geomagnetic field and others where it tends to oppose it. It follows that, when mapped over a given area around the body or 'source', some areas will show a positive magnetic anomaly value while others will show a negative one. A typical anomaly over a simple compact body is shown in Figure 17.

In general, the shape of any magnetic anomaly is a function of many factors, including the geomagnetic inclination and declination at the survey locality, the resultant direction of total (induced + remanent) magnetization within the body, the geometry of the body itself, its attitude in the ground (dip and strike), and the strength of its magnetization.

The shapes of anomalies over bodies of simple geometrical shape approximating to common geological bodies may be calculated directly, a process known as forward modeling. Such forward models help in interpreting the sources of observed anomalies in terms of the possible depth, dip, and geometrical form of the source body. While the inverse problem is, in principle, under-determined, reasonable geological assumptions or other *a priori* information can usually be brought to bear to add practical constraints in the inversion process that is often used in anomaly interpretation.

In practice, the flat-topped dipping dyke, extending down-dip to infinity and with parallel sides, is one of the more useful models for the geological sources of many anomalies. The anomaly to be expected over such a body with a vertical dip for a range of magnetic inclinations is illustrated in Figure 18.

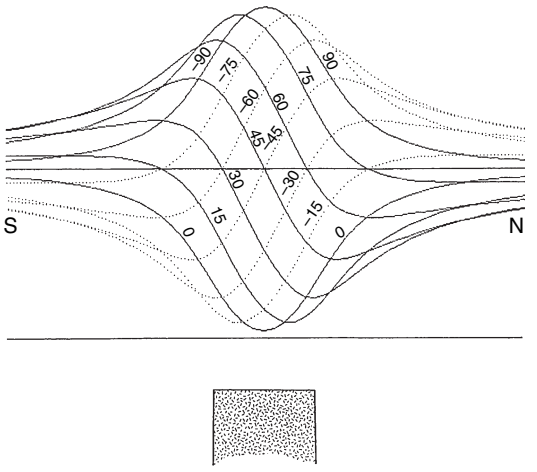

Figure 18 The magnetic anomaly over a vertical dyke-like body striking east–west and magnetized solely by induction varies with the angle of inclination *I* of the geomagnetic field at the locality of the body. The figure shows the curve family as I goes from $+90^\circ$ to 0° (northern hemisphere) as solid lines and from 0 degrees to -90° (southern hemisphere) as dotted lines. Note that the positive lobe of the anomaly is displaced from above the body in the direction of the equator in both hemispheres as the negative lobe grows on the side towards the nearest pole.

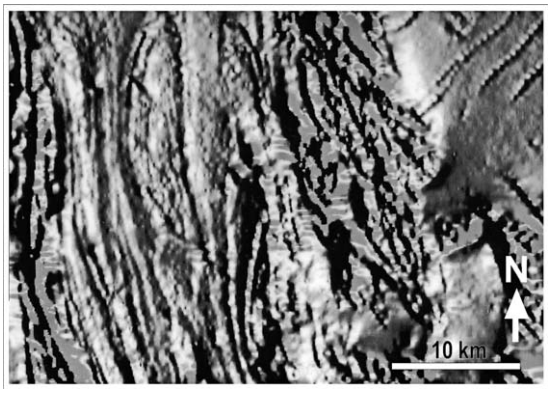

Figure 19 The magnetic anomalies in a certain area are displayed here as a gray-scale shaded-relief image. In many areas the geology gives rise to a plethora of anomalies that enable, in this case, the folds in the rock formations of the western half of the area to be traced quite clearly. Some subtle dyke anomalies appear in the NE corner of the area. Courtesy of Geoscience Australia.

Approximations of magnetic sources by isolated poles or dipoles are found to be of little value in serious interpretation, particularly now that computer algorithms are readily available to compute accurately the effects of realistically dimensioned geological bodies in two and three dimensions. In specific applications, such as understanding the structure and stratigraphy in a potential petroleum province, the interpretation of gravity and magnetic data in terms of geological bodies and horizons of specified densities and magnetizations can be a helpful adjunct to understanding the stratigraphic and structural information contained in seismic sections. Since most sedimentary rocks are essentially nonmagnetic, the anomalies in such an area are usually of deep-seated origin, arising from the igneous and metamorphic basement below the sediments. Hence a rather small number of deep-seated anomalies are seen and their interpretation can help understand the structure of these older rocks, the downfaulting and subsidence of which led to the development of the sedimentary basin of interest for petroleum resources.

In normal survey practice, particularly in areas of Precambrian basement typical of solid mineral exploration environments, many hundreds or even thousands of anomalies are often detected (**Figure 19**). The extent to which any one of them may be quantitatively interpreted as suggested above depends to some extent on the degree of interference from neighboring anomalies. In any event, the trailing off to zero at infinite distance, predicted mathematically for all anomalies, is seldom observable to any great distance from the source. Often the interference from nearby anomalies is quite severe and the emphasis of the interpretation must then be mostly on qualitatively tracing patterns of anomalies from one place to another and reconciling these patterns with the (often isolated) exposures of certain suites of rock in the survey area. Even so, aeromagnetic anomaly mapping has proven to be a powerful tool in extending geological mapping beyond areas of relatively well-exposed geology in old (particularly Precambrian) terrains where the topography has become subdued and overlain by younger weathering products (see later sections).

It should be noted that it is rarely the case that eye-catching magnetic anomalies arise directly from important ore bodies. While this may have been the initial hope in developing the aeromagnetic survey method, experience has shown that the real value of aeromagnetic surveying is its role in building up a picture of the regional geology. From this picture, and knowledge of the types of geological environments in which certain types of economic minerals occur, selections can be made of limited areas in which more detailed and expensive investigations (such as ground geochemistry and drilling) may be worthwhile in order to isolate ore bodies of potential

economic value. Even so, at a detailed scale of magnetic surveying on the ground surface, it is often the case that magnetic minerals occur in association with economic minerals even where the latter are themselves nonmagnetic. In such cases, magnetic anomalies may serve as pathfinders to economic targets and, in any case, provide an inexpensive way of tracing known economic occurrences along strike, for example.

5.04.3.3 Instrumentation Applied to Magnetic Surveying

5.04.3.3.1 Ground surveys

The earliest ground magnetometer surveys used sensitive dip needles, the deflections of which were sufficient to detect large deposits of magnetic iron ore. More sensitive mechanical instruments evolved, of which the Schmidt-type magnetic field balance became almost ubiquitous in mineral and petroleum exploration in the 1940s and 1950s, prior to the prevalence of electronic magnetometers. They were designed to measure the vertical (more rarely the horizontal) component of the geomagnetic field. The necessity to set up a tripod and level the instrument meant that progress was slow and surveys consequently costly, despite a poor sensitivity of only a few tens of nT.

The invention of the fluxgate magnetometer (Section 5.04.1.2) in the 1940s marked the arrival of the electronic age in magnetometry. Initially designed for airborne application, it was some time before the electronics were sufficiently lightweight and compact for hand-carried operations. The fluxgate element, if gimbaled to hang vertically in a damping medium, such as oil, could measure the vertical component of the magnetic field with a sensitivity sufficient to detect variations of a few tens of nT. Instruments such as the Jalander weighed only a few kilos and could be read in seconds so that long traverses (several kilometers) with frequent readings (every 5–50 m) could be accomplished each working day, even when combined with suitable survey practice to monitor and correct for temporal variations in the main geomagnetic field. As is often the case with exploration surveying, the quantity of observations and the uniformity of coverage of an area is more important than the absolute accuracy of each individual reading, the idea being to cover ground and detect interesting anomalies.

Improved performance in ground surveys was soon achieved by the PPM (see Section 5.04.1.3) in the 1950s and 1960s with the added advantage that it was the magnitude of the total field that was being measured, directly and absolutely to 1 nT accuracy, eliminating the need for any careful adjustment, orientation, or calibration of the instrument. This also brought ground surveys into line with airborne surveys where only the scalar magnitude of the total field has ever been measured from the early post-war days of the airborne fluxgate. Only relatively recently has the addition of a second or third magnetometer sensor been exploited to obtain magnetic gradient estimates either vertically, along track, or across track. Any possible theoretical advantages of making vector (as opposed to scalar) measurements in exploration practice have, even until the present, been outweighed by the additional technical complexity that would be entailed when working from a moving platform.

In the 1980s, with the advent of inexpensive and portable computer systems, ground magnetometry in which the operator had little to do except walk, push a button, and note down a reading became automated into integrated systems in which the x and y coordinates of each observation point and the time of the observation (for temporal variation corrections) were recorded directly in computer memory for later retrieval, correction with time-synchronized base-station readings, and plotted as contour maps or gray-scale images. Eventually, GPS readings became accurate enough that position could also be recorded directly (rather than the observer following pre-surveyed lines) and, in open terrain and small local areas, the use of multiple sensors could be employed to collect more than one line of observations with each passage of the observer or ground survey vehicle. Quad-bikes, mountain bikes, and many other types of transport suited to the terrain being surveyed have been pressed into service for this purpose. For archeological, unexploded ordinance, and engineering site investigation purposes, the readings may be as little as 50 cm apart giving resolution at a sub-meter scale where the sources are buried within the uppermost layers of the subsurface. Apart from ferrous metal objects that are magnetic, bricks and the clay in the immediate vicinity of open fireplaces will have acquired a magnetization that is detectable in such surveys and the method therefore offers considerable economy of effort in the excavation of sites of potential archeological interest. **Figure 20** shows, by way of example, the magnetic anomaly image over a settlement dated at 800–600 BC where ancient excavations of the subsoil to build

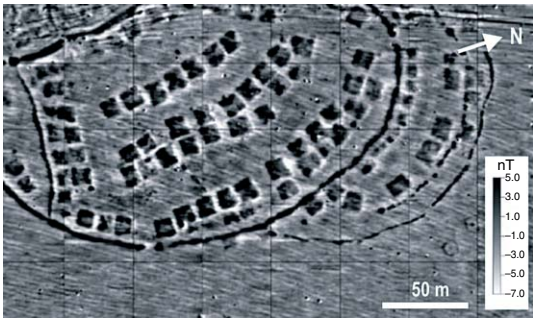

Figure 20 A carefully executed ground magnetometer survey over an archeological site in Siberia. The magnetic image reveals the locations of dwellings and ditches dated at 800–600 BC. The grid-squares on the figure are of dimension 40 m, and magnetic anomaly readings were made on a grid of 50 × 25 cm. Reproduced from Becker H and Fassbinder JWE (1999) Magnetometry of a Scythian settlement in Siberia near Cicah in the Baraba Steppe. In: Fassbinder JWE and Irlinger WE (eds.) *Archaeological Prospection, Arbeitsh. Bayerisches Landesamtf. Denkmalpflege*, Vol. 108, pp. 168–172. Munchen: Verlag Karl M. Lipp.

primitive habitations have left their mark in the details of the local magnetic field.

5.04.3.3.2 Airborne survey techniques

Airborne magnetic surveying has its origins in the Second World War in more ways than one. The necessary fluxgate magnetometer technology was originally developed for military applications such as submarine detection. But the war's legacy of aircraft and flying skills also contributed to a favorable environment for the application of the airborne magnetometer to exploration in peacetime. Early case histories were documented during the late 1940s (Reford and Sumner, 1964) as early fluxgate magnetometers underwent post-war refinement to improve their resolution and efficiency.

PPMs (see Section 5.04.1.3) made their appearance in the late 1950s and early adaptations to airborne use and to digital recording of the magnetic field readings are evident. Even so, the fluxgate magnetometer proved capable of further refinement and continued in service for many years. Optically pumped magnetometers (see Section 5.04.1.3) first came into airborne service in the early 1960s but they did not seriously replace earlier types until the late 1980s when expiry of the original patent led to their more general application. Since then they have become almost ubiquitous on account of their high sensitivity and fast reading rate. Helium, rubidium, cesium, and potassium types have all been used, but cesium vapor types seem now almost ubiquitous in the industry. SQUID-type magnetometers (see Section 5.04.1.2) with vector capability are under development but so far only approach the overall sensitivity of standard systems based on the cesium vapor instrument.

5.04.3.4 Design and Execution of Surveys

5.04.3.4.1 Practical airborne magnetometry

The development of suitable magnetometers is only part of the story of aeromagnetic surveying. Many survey practicalities need to be addressed before the profiles of readings can be combined into a contour map – a hand-drafted map being the end product of early surveys (pre-1975 approximately) after several manually intensive intermediate steps. These steps included the planning and execution of an appropriately regular grid of parallel flight lines and their recovery in map form. In many frontier areas this was sufficiently challenging (due to poor or nonexistent topographic mapping) that early satellite imagery (1970s) was able to play a significant role as base maps in many surveys. Offshore, the conventional application of a downward-looking 35 mm camera to record the flight path was of little use and necessitated pressing various electronic navigation systems such as inertial navigation and Doppler navigators into service. A summary of these techniques, written at the time when they were about to be replaced by GPS, is given by Bullock and Barritt (1989).

To achieve good resolution of closely spaced near-surface geological sources, the airborne magnetometer needs to be flown at a low ground clearance, typically 60 or 80 m these days, and often only 150 m, even in the early years. For a similar reason, close spacing of the parallel survey lines in the grid of observations is essential if small features of geological importance are not to be missed. (Kimberlite pipes containing economic concentrations of diamonds, e.g., may be no more than 100 m in diameter). In the days of early reconnaissance work, the line spacing was often 1 km or more, but in modern surveys, particularly over the hard rock terrain typical of mineral exploration work, this is now commonly reduced to 400 or even 200 m. Worldwide, many millions of kilometers have been flown already in the attempt to achieve appropriate coverage of the geology of all continents. The national coverage of Australia, for example, now includes almost 20 million line-km of data gathered

over more than 50 years (Geoscience Australia, website). Typical survey aircraft fly at about 250 km h^{-1} and operate for periods of 4–6 h each day, typically recording 20 000 line-km of data per month of operation.

Magnetometer readings are gathered at appropriately timed intervals – 1 s for the early proton magnetometer (equivalent to about 70 meters on the ground) and more recently ten or even one hundred times per second for modern cesium vapor instruments. Clearly there is a need for the electronic data gathering that made its appearance in the 1970s, first with dedicated custom-built systems and more recently with standard laptop computers and commercially available software.

Output of survey results in computer-generated anomaly contours, as opposed to contours hand-drafted from analog paper-chart records generated during each flight, gradually became the norm in the late 1970s. Almost simultaneously, new computer software, originally developed for use with digital satellite imagery, was adapted for the display of aeromagnetic anomaly data sets as grayscale and color maps using, for example, shaded-relief effects to emphasize the geological content of the anomaly data sets (e.g., **Figure 19**) (O'Sullivan, 1991). Individual aeromagnetic survey projects with more than 1 million line-km of data have been carried out in recent years with the latest technology in Africa and Arabia. In Europe (outside of Scandinavia) and North America, generally older coverage to a lower standard is the norm, except where upgraded for oil exploration or, quite rarely now in Europe at least, for mineral exploration purposes. Images of outstanding quality and detail at scales compatible with regional geological maps (say 1:250 000) are now published routinely from these surveys.

Gamma-ray spectrometers are usually flown simultaneously to add information streams on the abundances of thorium, uranium, and potassium to the graphical output of many surveys. Airborne gravity anomaly mapping is sometimes carried out simultaneously with aeromagnetic readings, but this is much less common on account of the added cost of the gravimeter technology, making it attractive only in limited commercial situations such as frontier oil exploration areas with difficult ground access (Reeves and Bullock, 2006).

Arguably the biggest single innovation in more than 50 years of airborne magnetometry was the introduction of the GPS in the early 1990s. So many of the tedious and labor-intensive aspects of previous survey practice centered around navigation of the survey aircraft as closely as possible along predetermined lines and, subsequently, the recovery of the flight path actually flown. Even after the arrival of the digital era in the 1970s, this part of the process remained primarily manual, up to the point where the flight path – recovered manually using the 35 mm strip films exposed during flight – was digitized and merged with the digitally acquired geophysical data. GPS provided quicker, better, and cheaper solutions to all these problems – in real time to an accuracy of about 5 m after the introduction of differential GPS. The regularity of the pattern of flight-lines so achieved was an added bonus to the quality of the survey data, quite apart from the accuracy with which individual features could be recovered on the ground. In addition, GPS facilitated the production of digital elevation models of the surveyed area, thanks to the combination of GPS (geocentric) heights for the aircraft and radar altimeter values for the aircraft's ground clearance.

5.04.3.4.2 Elimination of nongeological influences (aircraft, temporal changes)

A reading of a magnetometer on board an aircraft must clearly be corrected for any effect of the aircraft itself – primarily the engines and electrical currents, since most other parts of aircraft are now of nonferrous materials. The first-line approach is to mount the magnetometer sensor as far as possible away from such effects, usually in a fairing attached to the tail (**Figure 21**) and backing out as much as possible of any permanent magnetic effects.

Magnetic effects due to the varying attitude of the aircraft in the geomagnetic field (so-called maneuver noise) have been greatly reduced by the development of so-called automatic compensators. In calibration mode, such equipment records the variations in

Figure 21 An Aero-Commander Shrike aircraft fitted with a magnetometer in a tail stinger for aeromagnetic surveying. Courtesy of Geoscience Australia.

magnetometer reading as the aircraft executes a predetermined series of maneuvers in pitch, roll, and yaw at high altitude (distant from geological sources) while flying on each of the cardinal compass directions. When switched to survey mode, the instrument then automatically applies in real time the appropriate correction for the actual attitude of the aircraft at any moment. A 'figure-of-merit' – the sum of the 12 terms, three maneuvers in each of four cardinal compass directions – is an assessment of the performance of the airborne system and commonly now is as low as about 1 nT. From the point of view of revealing geological detail, a major achievement in airborne survey practice has been the reduction of noise from all sources on the magnetic anomaly profile to as little as 0.1 nT. Since the interest for geological mapping is not confined only to the most magnetic rocks, even the most subtle anomalies are of potential value. So reducing the noise level lowers the threshold of what is detectable in anomaly mapping generally.

Noise arises from various sources. Maneuver noise is discussed above. The elimination of time variations in the geomagnetic field itself is achieved largely by monitoring temporal variations at a fixed base station during survey flying. The limit to this is set by the fact that geomagnetic micropulsations vary detectably from place to place, even over a few tens of kilometers, so the records of a single fixed base station do not perfectly represent the temporal variations experienced by the magnetometer in the aircraft throughout a survey area, parts of which are typically hundreds of kilometers apart. Nevertheless, the time-synchronized subtraction of total field readings at the fixed base-station magnetometer from the readings made in the surveying aircraft eliminates the bulk of the temporal variations. Corrections of several tens of nT are made typically in this way. The base station magnetometer should be sited in a magnetically quiet locality and its output carefully filtered to avoid the addition of (negative) noise when subtracted from the airborne profiles. On days when geomagnetic activity is high (magnetic storms), survey operations must be suspended. The magnetic base stations are rarely tied to a geomagnetic observatory. While this would be ideal, the remoteness of many survey areas dictates that the additional logistic effort required and the low commercial value of the absolute background level in any single survey (as opposed to the anomalies) usually makes this prohibitive. As a result, tying together a patchwork of hundreds of independently acquired surveys into a consistent national system with a credible datum requires some innovative approaches (Tarlowski *et al.*, 1996).

The imperfections in the base-station subtraction process are almost always reduced further by flying surveys with a number of control lines or tie-lines at right-angles to the main survey direction. These are spaced such that an aircraft flying a survey line crosses a control line every few minutes – sufficiently often that departures from linearity in temporal variations are not severe. Once the aircraft magnetometer and compensator are properly calibrated, any difference between the two magnetometer readings (flight-line and tie-line) at each intersection point should be due only to temporal geomagnetic variations or, to be more precise, the imperfections of the base-station subtraction procedure in removing them. An iterative adjustment of each of the survey lines with low-order polynomial corrections to minimize these differences at all the hundreds or thousands of intersections in a survey usually makes, on average a few nT change to the near-DC level of each of the profiles.

The prevalent use of image-processing procedures for presentation of survey data as images (see next section) means that any remaining line-related noise may still be visible in certain image presentations. This residual can be reduced by applying a type of directional filtering procedure often called micro-leveling (Minty, 1992). Adjustments at this stage are at the level of a few tenths of a nT, but still as large as, or larger than, the noise level on each of the profiles. This is essentially a cosmetic procedure but it does significantly improve the signal-to-noise ratio in the final data when viewed as an image.

Exposing geological detail requires a minimum separation between airborne magnetometer and magnetic sources commensurate with operational safety of the aircraft. This leads to surveys with a terrain clearance of typically 60 or 80 m. This is achievable with safety in areas of subdued topography but needs to be adjusted in more rugged areas or around isolated hillocks due to the limited climbing capacity of any fixed-wing aircraft. Flying to a predetermined 'drape' on the topography means that similar altitudes are achieved at all the intersections of flight-lines with tie-lines in the survey, adding further precision to the data-reduction process in exchange for a small loss of geological resolution where terrain clearance needs to be greater than the minimum.

The free-air gradient of the undisturbed geomagnetic field with height is generally small (0.01–0.03 nT

per meter), meaning that height differences at intersections need to be 10 m or more for differences in magnetic values due to this gradient to exceed the noise envelope in the profiles. This is comparable with the height discipline normally achieved in survey operations.

Positional accuracy for the aircraft of ±5 m is achievable routinely with differential GPS, meaning that the location of cross-over points is well determined, but it may still be prudent to exclude some cross-overs from the error analysis where exceptionally high magnetic gradients are noted and errors of a few nT may arise simply through a slight mispositioning of the crossover.

With all these precautions, flight-lines executed repeatedly over terrain with only very subtle anomalies show repeatability to about ±0.1 nT. This is comparable with the noise level on the profiles in general in modern data.

At the end of the data-reduction and processing cycle, maps and images revealing geological detail on the scale of a 50 m pixel are produced for interpretation. Commonly these maps and digital data sets are published by national government agencies as part of a nation's geological mapping program and compilations of such maps over whole continents will, eventually, provide valuable new insights into the, often hidden, geology of all the continental areas of the world. Thanks to modern communications, internet, and software technology, these data sets may be exchanged between organizations and clients worldwide, ultimately meaning that exploration decisions may be based on access to a maximum of factual *x-y* registered information from which intelligent interpretations of exploration priorities may be made.

Over the world's oceans, the magnetic anomaly data is mostly of shipborne origin and lacks the quality and resolution of airborne surveys since marine research vessels travel comparatively slowly, remotely from good monitoring of temporal variations, and seldom execute a regular pattern of closely spaced lines. A wealth of shipborne magnetometer data still awaits inclusion in rational worldwide databases (Reeves *et al.*, 1998). Nevertheless, the mapping of oceanic magnetic anomalies has played a key role in establishing our understanding of the way in which oceans grow at mid-ocean ridges with consequent separation of the once-adjacent continents and the improved appreciation of geological evolution that came with global tectonics. Over continental shelf areas critical for petroleum exploration, airborne surveys will often be executed to the same critical standard as described above for land areas.

5.04.3.5 Data Presentation, Enhancement and Interpretation Methods

Since the data-capture and processing stream of modern magnetic anomaly surveys is entirely digital, the final product is also a digital data file or database in which all the collected data is preserved, organized sequentially by flight-lines, and where as many as necessary intermediate corrections are recorded against each reading. Assuming the data reduction and processing has been done correctly, a final corrected anomaly value will exist in this database for each of many millions of observation points. For a large survey this can involve gigabytes of data. Accessing small windows and individual profiles from such a database requires dedicated software if it is to be done conveniently and routinely. Commercial packages have been developed to enable users to do this on laptop PCs (e.g., Geosoft, website; Intrepid Geophysics, website).

For the human interpreter, the first priority is to visualize the data. This may be done on a profile-by-profile basis to inspect individual anomalies, but synoptic overviews of an entire survey are also necessary and best obtained by means of graphical displays of maps and images. The original method of display of magnetic anomaly data was contour maps. With the advent of personal computing power in the 1980s, contour displays have been largely replaced by images in which the anomaly values are converted to a gray scale or a color scale (Milligan *et al.*, 1991; Reeves *et al.*, 1997). The first step in this process is to interpolate the line-based data onto a regular raster or grid of values over the survey area. Typically the size of the grid element (pixel) is one-quarter to one-fifth of the flight-line spacing, so commonly 50–100 m for most surveys. Such a grid cannot represent the full information content of the original profiles along line (with samples at 7 m for a 0.1 s sampling interval) and anti-alias filtering is needed to avoid the smallest anomalies being represented as broader ones in the grid. Across-lines, there is often an under-sampling problem since the line spacing, for cost reasons, often does not meet the strictest sampling criteria. This can be solved in most cases by interpolation along the predominant strike direction of the geology where anomalies change most slowly from one flight-line to the next.

Once available in grid format, many methods of visualization of the gridded data are available (Milligan *et al.*, 1991). A gray-scale representation may be the simplest of these, with the highest magnetic values portrayed as white and the lowest as black (or vice versa) with a suitably stretched gray-scale between. Often more satisfactory is a gray-scale shaded-relief image in which the 'topography' of the anomaly field is displayed as though illuminated by a light source in a given direction (azimuth and altitude). Diffuse reflection from the surface of the magnetic topography is calculated such that slopes facing the illumination source appear brighter than those sloping away from it (**Figure 19**). This gives the human eye a clear impression of the undulations in the anomaly field and has the added benefit that the average magnetic anomaly background level (which may be ill-determined and of little value in studying the near-surface geology) is effectively lost among the average gray levels of the spectrum.

Color may also be used for display purposes, usually with a natural color spectrum and with the highest magnetic values in red and the lowest in blue. Such a presentation may even be combined with the gray-scale shaded-relief effect, or the color saturations may be adjusted to give the eye an optimum impression of the pseudo-topography (Milligan *et al.*, 1991).

All these techniques evolved quickly in the early 1990s and have become universally accessible to users working with commercial software packages. Display of the aeromagnetic data geographically registered with, for example, the pre-existing geological map (or any other geophysical or geochemical data set) is then a powerful tool for the interpreter to use and this is readily available in the geographical information systems (GIS) that are in common use with individuals and groups working with x,y-referenced geoscience data.

Once the data is in a digital gridded format, it is also readily amenable to digital filtering processes that may be operated in the space domain. These may be useful to smooth the data or to enhance certain types of feature, with a directional bias, for example. Calculating gradients across-strike will clearly enhance features striking in one direction, while the same features may be largely subdued by calculating the gradient along-strike. This is analogous to choosing a direction for illumination in the shaded-relief map. Clearly many different options are available.

A further suite of opportunities for data processing arises from the Laplacian nature of the magnetic anomaly field (Spector and Grant, 1970). Measurements of any potential field on one plane (if it is done thoroughly at all wavelengths, as is attempted in aeromagnetic surveys) are sufficient to calculate the field that would be observed on any different plane, permitting what is called upward and downward continuation of the data. Conveniently, this is done by way of a Fourier transform of the data into the wave number domain where upward and downward continuation operators are relatively simple filter functions that may be applied to the wave number and phase spectra. Inverse Fourier transformation restores the filtered result into a new grid in the space domain for display using any of the above gray-scale or color raster techniques.

Similar operations may be performed for calculating gradients in the data (vertical or in any chosen horizontal direction) and, by calculating suitable low-pass and high-pass filters based on the analysis of the wave number spectrum, regional and residual components of the anomaly field may be separated out.

The shape of a typical anomaly depends in part on the magnetic inclination at the survey locality (**Figure 18**). Through adjustments to the phase spectrum in the Fourier domain, anomalies may be transformed into the simple positive shape typical of bodies at the geomagnetic poles, bringing the positive anomaly above its source body. This process is called migration (or reduction) to the pole and is often considered an advantage in interpretation, though it is not without some problems at low magnetic inclinations where north–south trending bodies have very small amplitude anomalies in theory. The desired result assumes that source bodies are vertical and that remanent magnetization plays an insignificant role. Generally speaking, the results are nevertheless useful. The persistence of occasional negative anomalies in a map processed in this way is not disastrous and simply signals that one or both of these two assumptions is invalid locally.

The approach may be taken a step further by assuming the geology to be made up of a raster of vertical prisms of size equal to the grid-cell size of the data and calculating the equivalent magnetic susceptibility necessary for each prism to produce the observed magnetic anomalies. This, again, is seldom perfect in its application but is reasonably valid in many metamorphic terrains such as Precambrian shields. It can form an important step in the interpretation process that may be seen as attempting to

go from the continuous Laplacian magnetic anomaly field to the discontinuous geology where changes in lithology and, for example, faults bring different rock types with different magnetic susceptibilities into contact over very short distances.

Other techniques used routinely to process data and produce outputs that help the extraction of geological information include the calculation and plotting of Euler solutions that indicate the depth of source bodies based on the curvature of their anomalies (Reid *et al.*, 1990) and the calculation of analytic signal expressions (Roest *et al.*, 1992). The latter are the positive envelope to the curve family shown in **Figure 18** and so are independent of magnetic inclination. Positive analytic signal values are also to be found over faults and contacts; however, they do not necessarily highlight only the main magnetic bodies in an area, though in experienced hands they do have considerable value.

Despite all these modes of assistance, the translation of the aeromagnetic anomalies into a geological map – interpretation *sensu stricto* – remains a largely intellect-driven endeavor at present. This is based on the physical constraints surrounding the origin of anomalies and the integration of quantitative interpretation results with more qualitative approaches as well as the constraints provided by other data such as the pre-existing geological map and other layers of geophysical (gamma-ray spectrometry, gravity) or geochemical information. An illustration of magnetic anomalies over an area of Precambrian shield in western Australia and their interpretation at the hands of a skilled geologist is given in **Figure 22**. An understanding of the magnetic properties of rocks in general (next section) undoubtedly plays an important part in this process, though information in any given area on this latter point is almost always incomplete. While a geological map shows the formations that outcrop, or at least sub-outcrop below soils and overburden, the magnetic anomaly pattern also contains information from more deeply buried geological sources. An interpretation map often, therefore, has to include elements of this third dimension of the geology that does not appear on conventional geological maps.

5.04.3.6 The Link between Magnetic Properties of Rocks and Regional Geology

The fact that magnetic properties are retained at all temperatures below the Curie point means that virtually the whole of the Earth's crust contributes to magnetic anomalies and that it is the bulk of these igneous and metamorphic rocks that is represented in the anomaly patterns, though in general the effects of the shallower rocks will predominate over the deeper ones. The fact that the wavelength of anomalies increases with increasing vertical distance between source and magnetometer means that processes of wavelength-based filtering (e.g., after spectral analysis of anomaly patterns, see previous section) can be used to emphasize sources at different depths. Often, for geological mapping, it is the shallowest sources that are of most interest. These can be enhanced (and the deeper sources suppressed) by high-pass filtering or the calculation of a residual or a vertical derivative field from the observed field data (see previous section). Vertical gradient magnetometers similarly are more sensitive to the effects of shallow sources, so vertical gradient surveys tend to reveal the effects of near-surface rocks more clearly than total field surveys. Even quite magnetic rocks disposed in thin, flat-lying layers at or near the Earth's surface, such as lava flows, have relatively little effect in comparison to the 'basement' when it comes to geological mapping, however. So the ability to map underlying crystalline rocks below any surface formations is well-entrenched in the aeromagnetic method.

In the interpretation of anomalies, some understanding of the magnetic properties of rocks in general is an essential part of deriving useful solutions to the mathematically underdetermined problem of inverting anomaly patterns in two dimensions into models – even simplistic ones – of the subsurface in three dimensions. While the geometrical parameters of buried rock bodies in a given area may be unknown, the magnetic properties of representative rock-types may be determined independently in the field or laboratory. Experience gained from such measurements on common rock-types around the world may be helpful, even in an area where the local geology is essentially unknown.

Magnetic properties reside mainly, but not exclusively, in the magnetite grains that rocks contain. Magnetite content is, unfortunately, largely independent of the abundance of the main minerals that determine rock lithology as described by the geologist and petrologist. These basement rocks display a wide range of magnetic properties that are not readily summarized by simple rules that can be used to deduce rock types from their anomalies (Grant, 1985).

Apart from magnetite and the mixed oxides of iron and titanium, only the sulphide mineral

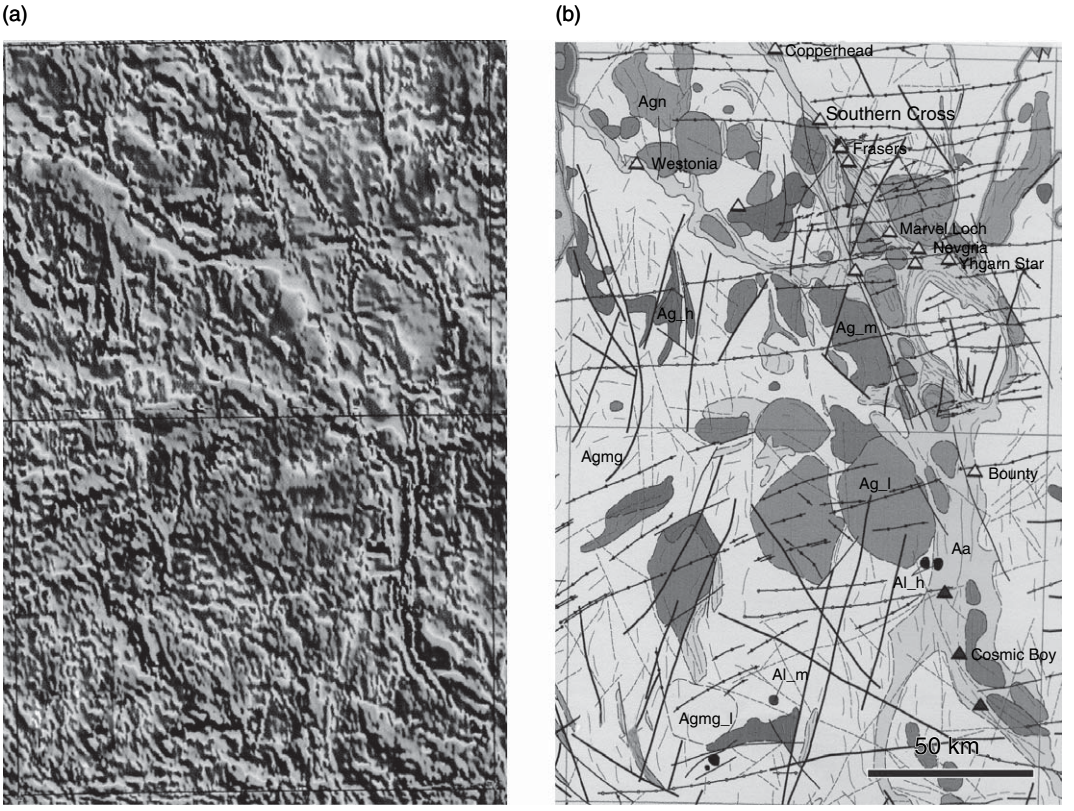

Figure 22 (a) An area of the composite aeromagnetic anomaly map of Western Australia and (b) its geological interpretation. Courtesy of Geoscience Australia and the Geological Survey of Western Australia.

pyrrhotite contributes to magnetic anomalies. At low concentrations, a fairly simple, monotonic relationship is found between magnetite (or pyrrhotite) content and the magnetic susceptibility of a rock. However, there is little relationship between magnetite content and the gross mineralogy of rocks and hence their more conventional petrological classification. It is more useful to relate the anomaly patterns to geological units known in the area, or known from their typical expressions elsewhere. For example, long rather straight anomalies cutting through all other patterns are typical of dykes intruded through cracks or fissures long after the bulk of the country-rock had solidified (**Figure 23**). Similarly, an oval area of anomalies with a texture distinctly different from the surrounding rocks is typical of a granite diapir emplaced long after the surrounding rock solidified.

While the direct relation of magnetic anomalies to specific igneous and metamorphic rock types is not possible in interpretational exercises (except where independent evidence is available from ground studies), the fact that rock types have a bimodal distribution of susceptibility with the two populations separated by at least two orders of magnitude (**Figure 24**) means that many lithological boundaries in such geological terrains are coincident with magnetic property boundaries. Hence, even where two adjacent rock types are both unknown, their contact can often still be traced through aeromagnetic mapping. Magnetic anomaly patterns therefore provide a wealth of information on the general disposition of rock types in an area – their fold patterns, the brittle faults separating terranes with different tectonic histories, and the intrusion of geologically younger features (such as dykes, for example) that cross-cut the older rocks . They have therefore become an essential part of systematic and efficient geological mapping and mineral exploration in most parts of the world.

These evident difficulties notwithstanding, there appears to be no let up in the application of aeromagnetic anomaly mapping as a method of extending geological understanding of our continents and their

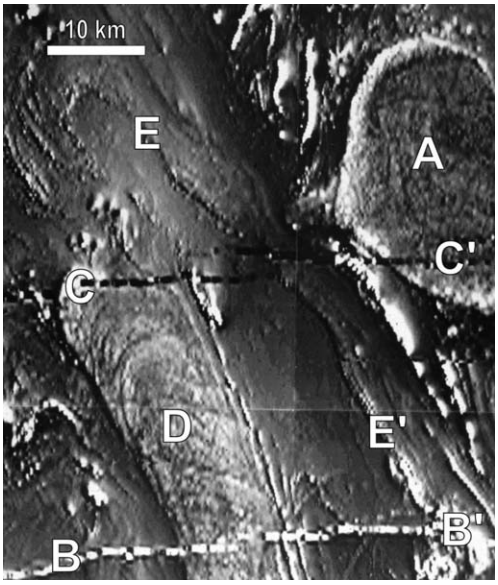

Figure 23 A gray-scale shaded-relief image of a small area of Western Australia showing the magnetic expression of several typical geological units. (A) Granite pluton with highly magnetized rim; (B-B′) dyke with normal magnetization; (C-C′) dyke with reversed magnetization; (D) granite; (E-E′): greenstones. Courtesy of Geoscience Australia.

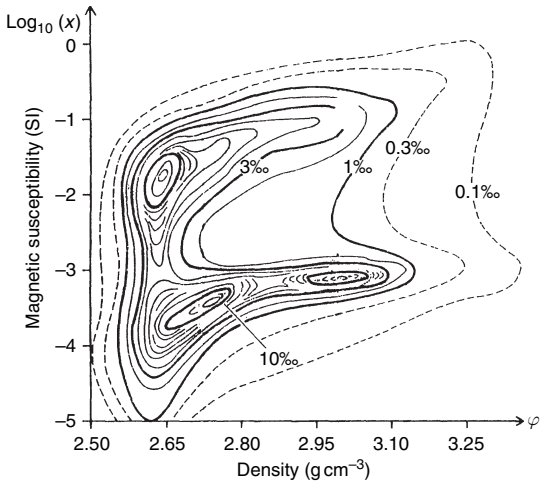

Figure 24 A frequency distribution plot of magnetic susceptibility against density for almost 30 000 rock specimens from northern Scandinavia shows a bimodal distribution between two populations of rocks with a difference in magnetic susceptibility of almost two orders of magnitude – effectively 'magnetic' and 'nonmagnetic' in terms of magnetic anomaly mapping. Note that, while some increase in susceptibility with density (and the higher proportion of mafic minerals) is evident, many highly magnetic rocks are of low density and must, therefore, contain few of the dark minerals found in mafic rocks. Modified from Henkel H (1991) Petrophysical properties (density and magnetisation) of rocks from the northern part of the Baltic shield. *Tectonophysics* 192: 1–19.

resources towards a more universal coverage of magnetic anomaly maps at global scale. Efforts are currently underway to compile the first global map of magnetic anomalies that, it is hoped, will be published in 2007.

5.04.3.7 Satellites and Space Probes

The first satellite to carry a magnetometer into Earth orbit was the Soviet Sputnik 3 in 1958. Since then most satellites and space probes have carried magnetometers of some sort. Early US missions were restricted by low payload requirements, and used a single search-coil design. Later on, single fluxgates were employed, and by varying the fluxgate orientation, three-component vector measurements were possible. The astronauts of the Apollo 12, 15, and 16 missions made vector measurements on the lunar surface, Apollo 16 using the newly developed ring-core fluxgate.

Relatively few satellites have been put into orbit specifically to carry out high-resolution magnetic surveys from space. MAGSAT (Langel *et al.*, 1982) carried a purpose-built fluxgate, together with a cesium vapor scalar instrument to calibrate the intensity while in space. It took measurements during 1979 and 1980. Twenty years later, the Danish satellite OERSTED, launched in 1999, carried a three-component fluxgate mounted alongside a star camera for absolute orientation, as well as an Overhauser effect proton magnetometer. However, a better resolution, spatial and temporal coverage are achieved by Challenging Minisatellite Payload (CHAMP), launched in July 2000 and managed by GFZ, Potsdam (CHAMP, website). CHAMP is in a low-altitude, near polar orbit, which makes it ideal for high-resolution gravity and magnetic measurements. The magnetometers carried by CHAMP are similar to OERSTED's, but the low Earth orbit and improved GPS technology result in much better imaging of crustal anomalies. CHAMP's lifetime was originally predicted to be 5 years, but at the time of writing it has been reliably transmitting data for nearly 7 years. This duration means it is possible to begin to investigate short-period features of the geomagnetic secular variation: sudden changes such as jerks, westward drift, etc.

5.04.4 Paleomagnetic Methods

Direct measurements of the direction of the geomagnetic field exist only for the past 400 years. The record of intensity measurements is even shorter. However, these records indicate that many of the interesting features of the geomagnetic field operate on much longer timescales. So, to gain a complete understanding of the geomagnetic field, or even to be able to say whether Earth has always possessed a magnetic field, much longer records, extending back into the geological past, are required.

Paleomagnetism provides such records through the remanent magnetization of natural materials and artifacts for which the age of the magnetization can be reliably estimated by independent means.

Most rocks and sediments contain small concentrations of ferrimagnetic minerals, for example, magnetite, hematite. The two main primary processes by which these can attain a stable natural remanent magnetization parallel to the ambient geomagnetic field are thermoremanent magnetization (TRM) and detrital remanent magnetization (DRM). A TRM is acquired as a lava, volcanic or igneous rock, or a fired pot or kiln cools; as magnetic grains pass through their Curie temperatures they acquire magnetic moments, and these stabilize on further cooling through an, often well-defined, blocking temperature. At ambient temperatures thermal relaxation times can be of geological duration. Theory and experiment show that the intensity of a TRM or a partial TRM is directly proportional to the intensity of the magnetizing field. Hence it is, in principle, possible to retrieve information on the paleointensity of the geomagnetic field by normalizing a TRM. Delesse (1849) and Melloni (1853) were the first to study TRM in volcanic rocks. Reversely magnetized lavas and baked contacts were reported by David (1904) and Brunhes (1906), sparking the suggestion of polarity reversals, while Chevallier (1925) published remanent directions from lava flows on Mt. Etna, that showed evidence of secular variation.

By contrast, in DRM the grains already carry stable magnetic moments, and, on the average, they align with the ambient magnetic field during depositional and post-depositional processes. DRM occurs in sediments, sedimentary rocks, and sometimes in wind-blown deposits or loess, and is generally, though not always, weaker than TRM. Retrieval of the paleointensity of the geomagnetic field from a DRM is complicated by the many sedimentological factors that affect the magnetization process; at present, it is possible only to estimate relative paleointensities from sequences of sediments that are extremely uniform in character.

The accuracy and age control of paleomagnetic records are very variable. In favorable situations an accuracy of a few degrees can be attained in direction, but 10–20% is usually regarded as good for absolute paleointensity determinations. Whereas archaeological artifacts can often be dated to within decades or even years, radiogenic isotope methods are most commonly used for natural materials, and uncertainties of a few percent of the age are common. The sequential ordering of sedimentary deposits and sedimentary features such as climate-induced cyclic structures that can be tied to astronomical cycles can also provide invaluable constraints in dating sedimentary records of the past few million years. The fact that the main geomagnetic field has reversed its polarity at irregular intervals throughout geological time more generally means that it can be used as the basis of a unique and global timescale of immense value in dating geological events. The development and dating of the geomagnetic polarity timescale (GPTS) is described in Chapter 5.12.

Natural materials may also be magnetized or remagnetized through reheating, recrystallization, diagenetic and other secondary physical or chemical changes. Detailed descriptions of natural magnetization processes are given in Chapter 5.08.

5.04.4.1 Sampling

5.04.4.1.1 Introduction

High-resolution rock magnetometers (see below) are precision instruments, housed and operated in modern sophisticated laboratories. Natural and archaeological materials must therefore be carefully sampled and brought to the paleomagnetic laboratory for measurement. A crucial part of the sampling procedure is the recording of the orientation of the sample while *in situ*, that is, before removal from the outcrop, exposure, or site. Without such orientation the magnetization vector cannot be referred back to a geographic reference frame. It is also important to establish whether the material is still in the orientation in which it was magnetized, or, if not, whether a correction can be made for any disturbance that has occurred since that time. In rocks this usually means looking for an indicator of the paleohorizontal, for

example, a bedding plane in sediments or possibly flow marks in lavas or ignimbrite flows, and careful measurement of its attitude.

5.04.4.1.2 Consolidated rocks

The most popular method of sampling consolidated rocks is by use of a high-speed drill with a diamond matrix-tipped drill stem, usually 2.5 cm in internal diameter, and usually water-cooled. Various models have been designed: modified chain-saw motors, petrol-fuelled; modified electric drills, used either with rechargeable batteries or a portable generator. A petrol-fuelled drill, with pressurized water-cooling is shown in **Figure 25(a)**. Outcrops are often remote and access is frequently difficult or awkward, so portability is important, as is the availability of water.

Drilled samples are usually between 5 and 15 cm in length, depending on the hardness and structural integrity of the rock. Before removal from the outcrop, the sample must be oriented with respect to north and the vertical. This is usually achieved by measuring the plunge below the vertical, and the azimuth of the core axis (or a pair of angles simply related to these), with an inclinometer and a compass (**Figure 25(b)**). A fiducial line is drawn lengthwise along the upper edge of the sample, the front (outside) face marked and the sample clearly labeled following laboratory conventions (**Figure 25(c)**). Every laboratory has its own set of conventions for the orientation and labeling of samples, which have usually been carefully worked out over many field seasons. Weakly magnetized rocks can usually be oriented with a geological magnetic compass;

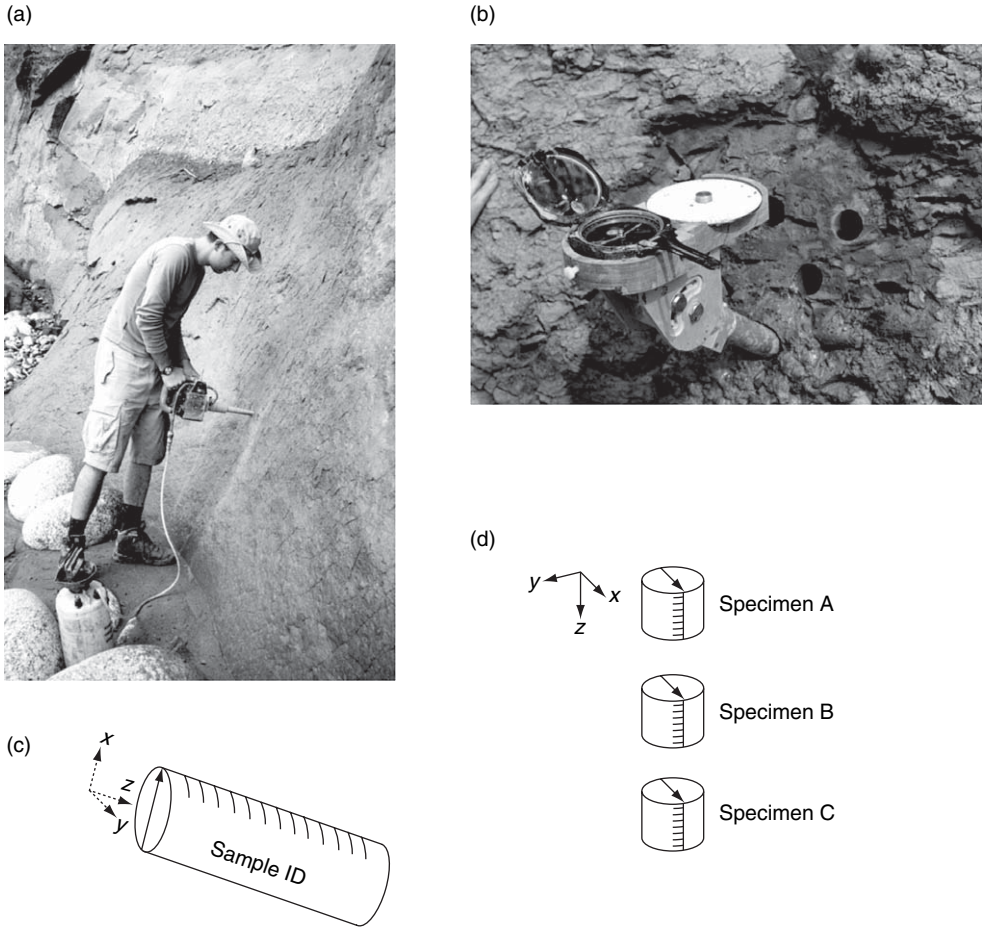

Figure 25 (a) Palaeomagnetic sampling using a water-cooled, petrol-fuelled drill with diamond tipped drill-stem. (b) Before the sample is broken loose, a line is marked on its exposed face and an orientation tool placed over it. A compass is used for azimuthal orientation of weakly magnetized rocks; the inclinometer level and scale are obscured beneath the compass. (c) A method of marking a drill sample once removed from the exposure; sample coordinate system. (d) Each sample is normally cut into a number of specimens. (a) Photo by S. Hüsing. (b) Photo by D. Michalk.

however, some basalts and other strongly magnetized rocks can influence the compass needle, and in such cases a sun compass is preferable. If a magnetic compass is used, the local magnetic variation (declination) must be known, so a correction to geographic north can be made. When a sun compass is used the location, date, and time of each measurement must be recorded, so that the azimuth can subsequently be calculated from tabulated or programmed positions of the sun.

Each drilled sample is normally cut into several 2.2 cm-long specimens for natural remanent magnetization (NRM) measurement (**Figure 25(d)**).

An alternative sampling method is to remove oriented blocks of rock by hand, or by breaking from the exposure with a hammer, and to subsequently drill samples from this block in the laboratory or workshop. The block is oriented in the field by marking strike and dip lines on a flat surface and orienting these lines with an inclinometer and compass. One advantage of this method is that the outcrop is not left with an unsightly array of holes. However, it is often difficult to find suitable outcrops as it is difficult to remove block-samples from rock that is completely firm, intact, and devoid of joints or cracks. Further, accurate orientation is much harder to achieve than with a drilled core.

Many unconsolidated sediments and soft materials such as ignimbrites and loess are too fragile to remain intact and keep their shape without being encased in some way. A popular practice with such materials is to carve a cube-shaped sample and to cover it with a small plastic box (one standard type is approx. 8 cm^3), which is then oriented in a manner modified from that described above for drill samples.

Most modern rock magnetometers are designed to accept both 2.5 × 2.2 cm cylindrical samples and one of the standard sized cubes.

5.04.4.1.3 Unconsolidated (lake and deep sea) sediments

Sedimentary sequences that represent periods of unbroken deposition often provide continuous records of geomagnetic changes spanning thousands, hundreds of thousands or even millions of years. Continuous cores of lacustrine or deep-sea sediments may thus yield invaluable information. Numerous coring devices have been designed for soft sediments. To obtain material suitable for paleomagnetic work, core samplers should not twist, shear, or vibrate the sediment: a simple push mechanism is preferable. Any twisting or shearing of material will compromise the determination of declination, while vibrating may cause reorientation of magnetic grains within the sediment. Corers should contain an absolute minimum of ferrous materials: steel core barrels are known to induce steep components of magnetization in drill cores. There are very few devices that incorporate absolute orientation of the core sample, or even relative orientation between consecutive drives or sections. Individual drives should therefore be as long as possible, to minimize azimuthal matching between sections and the possibility of lost material. The most appropriate method depends on the field environment and the resolution required.

In relatively calm environments and up to about 100 m water depths, the Mackereth corer (**Figure 26**) has proved invaluable. Originally developed for geochemical studies (Mackereth, 1958, 1969), versions of this corer have been designed to collect single-drive cores between 1 and 18 m in length, the most common being the 6-m corer. It is built entirely from nonmagnetic materials and is operated pneumatically from a small boat anchored near the coring site, using cylinders of compressed air. Air is expanded above a piston (MP), forcing the core tube into the sediment in a single smooth drive; a second, fixed piston (KP) inside the core tube sits on top of the sediment throughout, preventing disturbance. At the completion of the coring stroke, air is diverted into a large anchor chamber (AC), which, until this moment, has anchored the corer, but which now becomes buoyant, lifting the corer and core to the surface. When properly deployed, a buoy at the water surface and/or a float chamber near its upper end supports the corer, and the core tube penetrates the sediment vertically.

In deeper water or less clement conditions gravity-driven piston corers or mechanical drills are more commonly used.

In shallow water corers pushed into the sediment on the end of a system of connected rods are popular. This method necessitates a stable platform: a well-anchored raft, or a winter platform of solid ice, are two possible options. Such systems and most drilling systems retrieve sections that are rarely more than 1.5 m long necessitating matching to obtain declination records.

The rotary corers traditionally used to core hard sediments and igneous basement on the sea floor are not suitable for the soft sediments that carry high-resolution paleomagnetic and climatic records as they cause too much disturbance and shearing of the material. The Ocean Drilling Program, which operates the ship JOIDES Resolution, and has drilled throughout the world's oceans for several decades,

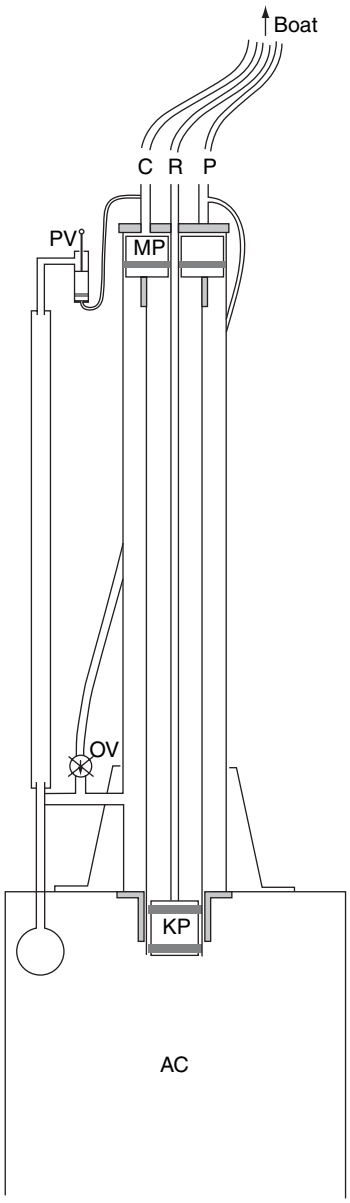

Figure 26 The Mackereth lake sediment corer is operated pneumatically from a boat. Passing air down line P, through a one-way valve OV, and the open valve PV creates a suction effect that pulls the anchor chamber AC into the sediment. Passing air down line C then closes PV and pushes the main piston MP and core tube into the sediment. The Kullenberg piston, KP, remains fixed with respect to the corer, minimizing disturbance to the uppermost sediment. At the completion of the coring stroke, air is diverted into the anchor chamber AC, which becomes buoyant lifting the corer to the lake surface for retrieval. Air-line R allows retraction of the core tube and emergency retrieval.

has developed an Advanced Piston Corer to overcome the problem (Ocean Drilling Program, website). The corer is dropped to the bottom of the coring wireline and then operates in a manner very similar to that of the Mackereth corer described above. Once the corer is in place, safety pins are broken by a burst of hydraulic pressure, which then drives the 9.5 m inner core barrel into the sediment in a single smooth stroke. The core section is brought to the surface for recovery, the drill bit and bottom hole assembly driven a further 9.5 m down and the whole process repeated to recover the next 9.5 m of sediment. The Advanced Piston Corer also carries an orientation tool so each section can be oriented for absolute paleomagnetic work. The Ocean Drilling Program quote a recovery rate of 1–4 sections per hour (9.5–38.0 m h^{-1}), depending on water depth and the hardness of the material cored.

5.04.4.2 Rock Magnetometers

5.04.4.2.1 Introduction

Since its infancy in the 1950s paleomagnetism has seen three generations of rock magnetometers. The first astatic system was possibly that used by Melloni (1853) in his pioneering investigation of the TRM of Vesuvian lava flows. Astatic systems continued to be developed and used extensively for over 100 years, until post second world war developments in electronics led to the fluxgate, spinner magnetometers with online computer control and signal processing. This new generation of magnetometers proved rugged, reliable, and versatile, and most laboratories still employ spinner magnetometers for certain types of work. The ultimate in sensitivity is, in principle, provided by the cryogenic magnetometers, which first appeared in the early 1970s following Josephson's discoveries in superconductivity, including quantum properties of the Josephson junction and its close cousins, the weak link, and the SQUID. Modern cryogenic systems offer unprecedented sensitivity, fast response, no spinning or vibrating, full automation, including some demagnetization procedures if desired, data logging and presentation.

5.04.4.2.2 Astatic systems

A single suspended magnet suffers from time variations of the torque provided by the time-varying ambient magnetic field, and is really only suitable for rough measurements on samples with magnetizations strong enough to exceed this variability.

The principle of an astatic system is to compensate for time variations in a uniform horizontal field by using two magnets of equal moment, mounted antiparallel, one above the other, from the same

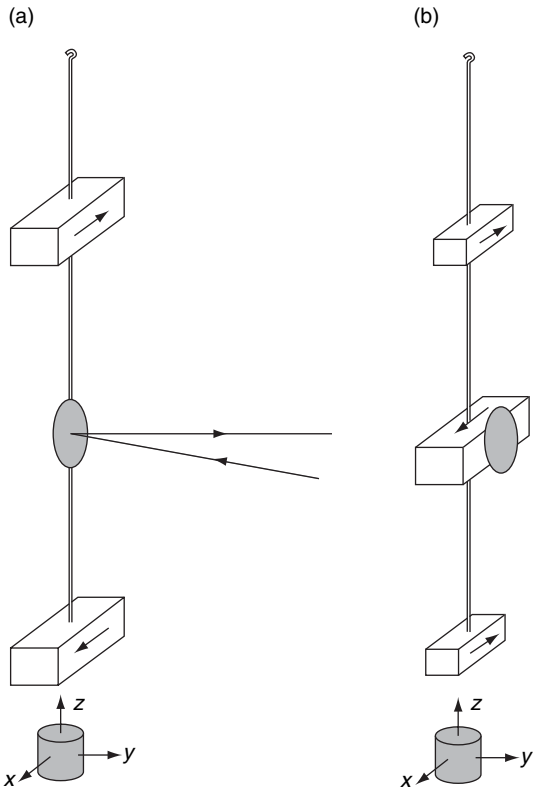

Figure 27 (a) Principle of the astatic magnetometer: the two magnets have equal and opposite moments. The angular deflection is measured for a number of different orientations of the specimen, one of which is shown. (b) Parastatic magnetometer system: the central magnet has a moment equal to twice that of the upper and lower magnets, and is oppositely oriented; this compensates for gradients in the horizontal magnetic field.

suspension (**Figure 27(a)**). The total moment of the system is weak, and a weak torsional suspension can be used. When a sample is brought up symmetrically beneath the lower magnet, a torque is exerted on the system that is proportional to the magnetic moment of the sample (and depends also on a number of geometric factors), this results in an angular deflection that is measured by means of an optical lever. By measuring the deflection with the sample in a number of different positions with respect to the magnets, it is possible to obtain all three components of its magnetic moment, and hence calculate its magnitude and direction. Blackett (1952) detailed the design features, construction, and use of a highly sensitive astatic magnetometer, and this was then used in many of the pioneering paleomagnetic studies of the 1950s.

Moderate-sensitivity astatic systems were relatively easy to set up in most laboratories. Such systems gave reliable results on standard-sized samples with magnetizations above about $0.2\,\mathrm{A\,m^{-1}}$: (most TRM-bearing volcanic and igneous rocks). However, their sensitivity was limited by vibration, field gradients, and variability caused by moving objects such as lifts, vehicles, etc.

These factors were particularly problematic in noisy city laboratories, and led to the establishment, in the 1960s, of many out-of-city laboratories, many of which are still in operation at the beginning of the twenty-first century. High-sensitivity astatic magnetometers housed in these quiet environments, usually mounted on stable concrete slabs, and set in the center of large sets of Helmholtz coils, were capable, with patience, of accurate measurements to $0.001\,\mathrm{A\,m^{-1}}$: (weak sediments and limestones).

An alternative in magnetically noisy environments is a parastatic system, which employs three suspended magnets, as shown in **Figure 27(b)**. The upper and lower magnets are antiparallel to and each have half the moment of the center magnet. This arrangement is less sensitive to changes in the gradient of a horizontal field. Parastatic systems were first described by Thellier (1933), and were further developed in the 1960s (Pozzi and Thellier, 1963). Larochelle and Christie (1967) quote an accuracy of 1° in the measurement of a sample of $10^{-3}\,\mathrm{A\,m^{-1}}$, in a measurement time of 6 min.

5.04.4.2.3 Spinner magnetometers

The basic principle of all spinner magnetometers is that of electromagnetic induction: when the magnetic moment of a sample is rotated in or near either a coil or a fluxgate system, an alternating voltage signal is induced in the coil or fluxgate circuitry. For this reason they have also been called 'rock-generator' magnetometers (e.g., Nagata, 1961). In general, the amplitude of the induced signal is proportional to the component of the magnetic moment perpendicular to the rotation axis, and the phase can be used to determine the direction of this component with respect to some reference direction in the sample. The sample must be spun about at least two axes to obtain three orthogonal components of the magnetic moment and so compute the total vector. Measurements are often made in 4, 6, or 12 different orientations, creating a redundancy of information, but also enabling the calculation of a statistical measure of confidence in the result. This can provide valuable information on the homogeneity of magnetization in a sample and its short timescale viscosity.

In induction coil-based systems, the induced voltage is actually a function of rotation frequency and the number of turns and dimensions of the coils, as well as the component of the magnetic moment of the sample perpendicular to the rotation axis. High rotation speeds (100–400 Hz) are required, and these have sometimes been achieved by means of an air turbine, to avoid magnetic field interference. However, rapid rotation is not always ideal for delicate samples.

Fluxgate sensors avoid the need for rapid rotation, since, in addition to the sample moment, the induced signal depends only on the fluxgate sensitivity (see Section 5.04.1.2) and the distance of the sample from it. Frequencies of less than 10 Hz are usual.

Several different designs of spinner magnetometers have been developed commercially. The Princeton Applied Research design includes a compensated (astatic) system of two coils connected in series opposition to eliminate field variations, while the Schonstedt magnetometer contains a single fluxgate housed in a mu-metal shield to eliminate external magnetic fields. The Institute of Applied Geophysics, Prague also manufactures a high-speed (85 Hz) spinner with a pair of uncompensated pick-up coils, housed in a three-layer mu-metal shield.

The Digico instrument (Molyneux, 1971; Molspin, website) incorporated an innovative ring-shaped fluxgate, within which the sample was rotated at about 4 Hz. It was also the first magnetometer to be controlled from a computer terminal and to employ online signal processing – features which, a decade later, had become virtually taken for granted, but which made the Digico the most advanced magnetometer of its day. The basic operating principles, which were later miniaturized in the portable Minispin magnetometer, are illustrated in **Figure 28**. The sample rotates in the circular fluxgate. The signal is sampled 128 times per revolution – this is controlled by a photo-gate arrangement mounted over a slotted disk that rotates with the sample, at the lower end of the drive shaft. The signals pass through an analog-to-digital converter to the computer, where they are averaged over a preset number of revolutions. When the measurement is complete the output signal is Fourier-analyzed and the first harmonic gives the magnetic moment in the plane of the fluxgate: its components are calculated with respect to a reference direction on the sample holder, printed out, and saved. Once the sample has been spun in four or six different orientations, the direction and intensity of the magnetic moment are calculated, together with a measure of uncertainty. Further calculations can be programmed to perform field and/or bedding corrections, and so output declination and inclination in various reference frames. By increasing the number of revolutions over which each measurement is averaged, the user can increase the precision of the result. Collinson (1983) quotes that the practical lower limit of sensitivity of the Digico magnetometer is about $10^{-4}\,\mathrm{A\,m^{-1}}$, with a measurement time of between 10 and 30 min, and a directional accuracy of about 5°.

5.04.4.2.4 Cryogenic magnetometers

Rock magnetometers incorporating superconducting (SQUID) sensors (see Section 5.04.1.2) were developed in the early 1970s and began to appear in paleomagnetic laboratories around the world later that decade. Cryogenic magnetometers offer enormous improvements in both the sensitivity and speed of measurement, while causing minimum disturbance to delicate samples. Sensor design and signal processing are not the only technical problems in the development of a cryogenic magnetometer: maintaining the extremely low temperatures at which the superconducting components operate is an equally important challenge.

The first cryogenic rock magnetometers were built by SCT in the USA and by Cryogenic Consultants Ltd. (CCL) in the UK, and incorporated RF-driven weak-link SQUID sensors. The practical design of the sensors is dictated by constraints on the size of the superconducting loop, which, in order to mitigate the effects of thermal noise must have a very small inductance, and have a diameter of 1–2 mm (Fuller, 1987). This is an order of magnitude smaller than the standard paleomagnetic specimen, so the most convenient way to link the specimen's magnetic flux to the sensor is indirectly, via a transformer-like coupling. The specimen is inserted into a sensor coil, which is connected by to a more tightly wound field transfer coil, and the flux of this coil is measured by the SQUID detector. Both coils and the connections are superconducting: the arrangement therefore acts somewhat like a DC transformer, the coupling depending on the actual flux linkage rather than its rate of change. **Figure 29** illustrates the arrangement of pick-up coils and SQUID sensors in the original SCT machine, which measured two components of magnetic moment, vertical and horizontal. The Helmholtz configuration of the sensor coils ensures optimum sampling of a homogeneous specimen placed at their center: the horizontal axis coils are

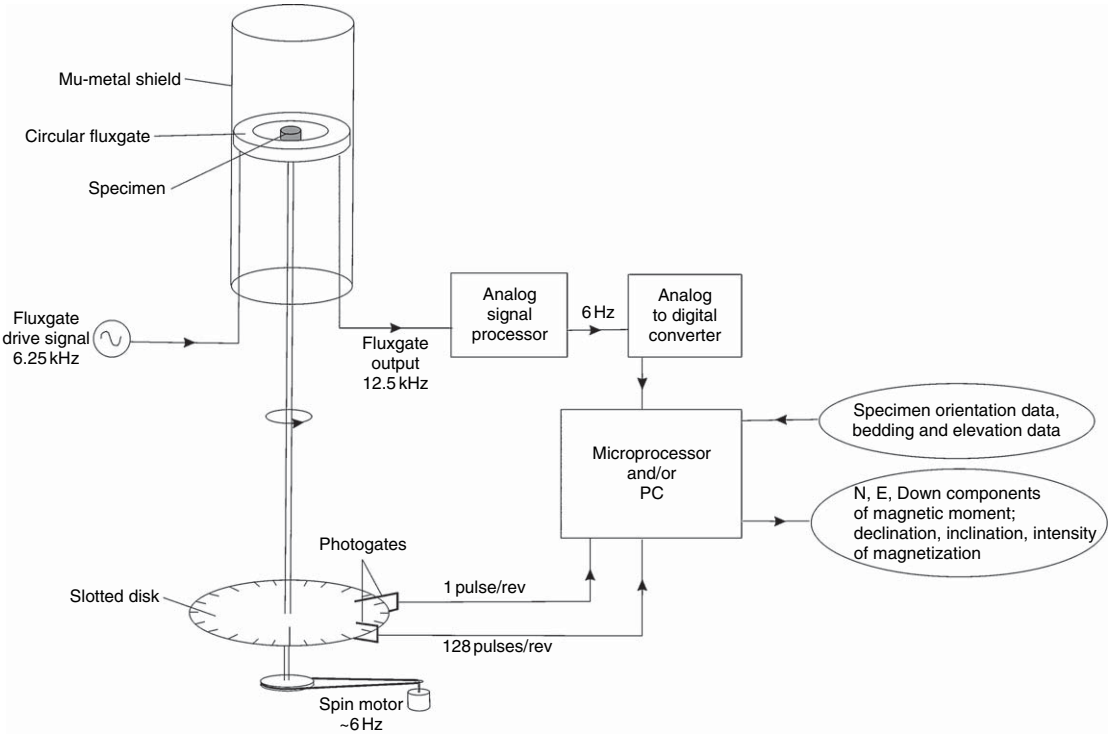

Figure 28 Principle of the Digico fluxgate magnetometer (Molyneux, 1971). The specimen is spun at the center of a single-axis ring-core fluxgate, signal processing is carried out by a microprocessor or computer, which calculates and outputs results as components of magnetic moment, or as required by the user.

less sensitive to sample position than the vertical axis set. Typically, a specimen is inserted into the sensor region, and measurements made at 90-degree steps as it is rotated about a vertical axis. This gives four estimates of the z component and two of each of the x and y components of magnetic moment. The specimen may then be inverted and the process repeated to give four more estimates of z and two more of x and y. Analyzing these, together with background and holder measurements allows calculation of the magnetic moment vector and estimation of the internal consistency of the overall measurement. The specimen holder is usually made of lightweight plastic or mylar, and the sensor region of the magnetometer is deep within a magnetically shielded, heavily insulated liquid helium cryostat.

Over the past 15 years several modifications and improvements have been made to commercially available cryogenic magnetometers. These include (1) replacement of RF-driven SQUIDS with DC SQUIDS, which effectively count individual flux quanta: improving sensitivity to ca. $10^{-12}\,\mathrm{Am^2\,Hz^{-1/2}}$ for a standard diameter access (2G Enterprises, website); and (2) design of a horizontal-axis machine, with room temperature access at both ends of the cryostat, allowing long samples to be passed right through the sensor region. Whole, or half-cores of sediment can thus be measured intact, by stepping them through the sensors. Whole sediment cores typically have diameters of 5 cm or more, so this necessitates a wider access, which lowers the sensitivity for smaller samples. A further development, the U-channel, solves this problem. A long rectangular plastic trough up to 1.5 m long and 20 mm by 20 mm cross-section, the 'U-channel', is pressed into the flat surface of a half-core, the resulting sample removed, and the open face of the U-channel sealed with a lid. The U-channel sample can be passed continuously through a standard small-access magnetometer. At other times the same magnetometer can be used for discrete sample measurement without loss of precision. Both whole-core and U-channel measurements inevitably result in a convolution of the magnetization signal with the sampling function(s) of the sensor(s), which has a smoothing effect on the output. Methods of deconvolution are available, but not commonly used.

Until very recently the only practical means of maintaining the very low temperatures necessary to

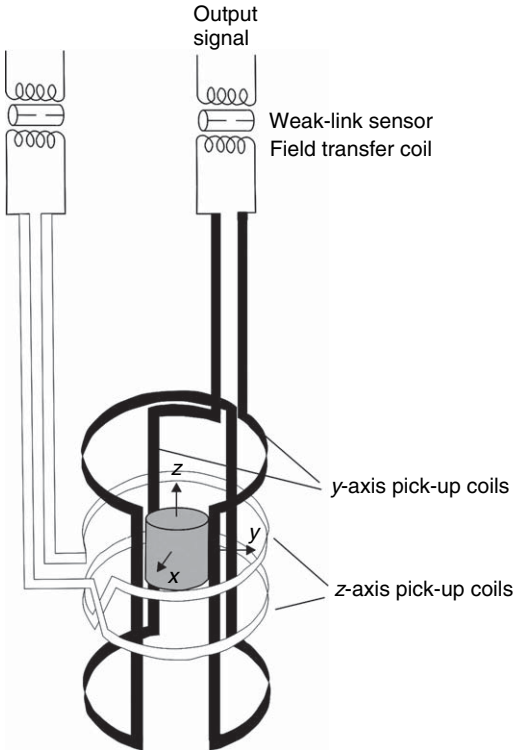

Figure 29 Arrangement of horizontal axis (black) and vertical axis (white) superconducting pickup coils, field transfer coils, and weak-link (SQUID) sensors in the early SCT cryogenic magnetometer. Modified from Superconducting Technologies User Manual.

operate superconducting sensors was by means of liquid helium. Helium 4 has a boiling point of 4.2 K. It has a very low heat of vaporization (0.082 kJ mol^{-1}, or 2.56 kJ l^{-1} of liquid He), but, due to its low atomic mass, a relatively high specific heat capacity. This means that, without extremely efficient insulation, a dewar of liquid helium evaporates very rapidly. The first cryogenic magnetometers were insulated by means of high vacuums, super-insulation (layers of reflective aluminized mylar separated by fiberglass sheets), heat shields cooled by contact with the evaporated helium gas, and/or an outer dewar filled with liquid nitrogen. It is crucial to ensure that helium gas is excluded from the vacuum spaces, as even small amounts can result in conduction of heat into the sensor region and loss of superconductivity. By these means the rate of heat flow into a 30 l dewar can be kept to about 75 mW, resulting in a boil-off of about 2.5 l of liquid helium per day.

Huge improvements in liquid helium retention may be achieved by incorporating an active cooling device or 'cryocooler' in the magnetometer. Unfortunately, the mechanical vibration and magnetic noise of such devices mean they must be physically separated from the magnetometer. A common arrangement is to place the compressor outside the building, or outside the magnetically shielded space or room which houses the magnetometer. The cryocooler cools a thermal shield around the helium reservoir, thus inhibiting evaporation. A modern magnetometer with a dewar of 50–90 l, and a well-maintained cryocooler, will typically run for between 500 and 900 days between fills.

An exciting new development in cryogenics is the 'pulse-tube cryocooler', which completely circumvents the need for liquid helium in order to reach temperatures of 4.2 K. The pulse tube cryocooler first appeared in 1999, and has very recently been incorporated in a rock magnetometer by 2G-Enterprises (2G Enterprises, website).

5.04.4.3 Progressive Demagnetization Techniques

5.04.4.3.1 Introduction

The NRM of a rock sample generally comprises several components carried by grains in different parts of the blocking temperature spectrum. The paleomagnetist usually (though not always) wants to isolate and determine the primary or characteristic component, acquired at the time of formation of the rock. In a straightforward situation involving only thermal activation/relaxation, but not chemical alteration of the magnetic minerals, the oldest component of magnetization will reside in the most stable grains, that is, those with the highest blocking temperatures and longest relaxation times. This will be the primary component unless the whole spectrum of grains has been remagnetized, for example, by a lightning strike or by heating to above the Curie temperature. Secondary partial thermoremanent magnetizations (pTRMs) and viscous components (VRMs) will be carried by less stable grains.

Such a situation is illustrated by the hypothetical example in **Figure 30**. Only those grains with blocking temperatures above T_2 retain a record of the primary magnetization. At some time in the rock's history, all the grains with blocking temperatures below T_2 have been remagnetized by a heating event and have gained a secondary pTRM in a different direction. Further, the least stable grains, those with $T_B < T_1$, have gained a VRM, probably parallel to the present-day field at the site. A single

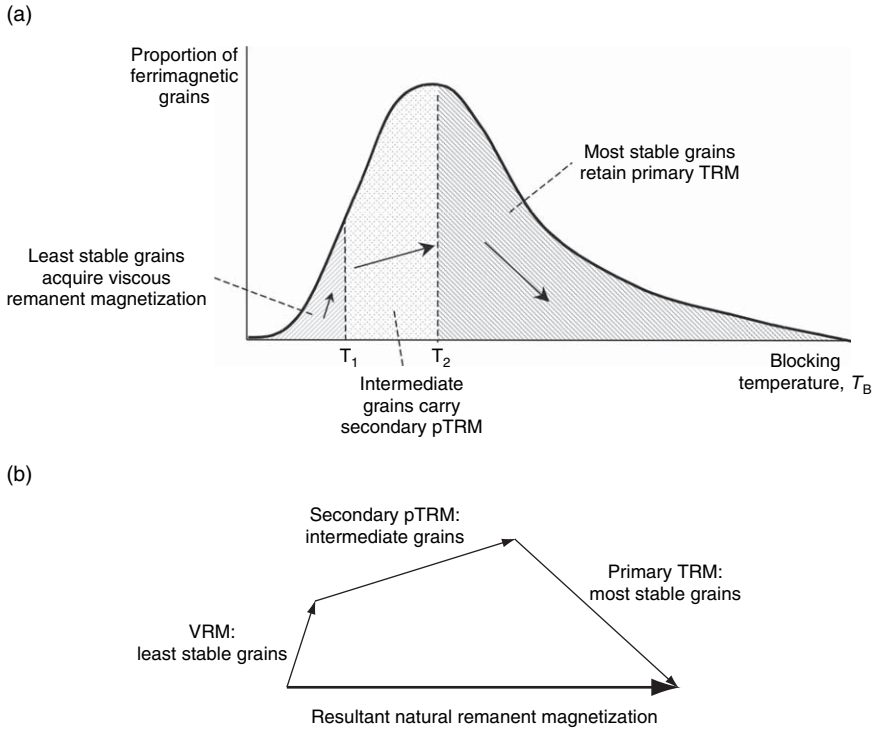

Figure 30 (a) Schematic diagram of the stability spectrum of ferrimagnetic grains in a typical rock sample, showing portions of the spectrum carrying the primary (TRM), secondary (pTRM), and viscous (VRM) components of remanent magnetization. (b) Vector diagram showing the addition of the various components of magnetization to yield the resultant natural remanent magnetization (NRM).

measurement of the NRM will yield the vector sum of these components, as shown in **Figure 30(b)**. In real situations there is almost always some overlap between the grains carrying each of the components of magnetization.

The association of the oldest component of magnetization with the most stable grains breaks down in more complex situations, for example, when chemical alteration has produced new, secondary ferrimagnetic minerals. In such cases it is possible to find a secondary chemical remanent magnetization carried by authigenic grains that have grown to such a size that they have the highest blocking temperatures in the sample, and which have formed at the expense of primary grains with high T_B's.

Partial or progressive demagnetization procedures are designed to incrementally remove the magnetization of a sample, working systematically through the blocking temperature or coercivity spectrum. This enables the separation and determination of components carried by grains in different intervals of the spectrum. Further information will be required to identify which is the primary or characteristic component and to piece together the magnetization history of the sample completely.

5.04.4.3.2 Thermal demagnetization

This method appeals directly to the blocking temperature spectrum of the ferrimagnetic grains in a rock sample.

After measurement of NRM, a specimen is heated to a predetermined temperature, T_H, and then cooled back to room temperature in a carefully controlled, zero magnetic field environment. This procedure randomizes the magnetic moments of all grains whose blocking temperatures are exceeded during the heating. A subsequent measurement of remanence will now give the vector sum of the moments of only those grains with blocking temperatures above T_H. Vector subtraction of this from the original NRM will give the removed magnetization, that carried by grains with $T_B < T_H$. In principle a series of incremental heating steps, alternated with measurements of the magnetization remaining after each cooling will enable a complete analysis of the components of magnetization carried by a specimen.

A number of thermal demagnetizers are available commercially. In addition many paleomagnetic laboratories have purpose-built equipment. The basic requirements of a thermal demagnetizer are a magnetic field-free furnace and cooling chamber. Most furnaces employ noninductive electrical windings, though gas-fired furnaces are also used. Various designs take between 12 and 50 specimens at a time: either arranged around the axis of a cylindrical furnace inside multiple, nested mu-metal shields, or in a layered arrangement at the center of a large Rubens coil set-up. It is during the cooling stage that it is most important to maintain as low a magnetic field as possible. Some designs incorporate a separate chamber into which the samples are passed for cooling, while a second set of samples may be heated in the already hot oven. In other designs the samples are cooled in the same space, without moving them.

It is important to allow sufficient time for the specimens to equilibrate both at the maximum temperature and back to room temperature before measurement: typically 20–30 min for each stage.

5.04.4.3.3 Alternating field (AF) demagnetization

Working progressively through the coercivity spectrum of a specimen provides an alternative way of separating different components of magnetization. In AF demagnetization, the specimen is placed inside a solenoid, which is connected to a variable AC supply, while being housed in an environment of zero direct field. The amplitude of the alternating current is increased to a preset maximum corresponding to a desired maximum magnetic field, it is then smoothly and slowly ramped back down to zero. When the current is at maximum amplitude, the magnetic moments of all grains with coercivities below the corresponding magnetic field follow the oscillations back and forth along the axis of the solenoid. As the peak field falls below the coercivity of each grain, its magnetic moment becomes blocked: ideally equal numbers of grains become blocked in each opposing direction. All directions in the specimen should be exposed equally to the demagnetizing field of the solenoid. This may be achieved by successively aligning each of the three axes of the specimen with the axis of the solenoid while the alternating magnetic field is cycled up and down (static method). Alternatively, the specimen may be tumbled simultaneously about two perpendicular axes, by means of a small motor and belt-driven turntable, while the field is cycled just once. There are advantages and disadvantages associated with each method. Certain specimens are susceptible to acquisition of a spurious magnetization during the tumbling procedure: a rotational remanent magnetization (RRM) antiparallel to the inner rotation axis was first documented by Wilson and Lomax (1972). RRM seems to be related to the more general phenomenon of gyroremanent magnetization (GRM), which may be acquired by single-domain grain-bearing specimens when they are rotated in steady or alternating magnetic fields (Stephenson 1980, 1981). Methods to correct for RRM and GRM have been proposed by Hillhouse (1977) and Giddings *et al.* (1997). However, these corrections are of an empirical nature, and to avoid any suspicion of doubt in results, many authors prefer to use thermal demagnetization in specimens that are likely to develop RRM or GRM.

5.04.4.4 Data Analysis and Statistics

Most rock magnetometers return the components of the magnetic moment of a specimen along the x, y, and z axes of the specimen. The operating software usually offers the provision to enter the field orientation of the specimen and this enables transformation of the result to the present-day geographic reference frame: northerly, easterly, and downward components of magnetic moment; or declination, inclination, and total magnetic moment. The intensity of magnetization is further obtained by dividing the total magnetic moment by the specimen volume. Finally, if the bedding attitude is known, this may be entered and the magnetization vector referred to the pre-tilting coordinate frame.

5.04.4.4.1 Progressive demagnetization data

Progressive demagnetization of a specimen yields a series of vectors, describing the magnetization left after each step of demagnetization. Three different plots are useful in interpreting such data. Examples are shown in **Figure 31**.

5.04.4.4.1.(i) Intensity of magnetization against demagnetization level If the direction of remanence changes little during demagnetization, then this plot gives an approximation to the blocking temperature or coercivity spectrum of the specimen. For multicomponent magnetizations its interpretation is less straightforward (**Figure 31(c)**).

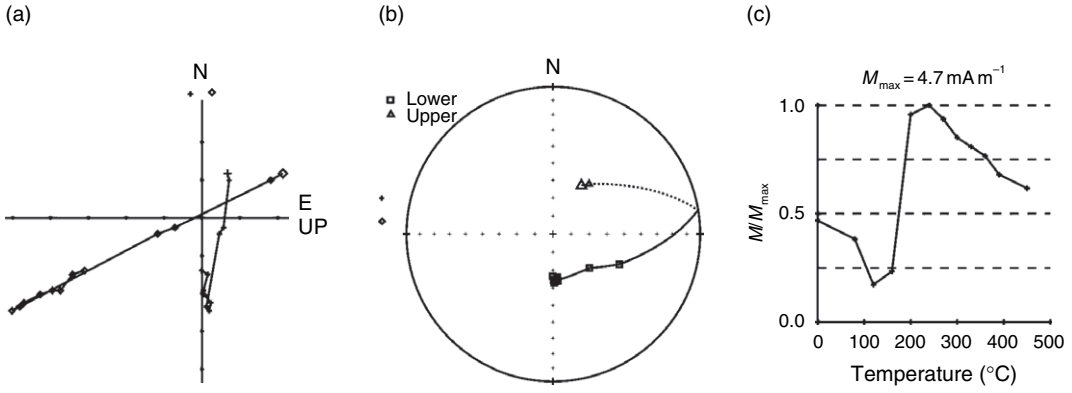

Figure 31 An example of progressive thermal demagnetization data for a (southern hemisphere) specimen carrying a primary magnetization of reversed polarity, overprinted by a normal polarity thermoviscous secondary component. (a) Vector component plot, showing the projection onto the horizontal plane (N vs E) and the projection onto the vertical NS plane (N vs UP), as crosses and diamonds respectively; (b) An equal angle stereographic projection of the sequence of remanent directions, (c) The intensity of magnetization plotted against demagnetization level (temperature).

5.04.4.4.1.(ii) Stereographic projection Stereographic projection of the directions of the remanence remaining at each step contains no information regarding the intensity of magnetization. For a single-component magnetization the direction does not change during demagnetization and all the data points overlie each other. For a two-component magnetization, the initial NRM is the vector sum of the two components. As the lower blocking temperature component is progressively removed, the tip of the remanent unit vector moves along a great circle path towards the direction of the underlying more stable component. The direction of the secondary component lies on the backward extrapolation of this great circle. This process is best seen in **Figure 31(a)**, where the primary magnetization is of reversed polarity (to the south and downward, since the specimen is from a southern hemisphere site), and the secondary magnetization is close to the present-day field at the site ($D = 20°$, $I = -66°$).

5.04.4.4.1.(iii) Vector component plots Vector component plots combine both intensity and direction data, by projecting the successive remanent vectors onto two different planes and presenting them in a single diagram (Zijderveld, 1967). The actual planes chosen vary; in **Figure 31(b)**, the horizontal plane (N vs E) and the vertical north–south plane (N vs Up) are shown, with the northerly component plotted on the same (y) axis in both cases. Linear segments correspond to the removal of single components of magnetization, and the direction of such a component can be measured directly from the diagram. The component residing in the grains with highest blocking temperatures or coercivities (often the primary component) should yield a linear segment terminating at the origin.

5.04.4.4.1.(iv) Principal component analysis In theory, the direction of a component of magnetization can be measured directly from a linear section of the vector component plot, as described above. In practice, however, the data are invariably scattered and estimation of the best straight line is often difficult and subjective. In such cases, principal component analysis, or PCA, (Kirschvink, 1980) provides a rigorous, objective way of estimating components of magnetization. In PCA the best-fit line is calculated to a pre-selected sequence of demagnetization data (vectors), which may be 'anchored' to the origin if desired, by analysis of a 3×3 matrix made up from the vector components: the 'orientation tensor'. The principal eigenvector gives the best-fit line, while a statistic of the quality of the fit, the 'maximum angular deviation' or MAD, is derived from the eigenvalues.

5.04.4.4.1.(v) Remagnetization circles In some situations involving multicomponent magnetization it is impossible to isolate the ChRM by progressive demagnetization. In such cases techniques involving extrapolation of trends in the demagnetization data (remagnetization circles) from a number of different samples until they intersect can be used to infer a common underlying component of magnetization or hypothetical endpoint (Halls, 1978; McFadden and

McElhinny, 1988). As with any extrapolation technique, extreme care is required in the interpretation of directions obtained from remagnetization circle analysis.

5.04.4.4.2 The statistical treatment of paleomagnetic data

When analyzing paleomagnetic data it is usual to treat the direction and intensity of the vectors separately. This is because the retrieval of the paleointensity of the geomagnetic field from magnetization intensity is a complex task and frequently cannot be achieved with the same degree of confidence as the paleodirection.

5.04.4.4.2.(i) Intensity of remanence and geomagnetic paleointensity The intensity of remanence (and also magnetic susceptibility and other laboratory-induced magnetizations) depends on the composition and concentration of the magnetic minerals and their granulometry, that is, grain size, shape distributions. Most such natural distributions do not follow a normal or Gaussian form, which is symmetrical about the mean value, but are highly skewed, with a long tail towards high values. It is often found that the logarithms of the values are normally distributed, however. The 'log-normal' distribution is found to give a good representation of natural remanent intensities and magnetic susceptibilities in rocks (Irving *et al.*, 1966; Tarling, 1966).

Methods for the determination of the intensity of the geomagnetic field from paleomagnetic measurements are covered in detail in Chapter 5.13, and only the rudimentary principles are given here. In general, the intensity of magnetization (TRM, DRM, CRM, etc.) of a sample will depend on many factors in addition to the strength of the prevailing field. These include intrinsic magnetic properties of the material such as the concentration of the remanence-bearing mineral(s), their saturation magnetization, and granulometry. In seeking the paleointensity one must firstly identify the portion of the ferrimagnetic grain spectrum that carries the primary or characteristic component of magnetization, and then normalize the intensity of magnetization of this portion to compensate for the intrinsic magnetic composition of the sample as described above.

Néel's theory of single-domain TRM (Néel, 1949, 1955) gives an analytical equation for magnetization intensity that is proportional to the external magnetic field (B_{ext}) in the weak-field approximation. Hence, in principle absolute determinations of paleointensity can be made from TRM-bearing materials. The relationship between magnetization and paleointensity is more complicated in the case of a DRM, where the degree of alignment of ferrimagnetic grains depends on external factors that are much more difficult to quantify. The intensity of DRM is nevertheless still predicted to be proportional to the prevailing magnetic field, and methods to retrieve logs of relative paleointensity from uniform sequences of sediments are often successful. Such methods usually employ normalization of a portion of the NRM with a laboratory-produced remanence, often anhysteretic or isothermal remanent magnetization.

5.04.4.4.2.(ii) Paleomagnetic directions: the Fisher distribution The analysis of remanent directions usually reduces to dealing with a set of unit vectors obtained from a set of N samples. Each unit vector $\mathbf{M}$ can be expressed in terms of its declination and inclination, or as direction cosines l, m, and n, which are the northerly, easterly, and downward components of the unit vector (**Figure 32(a)**).

$$l_i = \cos(D_i)\cos(I_i) \qquad D_i = \tan^{-1}\left(\frac{m_i}{l_i}\right)$$

$$m_i = \sin(D_i)\cos(I_i)$$

$$n_i = \sin(I_i) \qquad I_i = \sin^{-1} n_i$$

The mean direction is obtained via the vector sum $\mathbf{R}$ (**Figure 32(b)**).

$$\mathbf{R} = \left(\sum_{i=1}^{N} l_i, \sum_{i=1}^{N} m_i, \sum_{i=1}^{N} n_i\right) = (R_x, R_y, R_z)$$

$$\text{Mean } D = \tan^{-1}\left(\frac{R_y}{R_x}\right)$$

$$\text{Mean } I = \tan^{-1}\left(\frac{R_z}{\left(R_x^2 + R_y^2\right)^{1/2}}\right)$$

The length $R = \left(R_x{}^2 + R_y{}^2 + R_z{}^2\right)^{1/2}$ of the vector $\mathbf{R}$ forms the basis of the statistical analysis described below. If all N unit vectors are perfectly aligned, then $R = N$; the greater the scatter in the directions of the unit vectors, the smaller is the value of R.

The two-dimensional (2-D) probability density distribution function generally assumed to apply to paleomagnetic unit vectors is the Fisher distribution (Fisher, 1953). It is, in many ways, equivalent to a 2-D Gaussian or normal distribution, and is described mathematically by the function

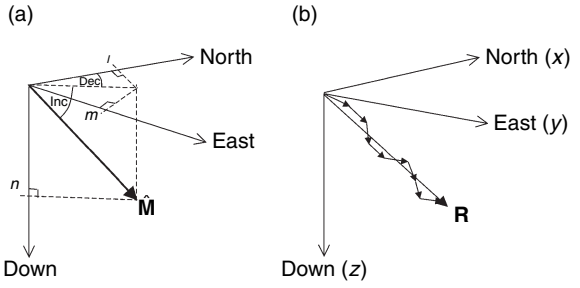

Figure 32 (a) The direction cosines l, m, and n of the unit magnetization vector $\hat{M}$ of a sample, and their relationship to declination and inclination. (b) Vector addition of unit magnetization vectors from a number of samples, $\hat{M}_1\,\hat{M}_2\,\hat{M}_3\cdots$, to yield the vector R (see text).

$$P(\varphi) = \frac{\kappa}{4\pi \sinh \kappa} \exp(\kappa \cos \varphi)$$

where φ is the angle between a direction and the true mean direction of the whole population. κ is known as the precision parameter, and reflects the dispersion of the distribution: it is analogous to the invariance, or the reciprocal of the variance, of a Gaussian distribution. κ ranges between zero for a random distribution (maximum scatter) and infinity for perfect alignment of the entire population.

A palaeomagnetic data set is a subset of N samples taken from the whole population. For $N \gtrsim 6$ and $\kappa \gtrsim 3$, the best (minimum variance, unbiassed) estimate of κ is given by $k = (N-1)/(N-R)$ (Fisher, 1953; McFadden, 1980). Naturally, as more of the population is sampled, that is, as N increases, k becomes a better estimate of κ.

The angular standard deviation, or angular dispersion, S, is a useful measure of scatter, for example, in studies where secular variation should be adequately sampled. For a Fisher distribution S is the semi-angle of the cone that includes 63% of the population. For low scatter a good approximation is given by

$$S = \theta_{63} \approx \frac{81}{\sqrt{k}}$$

The closeness of the mean of a given data set to the true mean of the population is clearly of crucial importance in palaeomagnetism. The ideal situation is obviously a large data set that samples the population randomly.

For $k \gtrsim 10$ the confidence that can be placed in the sample mean is quantified by the relation

$$\alpha_{(1-P)} = \cos^{-1}\left\{1 - \frac{N-R}{R}\left(\left(\frac{1}{P}\right)^{1/(N-1)} - 1\right)\right\}$$

where α is the semi-angle of the cone around the sample mean within which there is a probability $(1-P)$ of the true mean of the population lying. The levels of confidence most commonly quoted are 95% and 63%. The best estimates of α_{95} and α_{63} are given by

$$\alpha_{95} \cong \frac{140}{\sqrt{kN}} \quad \text{and} \quad \alpha_{63} \cong \frac{81}{\sqrt{kN}}$$

α_{63} is the direct analog of the standard error in the mean of a Gaussian distribution.

5.04.4.4.2.(iii) Comparison of directions In order to assess whether a paleomagnetically determined direction differs significantly from a direction that by comparison is completely specified, for example, the direction of the present-day field, α_{95} may be used directly. If the known direction lies outside the cone of 95% confidence of the paleomagnetic direction, then there is a 95% probability that the true directions differ.

It is frequently necessary to compare two paleomagnetically determined directions. It is often stated that the two directions are distinct (at the 95% level of confidence) if their cones of confidence do not overlap and are indistinguishable if they do. While the first statement is true, the second is not strictly correct. The cones may overlap by a small amount while the means are still distinct. More rigorous statistical tests have been devised and are discussed by McFadden and Lowes (1981) and Watson (1983).

5.04.4.4.3 Field tests

Progressive demagnetization experiments enable the analysis of natural remanent magnetization in terms of components carried by grains in different parts of the blocking temperature or coercivity spectrum. Statistical methods allow a meaningful comparison

to be made between determined paleomagnetic directions. However, neither gives any information regarding the ages of the various components of magnetization, or can prove that the characteristic magnetization was acquired at the time the rock formed. Application of some or all of the field tests discussed below can help order events in the geological and magnetization histories of a rock and so help date components of magnetization.

5.04.4.4.3.(i) Consistency test Demonstration of the reproducibility of results is an important aspect of all branches of science. In paleomagnetism it is usually necessary to show that the characteristic magnetization is of geomagnetic origin and not produced by some spurious or local effect such as a lightning strike or physical disturbance. Replication of a signal in rocks or sediments from different provenances or of different lithologies is a strong argument in favor of a regional or global magnetization process. Multiple records also provide data for more sophisticated levels of statistical analysis.

5.04.4.4.3.(ii) Fold test Paleomagnetists often sample beds or sediments that are no longer flat lying. It is usual to assume that such sediments originally accumulated on a horizontal surface, and have later been tilted or folded by tectonic processes of some sort. If a stable characteristic magnetization predates the tilting or folding, then the magnetization vector will have been tilted with the beds (**Figure 33**(**a**)), and a correction to restore the beds to the horizontal will also restore the magnetization to its original orientation. To this end, it is routine to measure the attitude of all sedimentary strata sampled during fieldwork. In cases of simple bedding tilt, a single rotation about the horizontal strike of the beds by an angle equal to the dip is required. In cases where folding is evident two steps are necessary: restoration of the fold axis to horizontal followed by untilting of the beds in the limbs of the fold. This requires the additional field measurement of the plunge of the fold axis. A fold test is successful if, after these field corrections, the characteristic magnetization vectors from individual sites move closer together or site-average vectors become indistinguishable within confidence levels. It is then possible to conclude that the magnetization predates the folding or tilting episode. An unsuccessful or partially successful fold test can also yield information about the magnetization history of a unit.

5.04.4.4.3.(iii) Reversals test When a study involves sampling through a number of geomagnetic polarity reversals, for example, for the calculation of paleomagnetic pole positions (see below) or for magnetostratigraphy, the resulting data set contains records of both normal and reversed polarity. According to the geocentric axial dipole (GAD) hypothesis (explained below), if secondary components of magnetization have been completely removed so that the records are accurate reflections of the geomagnetic field, and if sufficient time intervals have been sampled to average over secular variation (10^4–10^5 years), then the averages of the normal polarity directions and the reversed polarity directions should be antipodal. **Figure 33**(**b**) illustrates data from a magnetostratigraphic study in NZ. After progressive thermal demagnetization and PCA to estimate characteristic magnetization directions, the mean normal and reversed directions are antipodal to better than 95% confidence. In this case, the difference between the overall mean direction and the GAD direction for the site is a combination of an anomaly due to the movement of the Australian plate over the past 3 My, and a local vertical axis rotation associated with the proximity of the site to the Australian/Pacific plate boundary (Turner *et al.*, 2005)

5.04.4.4.3.(iv) Baked contact test When an igneous magma or volcanic lava is emplaced adjacent to a country rock, a temperature gradient develops in the country rock as heat is conducted away and the magma or lava cools and solidifies. As the temperature falls below the blocking temperatures of its constituent ferrimagnetic grains, the igneous or volcanic rock gains a TRM, which (ideally) is parallel to the ambient geomagnetic field. The maximum temperature reached in the country rock will be a decreasing function of distance from the magma or lava, and the magnetic moments of ferrimagnetic grains with blocking temperatures up to this maximum will be reset, that is, the baked contact will acquire a secondary pTRM. This will be parallel to the field at the time of emplacement of the lava or magma, and hence parallel to the TRM of the lava or magma. In those parts of the country rock closest to the magma the entire blocking temperature spectrum might be affected, but further away only the grains with lower blocking temperatures will become reset, while grains with higher blocking temperatures will retain the primary magnetization of the country rock. The description given above constitutes a positive baked contact test.

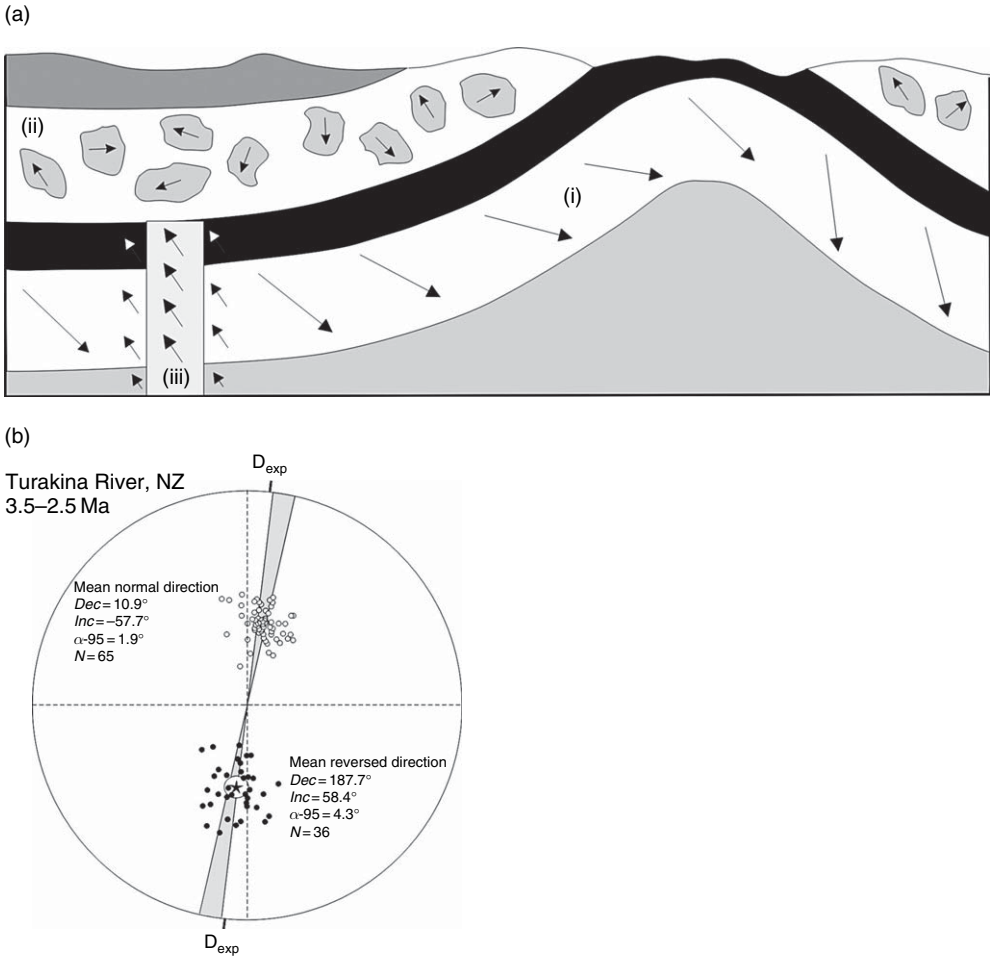

Figure 33 Paleomagnetic field tests: (a) Block diagram showing (i) the rotation of primary magnetization vectors during the folding of a rock unit (fold test); (ii) the randomization of the primary magnetization vectors of clasts incorporated in a conglomerate unit (conglomerate test); (iii) the remagnetization of country rocks immediately adjacent to an intruded dyke (baked contact test). (b) Example of a positive reversals test: equal area stereographic projection showing paleomagnetic directions from 101 sites sampled in a magnetostratigraphic study of the Turakina River Valley, New Zealand. The mean normal and reversed polarity directions are shown by stars, surrounded by an oval showing the cone of 95% confidence in the mean (alpha-95). (a) Adapted from Graham JW (1949) The stability and significance of magnetism in sedimentary rocks. *Journal of Geophysical Research* 54: 131–167. (b) From Turner GM, Kamp PJJ, McIntyre AP, Hayton S, McGuire DM, and Wilson GS (2005) A coherent middle Pliocene magnetostratigraphy, Wanganui Basin, New Zealand. *Journal of the Royal Society of New Zealand* 35: 197–227.

In the first part of the twentieth century baked contact tests provided invaluable evidence for the theory of polarity reversals. The opposing theory held that rocks found with reversed magnetizations had somehow become magnetized in the opposite direction to the ambient field (self-reversal). A worldwide compilation made by Wilson (1962a) listed 48 positive and three negative baked contact tests: 11 years later, McElhinny (1973) listed 154 positive results and still only 3 negative ones. Documented self-reversal mechanisms invariably involve particular, uncommon mineralogies, which are unlikely to be found simultaneously in large numbers of lavas and adjacent country rocks. As the number of positive baked contact tests accumulated, the likelihood of widespread self-reversal rapidly diminished and the idea of polarity reversals became generally accepted by the geomagnetism community. An unusual example of a doubly baked country rock was described by Wilson, (1962b). A lava flow and a dyke were successively emplaced in a laterite, which consequently carries secondary components of

magnetization from both heating episodes. Both are of reversed polarity, but they can be separated by progressive demagnetization since their directions differ significantly. It is virtually impossible to conceive of this situation occurring through self-reversal.

5.04.4.4.3.(v) Conglomerate test A conglomerate test may be applied when the rock (or sediment) of interest contains pebbles or clasts of a different lithology. It involves comparing the components of magnetization carried by the pebbles and by the matrix. If the pebbles retain a characteristic component of magnetization dating back to their previous history, then these vectors should have been randomized in the process of deposition, and no coherency should be observable in the data (**Figure 33(a)**). Any coherent component of magnetization found in the pebbles or between the pebbles and matrix raises the possibility of post-depositional remagnetization.

The conglomerate test is infrequently used, as it is not common to find suitable outcrops.

5.04.4.4.4 Poles

5.04.4.4.4.(i) Geomagnetic poles The present-day geomagnetic field can, to a first approximation, be modeled as a geocentric dipole. In 2005, the axis of the best-fitting geocentric dipole intersected Earth's surface at 79.7° N, 288.2° E and 79.7° S, 108.2° E (IGRF-10, 2005). These locations are called the 'geomagnetic poles'. This tilted geocentric dipole model (**Figure 34(b)**) describes about 80–90% of the present field at Earth's surface – the remaining 'non-dipole' part may be described by the higher-order components of a spherical harmonic representation, that is, quadrupole, octupole, etc.

5.04.4.4.4.(ii) Virtual geomagnetic poles If Earth's magnetic field could be modeled completely by a geocentric dipole aligned with the rotation axis (GAD) then at all points on the globe its horizontal component would be exactly northwards, that is, the declination would be zero, and the inclination would be a simple monotonic function of latitude (λ): $\tan(I) = 2\tan(\lambda)$. A corollary of this is that from any observed magnetic field direction (or paleomagnetically recorded direction), one can calculate the orientation of the geocentric dipole that would produce it, and the corresponding 'virtual geomagnetic poles' (VGPs). Imagine a globe: from the site of the observation draw a great circle in the direction of the horizontal component of the magnetic field or magnetization vector, the virtual pole must fall on this great circle. The angle (at the center of Earth) between the site and the pole (or the virtual geomagnetic latitude) is calculated from the recorded inclination according to the relation noted above, and corresponds to a distance measured along the great circle. This process is illustrated in **Figure 34(c)**.

Alternatively the latitude and longitude of the VGP (λ_p, φ_p) may be computed from the observed paleomagnetic direction (D, I) and the site latitude and longitude, (λ_s, φ_s) using the following equations

$$\sin\lambda_p = \sin\lambda_s \sin\lambda + \cos\lambda_s \cos\lambda \cos D$$

$$\phi_p = \phi_s + \beta \quad \text{if } \sin\lambda \geq \sin\lambda_s \sin\lambda_p$$

$$\phi_p = \phi_s + \beta + 180 \quad \text{if } \sin\lambda < \sin\lambda_s \sin\lambda_p$$

$$\text{where} \quad \tan\lambda = (1/2)\tan I$$

$$\text{and} \quad \sin\beta = \frac{\cos\lambda \sin D}{\cos\lambda_p}$$

A pole calculated in this way is virtual in the sense that the geocentric dipole model employed in the calculation cannot be justified for an observation from a single location and a single point of time: it has no real physical meaning unless the effect of the non-dipole field just happened to be zero at the time and place of the observation.

VGPs, however, remain a favorite way of presenting paleomagnetic directions and are used extensively, for example, in mapping sequences of transitional directions from polarity reversals when the field was almost certainly not dipolar.

5.04.4.4.4.(iii) The GAD hypothesis There is considerable evidence to indicate that, when the geomagnetic field is averaged over sufficiently long intervals of time (omitting intermediate directions recorded when the field was actually in the process of reversal), the mean positions of the geomagnetic poles coincide with the North and South poles of the rotation axis. For example, when the VGPs of a global distribution of rocks dated between 0 and 5 Ma are averaged the mean coincides with the rotation axis to within about 2° (McElhinny *et al.*, 1996). This leads to the GAD hypothesis: that the time-averaged geomagnetic field is a geocentric axial dipole field. There is some debate as to the minimum time period required to average out the secular variation (of both non-dipole and dipole fields): most sources quote between 10 000 and 100 000 years. The GAD hypothesis is fundamental to many applications

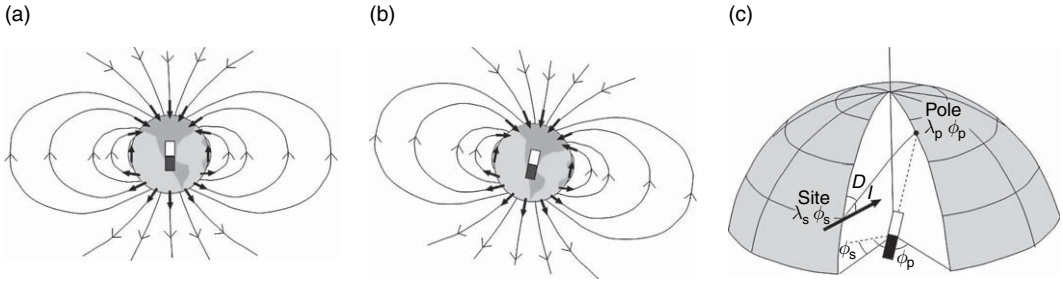

Figure 34 (a) The magnetic field due to a geocentric axial dipole. (b) The magnetic field due to a tilted geocentric dipole. (c) The principle of calculation of a virtual geomagnetic pole from an observed or recorded magnetic field direction at site (λ_S, ϕ_S).

of paleomagnetism, including providing crucial support for the theory plate tectonics and continental reconstructions.

5.04.4.4.4.(iv) Paleomagnetic poles and apparent polar wander paths The term 'paleomagnetic pole' is applied to a pole calculated by averaging a paleomagnetic data set that spans a time interval long enough to average secular variation. The GAD hypothesis implies that such a pole gives the position of the rotation axis with respect to the sampling location at the time the magnetization was acquired. Paleomagnetic poles for the past 5 million years are coincident with the rotation axis. However, older poles differ significantly – the discrepancy generally increasing with age. The time-sequence of paleomagnetic poles from a given continent or stable cratonic block is called an apparent polar wander path (APWP). The concept of an APWP was introduced by Creer *et al.* (1954). Originally it was thought that, while the orientation of the rotation axis remains fixed in space, APWPs were produced by rotation of the whole Earth with respect to its rotation axis: this is now termed 'true polar wander'. The steady accumulation of data over the years soon showed that APWPs from different continents differ significantly. However, it was also found that sometimes, the application of a finite rotation brought a segment of one APWPs into coincidence with the contemporaneous section of another. If one imagines an APWP tied to the continent from which it is derived, the implication is that there have been periods of time when some continents have moved together, producing similar APWPs, and other periods when they have moved separately over Earth's surface, causing separation and new segments of their APWPs. This is the basis of the theory of plate tectonics, whereby the continents move on thin lithospheric plates in response to mantle covection processes, constructive and destructive processes at plate boundaries.

References

Alexandrov EB, Balabas MV, Kulyasov VN, *et al.* (2004) Three-component variometer based on a scalar potassium sensor. *Measurement Science and Technology* 15: 918–922.

Alexandrov EB and Bonch-Bruevich VA (1992) Optically pumped magnetometers after three decades. *Optical Engineering* 31: 711–717.

Alexandrov EB and Primdahl F (1993) On gyro-errors of the proton magnetometer. *Measurement Science and Technology* 4: 737–739.

Alldredge LR and Saldukas I (1964) An automatic standard magnetic observatory. *Journal of Geophysical Research* 69: 1963–1970.

Aschenbrenner H and Goubau G (1936) Eine Anordnung Registrieung rascher magnetischer Storungen. *Hochfreg Tech. Elektroakust* 47: 178–181.

Bardeen J, Cooper LN, and Schrieffer JR (1957) Theory of superconductivity. *Physical Review* 108: 1175–1204.

Becker H and Fassbinder JWE (1999) Magnetometry of a Scythian settlement in Siberia near Cicah in the Baraba Steppe. In: Fassbinder JWE and Irlinger WE (eds.) *Archaeological Prospection, Arbeitsh. Bayerisches Landesamtf. Denkmlpflege*, Vol. 108, pp. 168–172. Munchen: Verlag Karl M. Lipp.

Bitterly J, Cantin JM, Schlich R, Folques J, and et Gilbert D (1984) Portable magnetometer theodolite with fluxgate sensor for earth's magnetic field component measurements. *Geophysical Surveys* 6: 233–239.

Blackett PMS (1952) A negative experiment relating to magnetism and the Earth's rotation. *Philosophical Transactions of the Royal Society Series A* 245: 309–370.

Blinov VE, Ginzburg BI, Zhitnikov RA, and Kuleshov PP (1984) Alkali-helium magnetometer with optically oriented potassium atoms. *Soviet Physics – Technical Physics* 29(2): 168–171. See also (in Russian): *Zhurnal Tekhnicheskoi Fiziki* 54: 287–292.

Bloch F (1946) Nuclear induction. *Physical Review* 70: 460–474.

Brunhes B (1906) Récherches sur les directions d'aimentation des roches volcaniques. *Journal of Physics* 5: 705–724.

Bullock SJ and Barritt SD (1989) Real-time navigation and flight-path recovery of aerial geophysical surveys: A review. In: Garland GD (ed.) *Proceedings of Exploration 87, Third*

Decennial International Conference on Geophysical and Geochemical Exploration for Minerals and Groundwater., Special Volume 3, pp. 960. Sudbury, Canada: Ontario Geological Survey.

Carver TR and Slichter CP (1953) Polarization of nuclear spins in metals. *Physical Review* 92: 212–213.

Carver TR and Slichter CP (1956) Experimenatl verification of the Overhauser nuclear polarization effect. *Physical Review* 102: 975–980.

Chave AD, Green AW, Evans RL, *et al.* (1995) *Report of a Workshop on Technical Approaches to Construction of a Seafloor Geomagnetic Observatory.* Technical Report WHOI-95-12. Woods Hole, USA: Woods Hole Oceanographic Institution.

Chevallier R (1925) L'aimentation des laves de l'Etna et l'orientation du champ terrestre en Sicile du XII^{e} au XVII^{e} siècle. *Annales de Physique* 4: 5–162.

Collinson DW (1983) *Methods in Rock Magnetism and Palaeomagnetism: Techniques and Instrumentation*. New York: Chapman and Hall.

Creer KM, Irving E, and Runcorn SK (1954) The direction of the geomagnetic field in remote epochs in Great Britain. *Journal of Geomagnetism and Geoelectricity* 6: 163–168.

David P (1904) Sur la stabilité de la direction d'aimentation dans quelques roches volcaniques. *Comptes Rendus Academie Sciences de Paris* 138: 41–42.

Delesse A (1849) Sur le magnétisme polaire dans les minéraux et dans les roches. *Annales Chimie et de Physique, Ser.* 325: 194–209.

Deumlich F (1980) *Instrumentenkunde der Vermessungstechnik*. Berlin (Ost): VEB Verlag für Bauwesen.

De Vuyst AP and Hus J (1966) Généralisation de la Mesure de l'Intensité des Composantes Verticale et Horizontale du Champ Magnétique Terrestre avec le Magnétomètre à Protons. *Annales De Geophysique* 22: 119–127.

Fisher RA (1953) Dispersion on a sphere. *Proceedings of the Royal Society of London, Series A* 217: 295–305.

Fuller M (1987) Experimental methods in rock magnetism and palaeomagnetism. In: Sammis CG and Henyey TL (eds.) *Methods of Experimental Physics*, pp. 303–471. Orlando: Academic Press.

Giddings JW, Klootwijk CT, Rees J, and Groenewoud A (1997) Automated AF-demagnetization on the 2G-Enterprises cryogenic magnetometer. *Geologie en Mijnbouw* 76: 35–44.

Gilbert G, Cantin JM, Bitterly J, Schlich R, and Folques J (1988) Absolute measurements of the Earth′s magnetic field in French Observatories: Results obtained with the portable theodolite fluxgate magnetometer for the period 1979–86. *Proceedings of the International Workshop on Magnetic Observatory Instruments*, *Geomagnetism Series 32*, paper 88–17. Ottawa, Canada: Geological Survey of Canada.

Gilles H, Hamel J, and Chéron B (2001) Laser pumped ^{4}He magnetometer. *Review of Scientific Instruments* 72: 2253–2260.

Goree WS and Fuller MD (1976) Magnetometers using RF-driven SQUIDs and their application in rock magnetism and palaeomagnetism. *Reviews of Geophysics and Space Physics* 14: 591–608.

Graham JW (1949) The stability and significance of magnetism in sedimentary rocks. *Journal of Geophysical Research* 54: 131–167.

Grant FS (1985) Aeromagnetics, geology and ore environments, I. Magnetite in igneous, sedimentary and metamorphic rocks: An overview. *Geoexploration* 23: 303–333.

Gravrand O, Khokhlov A, Le Mouël JL, and Léger JM (2001) On the calibration of a vectorial ^{4}He pumped magnetometer. *Earth Planets Space* 53: 949–958.

Green AW, Coles RL, Kerridge DJ, and LeMouël J-L (1998) INTERMAGNET, today and tomorrow. In: *Proceedings of the VIIth Workshop on Geomagnetic Observatory Instruments*, *Data Acquisition and Processing '96*, *Scientific Technical Report STR98/21*, pp. 277–286. Potsdam, Germany: GFZ-Potsdam.

Halls HC (1978) The use of converging remagnetization circles in paleomagnetism. *Physics of the Earth and Planetary Interiors* 16: 1–11.

Henkel H (1991) Petrophysical properties (density and magnetisation) of rocks from the northern part of the Baltic shield. *Tectonophysics* 192: 1–19.

Hillhouse JW (1977) A method for the removal of rotational remanent magnetization acquired during alternating field demagnetization. *Geophysical Journal of the Royal Astronomical Society* 50: 29–34.

Hrvoic I (2001) Standardization of total field magnetometers. *Contributions to Geophysics & Geodesy* 31: 93–97.

Hurwitz L and Nelson JH (1960) Proton vector magnetometer. *Journal of Geophysical Research* 65: 1759–1765.

Irving E, Molyneux L, and Runcorn SK (1966) The analysis of remanent intensities and susceptibilities of rocks. *Geophysical Journal of the Royal Astronomical Society* 137: 451–464.

Jankowski J, Marianiuk J, Ruta A, Sucksdorff C, and Kivinen M (1984) Long-term stability of a torque-balance variometer with photoelectric converters in observatory practice. *Geophysical Surveys* 6: 367–380.

Jankowski J and Sucksdorff C (1996) *IAGA Guide for Magnetic Measurements and Observatory Practice.* International Association of Geomagnetism and Aeronomy.

Josephson BD (1962) Possible new effects in superconducting tunnelling. *Physics Letters* 1: 251–253.

Kastler A (1950) Quelques suggestions concernant la production optique et la détection optique d′une inégalité de population des niveaux de quantification spatiale des atomes. *Journal of Physics, Radium* 11: 255–265.

Kirschvink JL (1980) The least-squares line and plane and the analysis of palaeomagnetic data. *Geophysical Journal of the Royal Astronomical Society* 62: 699–718.

Korepanov V, Berkman R, Rakhlin L, *et al.* (2001) Advanced field magnetometers comparative study. *Measurement* 29: 137–146.

Langel R, Ousley G, Berbert J, Murphy J, and Settle M (1982) The MAGSAT mission. *Geophysical Research Letters* 9: 243–245.

Larochelle A and Christie KW (1967) An automatic 3-magnet or biastatic magnetometer. *Geological Survey of Canada* Paper 67–26: 28 pp.

Lauridsen KE (1985) Experiences with the DI-fluxgate magnetometer: Inculsive theory of the instrument and comparison with other methods. Danish Meteorological Institute Geophysical Papers, R–71.

Laursen V and Olsen J (1971) Classical methods of geomagnetic observations. In: Flugge S and Rawer K (eds.) *Encyclopedia of Geophysics, Geophysics III/3, Volume XLIX/3*, pp. 276–322. Berlin: Springer.

Lilley FEM and Day AA (1993) D'Entrecasteaux 1792: Celebrating a bicentennial in geomagnetism. *EOS, Transactions of the American Geophysical Union* 74(97): 102–103.

Mackereth FJH (1958) A portable core sampler for lake deposits. *Limnology and Oceanography* 3: 181–191.

Mackereth FJH (1969) A short core sampler for subaqueous deposits. *Limnology and Oceanography* 14: 145–151.

McElhinny (1973) *Palaeomagnetism and Plate Tectonics*. Cambridge, UK: Cambridge University Press.

McElhinny MW, McFadden PL, and Merrill RT (1996) The time-averaged palaeomagnetic field. *Journal of Geophysical Research* 101: 25007–25027.

McFadden PL (1980) The best estimate of Fisher's precision parameter κ. *Geophysical Journal of the Royal Astronomical Society* 60: 397–407.

McFadden PL and Lowes FJ (1981) The discrimination of mean directions drawn from Fisher distributions. *Geophysical Journal of the Royal Astronomical Society* 67: 19–33.

McFadden PL and McElhinny MW (1988) The combined analysis of remagnetization circles and direct observations in paleomagnetism. *Earth and Planetary Science Letters* 87: 161–172.

Melloni M (1853) Du magnétisme des roches. *Comptes Rendus Academie Sciences de Paris* 37: 966–968.

Merayo MG, Brauer R, Primdahl F, Petersen JR, and Nielsen OV (2000) Scalar calibration of vector magnetometer. *Measurement Science and Technology* 11: 120–132.

Meyer O and Voppel D (1954) Ein Theodolit zur Messung des Erdmagnetischen Feldes mit der Förstersonde als Nullindicator. *Deutsche Hydrographische Zeitschrift* 12: 73–77.

Milligan PR, Morse MP, and Rajagopalan S (1991) Pixel map preparation using the HSV colour model. *Exploration Geophysics* 23: 219–224.

Minty BRS (1992) Simple micro-levelling for aeromagnetic data. *Exploration Geophysics* 22: 591–592.

Molyneux LA (1971) A complete result magnetometer for measuring the remanent magnetization of rocks. *Geophysical Journal of the Royal Astronomical Society* 24: 429–433.

Nagata T (1961) *Rock magnetism,* 2nd edn. Tokyo, Japan: Maruzen.

Néel L (1949) Théorie du trainage magnétiique des ferromagnétiques aux grains fins avec applications aux terres cuites. *Annales De Geophysique* 5: 99–136.

Néel L (1955) Some theoretical aspects of rock magnetism. *Advances in Physics* 4: 191–243.

Newitt LR, Barton CE, and Bitterly J (1996) *IAGA Guide for Magnetic Repeat Station Surveys. International Association of Geomagnetism and Aeronomy.*

Nielsen OV, Petersen JR, Primdahl F, *et al.* (1995) Development, construction and analysis of the ''Oersted'' fluxgate magnetometer. *Measurement Science and Technology* 6: 1099–1115.

O'Sullivan KN (1991) A map for all reasons: The role of image processing in mineral exploration. *Minerals Industry International* 8–14 (January 1991).

Overhauser AW (1953a) Polarization of nuclei in metals. *Physical Review* 91: 476 (abstract only).

Overhauser AW (1953b) Polarization of nuclei in metals. *Physical Review* 92: 411–415.

Packard ME and Varian RH (1954) Free nuclear induction in the Earth's magnetic field. *Physical Review* 93: 941 (abstract only).

Papitshvili VO, Petrov VG, Saxena AB, Clauer CR, and Papitshvili NE (2006) A virtual global magnetic observatory network: VGMO.NET. *Earth Planets Space* 58: 765–774.

Pozzi JP and Thellier E (1963) Sur des perfectionments récents apportés aux magnétometre a très haute sensibilité utilisés en minéralogie magnétique et en paléomagnétisme. *Comptes Rendus Academie Sciences de Paris* 257: 1037–1040.

Primdahl F (2002) Resonance magnetometers. In: Ripka P (ed.) *Magnetic Sensors and Magnetometers*, pp. 267–304. Boston and London: Artech House.

Primdahl F, Merayo JMG, Brauer P, Laursen I, and Risbo T (2005) Internal field of homogeneously magnetized toroid sensor for proton free precession magnetometer. *Measurement Science and Technology* 16: 590–593.

Pulz E, Jäckel KH, and Linthe HJ (1999) A new optically pumped tandem magnetometer: Principles and experiences. *Measurement Science and Technology* 10: 1025–1031.

Rasmussen O (1990) Improvements in fluxgate magnetometers at Danish meteorological Institute's magnetic observatories. In: *Proceedings of the International Workshop on Geomagnetic Observatory Data Acquisition and Processing.* Finnish Meteorological Institute Geophysical Publications No. 15. Helsinki, Finland.

Rasson JL (1996) Progress in the design of an automatic diflux. In: Rasson JL (ed.) *Proceedings of the VIth Workshop on Geomagnetic Observatory Instruments, Data Acquisition and Processing*, Publ. Sci. et Techn. No 003, pp. 190–194. Brussels: Institut Royal Meteorologique de Belgique.

Rasson JL (2005) About absolute geomagnetic measurements in the observatory and in the field. *Publication Scientifique et Technique de l'Institut Royal Météorologique de Belgique* 40: 42.

Reeves CV (2007) The role of airborne geophysical reconnaissance in exploration geoscience. *First Break* 19.9: 501–508.

Reeves CV and Bullock SJ (2006) *Airborne exploration.* Fugro Airborne Surveys Limited (in press).

Reeves CV, Macnab R, and Maschenkov S (1998). Compiling all the world's magnetic anomalies. *EOS American Geophysical Union*, **July 14**, p. 338.

Reeves CV, Reford SW, and Milligan P R (1997) Airborne geophysics: Old methods, new images. In: Gubbins AG (ed.) *Proceedings of Exploration 97*, *Fourth Decennial International Conference on Mineral Exploration*, pp. 13–30. Toronto, Canada: GEO F/X.

Reford MS and Sumner JS (1964) Aeromagnetics. *Geophysics* 29: 482–516.

Reid AB, Allsop JM, Gransser H, Millett AJ, and Somerton IW (1990) Magnetic interpretation in three dimensions using Euler deconvolution. *Geophysics* 55: 80–61.

Roest WR, Verhoef J, and Pilkington M (1992) Magnetic interpretation using the 3-D analytic signal. *Geophysics* 57: 116–125.

Sapunov V, Denisov A, Denisova O, and Saveliev D (2001) Proton and Overhauser magnetometers metrology. *Contributions to Geophysics & Geodesy* 31: 119–124.

Sapunov V, Rasson J, Denisov A, *et al.* (2006) Theodolite-borne vector Overhauser magnetometer: DIMOVER, In: Yumoto E (ed.) *Proceedings of the XIth Workshop on Geomagnetic Observatory Instruments*, *Data Acquisition and Processing.* Kakioka.

Schmidt H and Auster V (1971) Neuere Messmethoden de Geomagnetik. In: Flugge S and Rawe K (eds.) *Encyclopedia of Geophysics, Geophysics III/3, Volume XLIX/3*, pp. 323–383. Berlin: Springer.

Schnegg PA and Fischer G (1991) The TURBOMAG vector magnetometer. *Münchner Geophysikalische Mitteilungen* 5: 121–130.

Serson PH and Hannaford WLW (1956) A portable electrical magnetometer. *Canadian Journal of Technology* 34: 232–243.

Shifrin VYa, Alexandrov EB, Chikvadze TI, *et al.* (2000) Magnetic flux density standard for geomagnetometers. *Metrologia* 37: 219–227.

Spector A and Grant FS (1970) Statistical models for interpreting aeromagnetic data. *Geophysics* 35: 293–302.

Stephenson A (1980) Rotational remanent magnetization and the torque exerted on a rotating rock in an alternating magnetic field. *Geophysical Journal of the Royal Astronomical Society* 62: 113–132.

Stephenson A (1981) Gyromagnetic remanence and anisotropy in single domain particles, rocks and magnetic recording tape. *Philosophical Magazine Series B* 44: 635–644.

Tarling DH (1966) The magnetic intensity and susceptibility distributions in some Cenozoic and Jurassic basalts. *Geophysical Journal of the Royal Astronomical Society* 11: 423–432.

Tarlowski C, McEwin AJ, Reeves CV, and Barton CE (1996) Dewarping the composite aeromagnetic anomaly map of Australia using control traverses and base stations. *Geophysics* 61: 696–705.
Tenani M (1941) Nuovo Metodo di misura della declinazione e della inclinazione magnetica. *La Ricerca Scientifica* 20: 1135–1140.
Thellier E (1933) Magnétometre insensible aux champs magnétiques troubles des grandes villes. *Comptes Rendus Academie Sciences de Paris* 197: 224–234.
Trigg DF (1970) A portable D and I magnetometer. *Geomagnetic Laboratory Report n°70-3*, *Direction de la Physique du Globe*, *Energy*, *Mines and Resources*. Ottawa, Canada.
Turner GM, Kamp PJJ, McIntyre AP, Hayton S, McGuire DM, and Wilson GS (2005) A coherent middle Pliocene magnetostratigraphy, Wanganui Basin, New Zealand. *Journal of the Royal Society of New Zealand* 35: 197–227.
van Loo SA and Rasson JL (2006) Development of an automatic declination–inclination magnetometer. In: Rasson JL and Delipetrov T (eds.) *Geomagnetics for Aeronautical Safety: A Case Study in and Around the Balkans*, Nato Science Series, Sub-Series C. Netherlands: Springer.
Watson GS (1983) *Statistics on Spheres*, University of Arkansas Lecture Notes in the Mathematical Sciences, pp. 177–186. New York: Wiley.
Wienert KA (1970) *Notes on Geomagnetic Observatory and Survey Practice.* Brussels: UNESCO.
Wilson RL (1962a) The palaeomagnetic history of a doubly baked rock. *Geophysical Journal of the Royal Astronomical Society* 6: 397–399.
Wilson RL (1962b) The palaeomagnetism of baked contact rocks and reversals of the earth's magnetic field. *Geophysical Journal of the Royal Astronomical Society* 7: 194–202.
Wilson RL and Lomax R (1972) Magnetic remanence related to slow rotation of ferromagnetic material in alternating magnetic fields. *Geophysical Journal of the Royal Astronomical Society* 30: 295–303.
Zijderveld JDA (1967) AC demagnetization of rocks: Analysis of results. In: Collinson DW, Creer KM, and Runcorn SK (eds.) *Methods in Palaeomagnetism*. Amsterdam: Elsevier.

Relevant Websites

http://www.2genterprises.com – 2G Enterprises.
http://www.gemsys.ca – GEM Systems.
http://www.ga.gov.au – Geoscience Australia.
http://www.geosoft.com – Geosoft.
http://www.gfz-potsdam.de – GFZ Potsdam: CHAMP.
http://www.intrepid-geophysics.com – Intrepid Geophysics.
http://www.intermagnet.org – INTERMAGNET.
www.molspin.com – Molspin.
http://www.physics.nist.gov – NIST Physics Laboratory Home Page: Values of physical constants recommended by CODATA, 2002.
http://www-odp.tamu.edu – Ocean Drilling Programme.
http://home.ural.ru – Quantum Magnetometry Laboratory of Ural State Technical University.
http://www.ngdc.noaa.gov – USDOC/NOAA/NESDIS/ National Geophysical Data Center(NGDC) Home. Page: IAGA 2002 Data Exchange Format; IGRF-10; World Data Center Systems.